# ตัวเร่งปฏิกิริยาวิวิธพันธุ์ชนิดเบสจากโดโลไมต์ธรรมชาติสำหรับทรานส์เอสเทอริฟิเคชันของน้ำมันพืช

นางสาวทิฆัมพร นารี

วิทยานิพนธ์นี้เป็นส่วนหนึ่งของการศึกษาตามหลักสูตรปริญญาวิทยาศาสตรมหาบัณฑิต
สาขาวิชาปิโตรเคมีและวิทยาศาสตร์พอลิเมอร์
คณะวิทยาศาสตร์ จุฬาลงกรณ์มหาวิทยาลัย
ปีการศึกษา 2554

# HETEROGENEOUS BASE CATALYSTS FROM NATURAL DOLOMITE FOR TRANSESTERIFICATION OF VEGETABLE OIL

Miss Thikumbhorn Naree

A Thesis Submitted in Partial Fulfillment of the Requirements

for the Degree of Master of Science Program in Petrochemistry and Polymer Science

Faculty of Science

Chulalongkorn University

Academic Year 2011

| | |
|---|---|
| Thesis Title | HETEROGENEOUS BASE CATALYSTS FROM NATURAL DOLOMITE FOR TRANSESTERIFICATION OF VEGETABLE OIL |
| By | Miss Thikumbhorn Naree |
| Field of Study | Petrochemistry and Polymer Science |
| Thesis Advisor | Assistant Professor Chawalit Ngamcharussrivichai, Ph.D. |

---

Accepted by the Faculty of Science, Chulalongkorn University in Partial Fulfillment of the Requirements for the Master's Degree

……...Dean of the Faculty of Science

(Professor Supot Hannongbua, Dr. rer. nat.)

THESIS COMMITTEE

……...Chairman

(Professor Pattarapan Prasassarakich , Ph.D.)

……...Thesis Advisor

(Assistant Professor Chawalit Ngamcharussrivichai, Ph.D.)

……...Examiner

(Associate Professor Voravee P. Hoven, Ph.D.)

……...External Examiner

(Anurak Winitsorn, Ph.D.)

ทิฆัมพร นารี : ตัวเร่งปฏิกิริยาวิวิธพันธุ์ชนิดเบสจากโดโลไมต์ธรรมชาติสำหรับทรานส์เอสเทอริฟิเคชันของน้ำมันพืช. (HETEROGENEOUS BASE CATALYSTS FROM NATURAL DOLOMITE FOR TRANSESTERIFICATION OF VEGETABLE OIL) อ. ที่ปรึกษาวิทยานิพนธ์หลัก : ผศ.ดร. ชวลิต งามจรัสศรีวิชัย, 104 หน้า.

งานวิจัยนี้ศึกษาการเตรียมตัวเร่งปฏิกิริยาวิวิธพันธุ์ชนิดเบสจากโดโลไมต์ธรรมชาติสำหรับทรานส์เอสเทอริฟิเคชันของน้ำมันปาล์มกับเมทานอล ด้วยวิธีการละลาย-การตกตะกอน (dissolution-precipitation method) ขั้นตอนทั่วไปประกอบด้วย นำโดโลไมต์ที่ผ่านการเผามาผสมกับอะลูมินาที่ใช้เป็นตัวประสาน, โซเดียมอะลูมิเนตที่ใช้เป็นสารเพิ่มความแข็งของตัวเร่งปฏิกิริยา และไฮดรอกซีเอทิลเซลลูโลส (hydroxyethyl cellulose) ที่เป็นสารเสริมสภาพพลาสติก (plasticizer) ในสารละลายกรดไนตริกที่ pH 1 ของผสมนี้จะนำไปขึ้นรูปให้มีลักษณะแบบเส้น (extrudates) โดยใช้เครื่องอัดรีด (manual extruder ) หลังจากนั้นนำตัวเร่งปฏิกิริยาที่ผ่านการขึ้นรูปมาหักให้มีขนาด 5 มิลลิเมตรแล้วนำไปเผาที่ 500-800 องศาเซลเซียส ปัจจัยที่ศึกษาในการเตรียมตัวเร่งปฏิกิริยา ได้แก่ pH ของสารละลายกรดไนตริก ปริมาณน้ำ ปริมาณไฮดรอกซีเอทิลเซลลูโลส อุณหภูมิในการอบแห้ง อุณหภูมิในการเผาตัวเร่งปฏิกิริยา ผลของการเติมโซเดียม อะลูมิเนตต่อลักษณะสมบัติของตัวเร่งปฏิกิริยาและพิสูจน์เอกลักษณ์ของตัวเร่งปฏิกิริยาวิวิธพันธุ์ชนิดเบสเตรียมจากโดโลไมต์ธรรมชาติด้วยเทคนิคต่างๆ ได้แก่ X-ray fluorescence spectroscopy (XRF), X-ray diffraction (XRD), scanning electron microscopy (SEM), thermogravimetric /differential thermal analysis (TG/DTA), $N_2$ adsorption desorption measurement, temperature-programmed desorption ของ $CO_2$ ($CO_2$-TPD) และ $CO_2$-pluse chemisorption ภาวะที่เหมาะสมในการเตรียมตัวเร่งปฏิกิริยาคือ อัตราส่วนน้ำหนักของโดโลไมต์/อะลูมินา/โซเดียมอะลูมิเนต เท่ากับ 70:20:10, ปริมาณของไฮดรอกซีเอทิลเซลลูโลส ร้อยละ 3 เทียบกับน้ำหนักของของแข็งที่ใช้, pH ของสารละลายกรดไนตริกเท่ากับ 1, ปริมาณของน้ำ 1.5 เท่าของน้ำหนักของของแข็งที่ใช้ และอุณหภูมิในการเผาตัวเร่งปฏิกิริยา 800 องศาเซลเซียส ตัวเร่งปฏิกิริยาแบบเส้นที่เตรียมได้สามารถเร่งปฏิกิริยาทรานส์เอสเทอริฟิเคชันของน้ำมันปาล์มกับเมทานอลในระบบเบดนิ่งได้และให้ผลได้ของเมทิลเอสเทอร์ที่สูงถึง 54.3% โดยที่ตัวเร่งปฏิกิริยาไม่มีการเปลี่ยนรูปทรง

สาขาวิชา ปิโตรเคมีและวิทยาศาสตร์พอลิเมอร์ ลายมือชื่อนิสิต .....

ปีการศึกษา 2554 ลายมือชื่อ อ.ที่ปรึกษาวิทยานิพนธ์หลัก .....

# # 52727017 23: MAJOR PETROCHEMISTRY AND POLYMER SCIENCE
KEYWORDS: DOLOMITE/ CALCIUM OXIDE/ TRANSESTERIFICATION

THIKUMBHORN NAREE: HETEROGENEOUS BASE CATALYSTS FROM NATURAL DOLOMITE FOR TRANSESTERIFICATION OF VEGETABLE OIL. ADVISOR: ASST.PROF. CHAWALIT NGAMCHARUSSRIVICHAI, Ph.D., 104 pp.

The present thesis investigated preparation of heterogeneous base catalysts from natural dolomite for transesterification of plam oil with methanol. The catalysts were prepared by dissolution-precipitation method. Typically, the calcined dolomite was mixed with aluminium oxide as a binder, sodium aluminate and hydroxyethyl cellulose (HEC) as a plasticizer in a solution of nitric acid with pH of 1. The resulting catalyst paste was formulated as extrudates (5 mm) by using a manual extruder. The extrudates attained were finally calcined at 500-800 °C. Effects of the preparation conditions, including pH of nitric acid solution, amount of deionized water, amount of HEC, drying temperature, calcination temperature and addition of sodium aluminate on the physicochemical and the catalytic properties were investigated. The properties of the catalysts were studied by using X-ray fluorescence spectroscopy (XRF), X-ray diffraction (XRD), scanning electron microscopy (SEM), thermogravimetric/ differential thermal analysis (TG/DTA), $N_2$ adsorption-desorption measurement, temperature-programammed desorption of $CO_2$ ($CO_2$-TPD) and $CO_2$-pluse chemisorption analysis. The suitable conditions for the catalyst preparation are the mass ratio of dolomite/alumina/sodium aluminate = 70:20:10, the amount of HEC is 3 wt.% relative to the solid mass, the pH of nitric acid solution of 1, the amount of deionized water of 1.5 times of the total solid, the calcination temperature of 800 °C. The catalyst extrudates attained can catalyze the transesterification of palm oil with methanol in a fixed-bed reactor giving a high fatty acid methyl ester yield (54.3%) with retention of the extrudate shape.

Field of Study: Petrochemistry and Polymer Science Student's Signature .....

Academic Year: 2011 Advisor's Signature .....

# ACKNOWLEDGEMENTS

The author would like to express her sincere gratitude to his advisor, Asst. Prof. Dr. Chawalit Ngamcharussrivichai for his excellent supervision, inspiring guidance and encouragement throughout this research. The author also would like to acknowledge Prof. Dr. Pattarapan Prasassarakich, Assoc. Prof. Dr. Voravee P. Hoven and Dr. Anurak Winitsorn for serving as chairman and members of thesis committee, respectively.

The author wishes to express her thankfulness to all people in the associated institutions for their kind assistance and collaboration.

Many thanks are going to technicians of the Department of Chemical Technology, Chulalongkorn University.

The author also gratefully acknowledged the funding support from Center for Petroleum, Petrochemical and Advanced Materials (NCE-PPAM) and the PTT Public Company Limited.

Finally, the author wishes to express her deep gratitude to her family for their love, support, understanding and encouragement throughout graduate study.

# CONTENTS


| | Page |
|---|---|
| ABSTRACT (THAI)……..... | iv |
| ABSTRACT (ENGLISH)……..... | v |
| ACKNOWLEDGEMENTS..... | vi |
| CONTENTS..... | vii |
| LIST OF TABLES……..... | xi |
| LIST OF FIGURES ……..... | xiii |
| LIST OF ABBREVIATIONS……..……... | xviii |
| **CHAPTER I INTRODUCTION**……..... | 1 |
| 1.1 Statement of Problems……..... | 1 |
| 1.2 Objectives……..……... | 2 |
| 1.3 Scopes of Work ……...……....…….…….... …….... | 3 |
| **CHAPTER II THEORY AND LITERATURE REVIEWS**……..... | 5 |
| 2.1 Vegetable oils……..…….... | 5 |
| 2.1.1 Chemical composition of vegetable oils…… | 5 |
| 2.1.2 Fuel properties of vegetable oils…… | 8 |
| 2.1.3 Oil plants..... | 9 |
| 2.2 Biodiesel and Biodiesel production..... | 11 |
| 2.2.1 Biodiesel..... | 11 |
| 2.2.2 Biodisel production..... | 12 |
| 2.2.2.1 Direct use and blending..... | 12 |
| 2.2.2.2 Thermal cracking (pyrolysis)..... | 12 |
| 2.2.2.3 Transesterification (Alcoholysis)..... | 13 |
| 2.3 Biodiesel production technology..... | 14 |
| 2.3.1 Transesterification..... | 14 |
| 2.3.1.1 Batch processing..... | 15 |
| 2.3.1.2 Continuous process..... | 16 |
| 2.3.2 Esterification and transesterification..... | 17 |
| 2.3.3 Hydrolysis and esterification..... | 18 |

**Page**

2.4 Catalytic transesterification..... 20
2.4.1 Homogeneously acid-catalyzed transesterification..... 21
2.4.2 Homogeneously base-catalyzed transesterification..... 22
2.4.3 Heterogeneously acid-catalyzed transesterification..... 23
2.4.4 Heterogeneously base-catalyzed transesterification..... 24
2.4.5 Enzyme- catalyzed transesterification..... 24
2.5 Preparation of heterogeneous catalyst..... 25
2.5.1 Bulk catalysts and support preparation…….. 26
2.5.1.1 Precipitation……..... 26
2.5.1.2 Co-precipitation……..... 26
2.5.2 Supported catalysts preparation……. 26
2.5.2.1 Impregnation……. 26
2.5.2.2 Ion exchange……..... 27
2.5.2.3 Adsorption……..... 28
2.5.2.4 Dissolution- precipitation……. 28
2.6 Formulation of heterogeneous of heterogeneous catalysts…….. 28
2.6.1 Paste extrusion process…….. 29
2.6.2 Types of extruder……... 31
2.6.2.1 Rotary extruders…… 32
2.6.2.1 Ram extruders……... 32
2.6.2.3 Screw extruder…….. 33
2.6.2.4 Manual extruder……..... 34
2.7 Calcium oxide (CaO) as heterogeneous base catalyst……. 34
2.8 Dolomite……..... 36
2.8.1 Properties……... 36
2.8.2 Thermal decomposition of dolomite…….. 37
2.8.3 Sources of dolomite in Thailand……..... 37
2.8.4 Applications of dolomitge……..... 38
2.9 Literature review……..... 38
**CHAPTER III EXPERIMENTALS**..... 45
3.1 Chemicals..... 45

**Page**

3.1.1 Chemicals for synthesis of catalysts……..... 45
3.1.2 Chemicals for transesterification……..... 45
3.1.3 Chemical for reaction products analysis……..... 45
3.1.4 Chemical for quantitative analysis of monoglycerides, diglycerides and triglycerides in FAME yield..... 46
3.2 Instruments and Equipments..... 46
3.2.1 Instruments and equipments for catalyst preparation..... 46
3.2.2 Instrument and equipments for transesterification…..... 47
3.3 Instrument and Equipments for Characterization of catalyst..... 48
3.3.1 X-ray fluorescence spectrometer……..... 48
3.3.2 X-ray diffractometer……..... 49
3.3.3 Thermogravimetric/differential thermal analyzer…..... 50
3.3.4 Chemisorption analyzer……..... 51
3.3.5 Scanning electron microscope……..... 52
3.3.6 Surface area and porosity analyzer……..... 53
3.4 Reaction Products Analysis..... 54
3.5 Preparation of catalyst from natural dolomite by dissolution-precipitation method..... 56
3.6 Formulation of catalyst from natural dolomite by dissolution-precipitation method……..... 56
3.7 Transesterifition of RBD plam oil with methanol in a batch reactor….. 56
3.8 Transesterification of RBD plam oil with methanol in a fix- bed reactor..... 57
3.9 Quantitative analysis of monoglycerides, diglycerides and triglycerides on FAME yield…….. 58
**CHAPTER IV RESULTS AND DISCUSSIONS**……..... 59
4.1 Dolomite as a heterogeneous base catalyst for Transesterification of vegetable oil……. 59
4.1.1 Physical properties of dolomite..... 59
4.1.2 Transesterification of vegetable oil over natural dolomite calcined at different temperature……..... 61
4.2 Preparation of heterogeneous base catalysts from dolomite by dissolution-precipitation method..... 61
4.2.1 Effects of pH of nitric acid solution..... 61
4.2.2 Effect of adding binder ($Al_2O_3$)..... 63
4.2.3 Effects of adding plasticizer (HEC)…….... 66

**Page**

4.2.3.1 Effect of HEC grade..... 66
4.2.3.2 Effect of drying temperature……..... 68
4.2.3.3 Effect of calcinations temperature of catalysts extrudates... 69
4.2.3.4 Effect of water amount……..... 71
4.2.3.5 Effect of amount of HEC…….. 73
4.2.4 Effect of addition of sodium aluminate……. 78
4.3 Dependence of product distribution on reaction time in the transesterification of palm oil……..... 84
4.4 Mechanical testing of DM800+$Al_2O_3$+$NaAlO_2$+3%HEC catalyst extrudate..... 85
**CHAPTER V: CONCLUSIONS AND FUTURE DIRECTION**...……... 87
5.1 Conclusion..... 87
5.2 Recommendations..... 88
**REFERENCES**…… 89
**APPENDICES**…….. 96
**APPENDIX** A……..... 97
**APPENDIX** B……..... 98
**APPENDIX** C……..... 99
**APPENDIX** D……..... 100
**APPENDIX** E……..... 101
**VITAE**……..... 104

# LIST OF TABLES


| Table | | Page |
|---|---|---|
| 2.1 | Fatty acid composition of various vegetable oils…..... | 6 |
| 2.2 | Fuel properties of various vegetable oils……..... | 8 |
| 2.3 | Palm oil plantation and production in Thailand……..... | 10 |
| 2.4 | Comparison of homogeneously and heterogeneously catalyzed transesterification……..... | 21 |
| 2.5 | Processing stages……..... | 30 |
| 2.6 | Shapes of catalyst……..... | 31 |
| 3.1 | GC conditions for determination of FAME yield…..... | 55 |
| 4.1 | Elemental composition of natural dolomite analyzed by XRF spectroscopy ……..... | 59 |
| 4.2 | Effects of calcination temperature of natural dolomite on FAME yield attained from transesterification of palm oil with methanol in batch reactor..... | 61 |
| 4.3 | Effects of pH of nitric acid solution used in preparation of dolomite catalyst on FAME yield attained from transesterification of palm oil with methanol in batch reactor..... | 63 |
| 4.4 | Effects of adding $Al_2O_3$ and calcination temperature of DM800+$Al_2O_3$ catalyst on FAME yield attained from transesterification of palm oil and methanol in batch reactor..... | 65 |
| 4.5 | Effects of HEC grade used in the preparation of DM800+$Al_2O_3$+ 3%HEC extrudates on FAME yield attained from transesterification of palm oil and methanol in batch reactor..... | 67 |
| 4.6 | Effects of drying temperature of DM800+$Al_2O_3$+3%HEC on extrudates characteristics..... | 68 |
| 4.7 | Total basicity of DM800+$Al_2O_3$+3%HEC extrudates calcined at different temperatures..... | 70 |
| 4.8 | Effects of calcination temperature of DM800+$Al_2O_3$+3%HEC on extrudates characteristics and transesterification activity | 71 |

**Table** **Page**


| | | |
|---|---|---|
| 4.9 | Effects of water amount on extrudate characteristics..... | 72 |
| 4.10 | Effects of amount of HEC on textural properties of DM800+ $Al_2O_3$+HEC extrudates..... | 73 |
| 4.11 | Total number of basic sites of calcined DM800+$Al_2O_3$+$NaAlO_2$ extrudates determined by $CO_2$-pulse chemisorption..... | 82 |
| 4.12 | Dependence of product distribution on reaction time in transesterification[b] of palm oil with methanol over DM800+ $Al_2O_3$+$NaAlO_2$(70:10:20)+3%HEC extrudates in a fixed-bed reactor..... | 85 |
| 4.13 | Crushing strength of DM800+$Al_2O_3$+$NaAlO_2$(70:10:20)+3% HEC catalyst extrudates..... | 86 |

# LIST OF FIGURES


| Figure | | Page |
|---|---|---|
| 2.1 | Representative chemical structures of monoglyceride and diglyceride ……..... | 5 |
| 2.2 | Palm bunches (A) and palm fruits (B)…… | 11 |
| 2.3 | Mechanism of thermal decomposition of triglycerides…….. | 13 |
| 2.4 | Three-consecutive transesterification for methyl esters synthesis from triglyceride……..... | 14 |
| 2.5 | Diagram of batch processing for biodiesel production……... | 16 |
| 2.6 | Diagram of continuous processing for biodiesel production in plug flow reactor..... | 16 |
| 2.7 | Diagram of processing for eliminating free fatty acid in oil…….. | 17 |
| 2.8 | Hydrolysis of high free fatty acid oil in counter-current continuous flow reactor..... | 18 |
| 2.9 | Esterfip-H process developed by the French Institute of Petroleum (IFP) development……..... | 20 |
| 2.10 | Mechanism of the transesterification of vegetable oils catalyzed by acid……..... | 22 |
| 2.11 | Mechanism of the transesterification of vegetable oils catalyzed by base……..... | 23 |
| 2.12 | Left: Schematic plan view of the Roll-Caster. Two parallel rollers counter-rotate at a fixed separation controlled by a micrometer. Right: Cross-sectional view……..... | 32 |
| 2.13 | Ram extruder……..... | 33 |
| 2.14 | A single screw extruder with barrier-screw with shearing and mixing parts……..... | 33 |
| 2.15 | Manual extruder……..... | 34 |

**Figure** **Page**


| | | |
|---|---|---|
| 3.1 | Manual extruder used for formulation of catalyst……..... | 47 |
| 3.2 | Schematic of the XRF principle……..... | 48 |
| 3.3 | Diffraction of X-ray by a crystal……..... | 49 |
| 3.4 | Thermogravimetric/differential thermal analyzer……..... | 50 |
| 3.5 | Chemisorption analyzer……..... | 51 |
| 3.6 | Schematic diagram of scanning electron microscope..... | 53 |
| 3.7 | Surface area and porosity analyzer……..... | 54 |
| 3.8 | Gas chromatograph……..... | 55 |
| 3.9 | Experimental setup for transesterification of vegetable oil under fixed bed conditions……..... | 58 |
| 4.1 | XRD patterns of non-calcined dolomite (a), dolomite calcined at 600 °C (b), and 800°C (c)……..... | 60 |
| 4.2 | Weight loss and DTG curves of natural dolomite……..... | 60 |
| 4.3 | XRD patterns of DM800 merged in nitric acid solution with pH of 1 (a), 2 (b) and 3 (c). The samples were dried at 100 °C prior to the analysis. ..... | 62 |
| 4.4 | XRD patterns of DM800 merged in nitric acid solution with pH of 1 (a), 2 (b) and 3 (c), followed by calcination at 800 °C for 2 h. ..... | 62 |
| 4.5 | XRD patterns of non-calcined DM800+$Al_2O_3$ (a), and DM800 +$Al_2O_3$ calcined at 500 °C (b), 600 °C (c), 700 °C (d) and 800 °C (e)..... | 64 |
| 4.6 | Weight loss and DTG curves of as-synthesized DM800+$Al_2O_3$ catalyst..... | 64 |
| 4.7 | Pastes of DM800+$Al_2O_3$+3%HEC catalyst containing different HEC; (a) Fluka, (b) Thai Specialty Chemical and (c) A.H.A International..... | 66 |

**Figure** **Page**


4.8 Extrusion of DM800+$Al_2O_3$+3%HEC catalyst containing different HEC; (a) Fluka, (b) Thai Specialty Chemical and (c) A.H.A International..... 67

4.9 Images of DM800+$Al_2O_3$+3%HEC extrudates dried at room temperature (a)**,** 100°C (b) and 130°C (c), followed by the calcination at 800°C..... 69

4.10 XRD patterns of non-calcined DM800+$Al_2O_3$+3%HEC catalyst (a), and DM800+$Al_2O_3$+3%HEC calcined at 500 °C (b), 600 °C (c), 700 °C (d) and 800 °C (e)..... 69

4.11 Effect of water content on surface fracture of extrudates; (a) 1 and (b) 1.5 times..... 72

4.12 Effect of water amount on FAME yield attained from transesterification of palm oil with methanol over DM800+$Al_2O_3$+4%HECextrudates in a fixed-bed reactor..... 73

4.13 $N_2$ adsorption-desorption isotherms of DM800+$Al_2O_3$+HEC extrudates prepared with different amounts of HEC; 0% HEC (a), 1%HEC (b), 3%HEC (c) and 4%HEC (d). The extrudates were calcined at 800 °C before the measurement..... 74

4.14 BJH plots of DM800+$Al_2O_3$+HEC extrudates prepared with different amounts of HEC; 0% HEC (a), 1%HEC (b), 3%HEC (c) and 4%HEC (d). The extrudates were calcined at 800 °C before the measurement..... 75

4.15 SEM images of cross-sectional area of non-calcined DM800+$Al_2O_3$ +HEC extrudates prepared with different amounts of HEC; 0% HEC (a), 1% HEC (b), 3%HEC (c) and 4%HEC (d)..... 76

**Figure** **Page**


4.16 SEM images of side area of calcined DM800+$Al_2O_3$+HEC extrudates prepared with different amount of HEC; 0% HEC (a), 1% HEC (b), 3%HEC (c) and 4%HEC (d)..... 77

4.17 Effect of HEC amount on FAME yield attained from transesterification of palm oil with methanol over DM800+ $Al_2O_3$+HEC in a fixed-bed reactor..... 78

4.18 XRD patterns of non-calcined DM800+$Al_2O_3$+$NaAlO_2$ catalysts: DM800+$Al_2O_3$+$NaAlO_2$(70:10:20) (a), DM800+$Al_2O_3$+$NaAlO_2$ (70:10:20)+3%HEC (b) and DM800+$Al_2O_3$+$NaAlO_2$(70:20:10) +3%HEC (c)..... 79

4.19 XRD patterns of calcined DM800+$Al_2O_3$+$NaAlO_2$ catalysts: DM800+$Al_2O_3$+$NaAlO_2$(70:10:20) (a), DM800+$Al_2O_3$+$NaAlO_2$ (70:10:20)+3%HEC (b) and DM800+$Al_2O_3$+$NaAlO_2$(70:20:10) +3%HEC (c)..... 79

4.20 Weight loss and DTG curves of DM800+$Al_2O_3$+$NaAlO_2$ (70:10:20)+3%HEC..... 80

4.21 SEM images of side area of calcined DM800+$Al_2O_3$+3%HEC catalyst extrudates prepared with and without $NaAlO_2$ addition; DM800+$Al_2O_3$+3%HEC (a) and DM800+$Al_2O_3$+$NaAlO_2$ (70:10: 20)+3%HEC (b)..... 81

4.22 $CO_2$-TPD profiles of calcined DM800+$Al_2O_3$+$NaAlO_2$(70:10: 20) (a), DM800+$Al_2O_3$+$NaAlO_2$(70:10:20)+3%HEC (b) and DM 800+$Al_2O_3$+$NaAlO_2$ (70:20:10)+3%HEC (c)..... 82

4.23 FAME yield attained from transesterification of palm oil with methanol over DM800+$Al_2O_3$+3%HEC catalyst extrudates prepared with and without $NaAlO_2$ addition in a fixed-bed reactor..... 83

**Figure** **Page**


| | | |
|---|---|---|
| 4.24 | FAME yield attained from transesterification of palm oil with methanol over DM800+$Al_2O_3$+$NaAlO_2$ extrudates in a fixed-bed reactor. The catalyst bed height was reduced to 15 cm..... | 84 |
| D-1 | The chromatograms of methyl ester content..... | 100 |
| E-1 | Standard curve of monopalmitin..... | 101 |
| E-2 | Standard curve of dipalmitin..... | 101 |
| E-3 | Standard curve of tripalmitin..... | 102 |
| E-4 | Standard curve of monoolein..... | 102 |
| E-5 | Standard curve of diolein..... | 103 |
| E-6 | Standard curve of triolein..... | 103 |

# LIST OF ABBREVIATIONS

| | |
|---|---|
| BET | Brunauer-Emmett-Teller |
| BJH | Barret, Joyner, and Halenda |
| $^{o}$C | Degree Celsius |
| g | Gram (s) |
| h | Hour (s) |
| cm | Centimeter |
| μm | Micrometer (s) |
| mL | Milliliter (s) |
| min | Minute (s) |
| M | Molarity |
| nm | Nanometer (s) |
| % | Percentage |
| SEM | Scanning Electron Microscopy |
| XRD | X-ray diffraction |
| XRF | X-ray fluorescence spectroscopy |
| TGA | Thermogravimetric analysis |
| LHSV | Liquid Hourly Space Velocity |

# CHAPTER I
# INTRODUCTION

## 1.1 Statement of Problems

Biodiesel is an alternative fuel for diesel engines, which is produced from triglycerides, as the major components in vegetable oils and animal fats. Transesterification of triglycerides with small alcohols, so-called alcoholysis, in the presence of a catalyst is an effective route for producing biodiesel [1]. Sodium and potassium hydroxides are base catalysts commonly used in industrial scale. However, these processes generate a lot of alkali wastewater discharged from the product purification step, and the catalysts are not reusable. To avoid these disadvantages, many groups have extensively researched and focused on replacement of the homogenous catalysts for heterogeneous ones [2]. The heterogeneous catalysts are easily seperated from the biodiesel product, resulting in a reduction of wastewater and a possibility to reuse the catalysts. Calcium oxide (CaO) is one of the most active heterogeneous catalysts, which has been widely investigated in the transesterification [3,4], as its high basicity, low solubility in methanol and low cost. CaO can be achieved from a thermal decomposition of calcium carbonate ($CaCO_3$) at high temperatures (Eq. (1)) [5].

$$CaCO_3 \xrightarrow[\Delta]{898\ ^\circ C} CaO + CO_2 \qquad (1)$$

$CaCO_3$ sources are cheap since they are found in several areas of Thailand in forms of natural rocks, e.g. limestone and dolostone, and animal organs, such as shell and cuttlebone.

A direct use of CaO in powdery form in a fixed-bed reactor is not permitted due to the problems relating to reactor blockage and pressure drop [6]. Therefore, the catalyst has to be shaped in forms of pellet, sphere, ring or extrudate with a certain particle size. Extrusion is a simple but effective method for shaping the catalyst to which a binder must be compounded with the catalyst for improving strength of the resulting extrudates [7]. Alumina, silica and clay are mostly common binders used in the process. However, the co-existence of the binders results in lower catalytic

activity due to a decrease in specific surface area, pore volume and number of active sites [8]. In this research, the dissolution-precipitation method was selected as the process for simultaneous preparation of catalytic material and paste for the extrusion. This process uses an acid solution to partially dissolve metal compounds from a calcium source. The slurry of calcium source was then mixed with a binder to allow precipitation of soluble ions and formation of specific phase (if any) through an adjustment of the mixture pH. After calcination, CaO is believed to be the main active sites, whereas other phases work as pasticizers or solid lubricants besides the enhancement of mechanical strength. Comparing to conventional mixing of calcium source with binder, this method would bring about a relatively small loss of active sites due to binder blockage. Good extrudates can be formulated by regulating composition of ingredients, including calcium source, binder, and water, and thermally treating the extrudates under appropriate conditions. Besides, adding hydroxylethyl cellulose (HEC) as a plasticizer in the ingredients would improve porosity of the catalyst extrudates, and promote diffusion of reactants into the active sites.

In the present study, we emphasized on the formulation of heterogeneous base catalysts as extrudates via the dissolution-precipitation method. Natural dolomite, a mixed carbonate of calcium and magnesium ($CaMg(CO_3)_2$), was used as a calcium source. The suitable conditions for the catalyst preparation and the effects of HEC addition on the catalyst properties were investigated. Characterization of the catalysts was carried out by various techniques, i.e. XRD, XRF, SEM, TG/DTA, chemisorption analysis and $N_2$ adsorption-desorption measurement. The extrudates prepared were tested their catalytic performance in the transesterification of palm oil with methanol in both batch and fix-bed reactor at 65 °C.

### 1.2 Objectives

1. To prepare and characterize heterogeneous base catalysts derived from natural dolomite.

2. To study transesterification of vegetable oil with methanol over the heterogeneous base catalysts prepared from natural dolomite in batch and fix-bed reactor.

### 1.3 Scopes of work

1. Literature survey
2. Preparation of heterogeneous base catalysts from natural dolomite by dissolution-precipitation method. The preparation procedure is divided into 2 parts. The first one is the preparation of powdery catalysts and the second part is the formulation of the catalysts into an extrudate form. The parameters studied in both parts include:

   2.1 Preparation of heterogeneous base catalysts in powdery form
   - Calcination temperature of natural dolomite: 600-800 °C
   - pH of nitric acid solution : 1-3

   2.2 Formulation of heterogeneous base catalysts into extrudates
   - Amount of hydroxyethyl cellulose: 0-5 wt.% of total solid
   - Amount of deionized water : 1-2 times of total solid
   - Drying temperature: 80-150 °C
   - Calcination temperature of the extrudates: 300-900 °C
   - Effects of addition of sodium aluminate
3. Characterization of the catalysts prepared by following techniques:
   - X-ray fluorescence spectrometry (XRF)
   - X-ray diffraction (XRD)
   - Scanning electron microscopy (SEM)
   - Thermogravimetric and differential thermal analysis (TG/DTA)
   - Temperature-programmed desorption of $CO_2$ ($CO_2$-TPD)
   - $CO_2$-pluse chemisorption
   - $N_2$ adsorption-desorption measurement
4. Testing the catalyst extrudates for mechanical properties
   - Crush strength: ASTM D-4179-82

5. Evaluation of the catalysts activity in the transesterification of vegetable oil with methanol in batch and fix-bed reactors at 65 °C.
6. Characterization of the reaction products by using a gas chromatography technique.
7. Summarize the results and write thesis.

# CHAPTER II
# THEORY AND LITERATURE REVIEWS

## 2.1 Vegetable oils

### 2.1.1 Chemical composition of vegetable oils

Vegetable oils are naturally composed of triglycerides from 90 to 98% and small amounts of monoglycerides and diglycerides. To synthesize a triglyceride, an important reaction is esterification (Eq.(2.1)) that three moles of fatty acids react to one mole of glycerol.

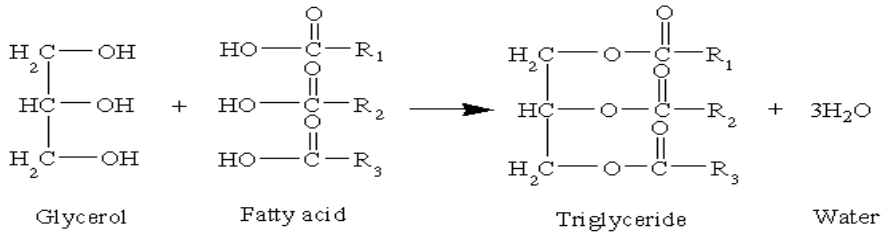


(2.1)

When all of three fatty acids are the same, the product is a simple triglyceride, whereas using different fatty acids gives mixed triglycerides [9]. The terms of monoglyceride or diglyceride refer to the numbers of fatty acids that are attached to the glycerol backbone. Monoglyceride has two hydroxyl groups and one fatty acid molecule attached to the glycerol backbone, while diglyceride has one hydroxyl group and two fatty acid molecules attached to the glycerol backbone as shown in Figure 2.1.

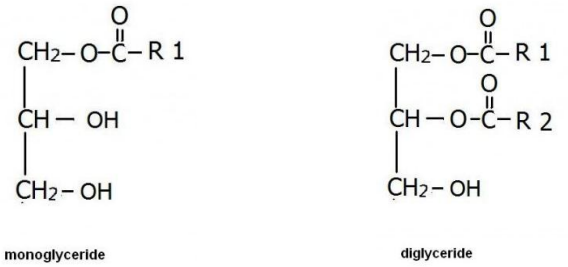


**Figure 2.1** Representative chemical structures of monoglyceride and diglyceride.

To describe precisely the structure of a fatty acid molecule, one must give the length of hydrocarbon chain (number of carbon) and the number of double bonds. For example, C18:1 (oleic acid) represents the fatty acid with 18 carbon atoms and 1 double bond. Most fatty acids in vegetable oils are straight-chain compounds with the most frequently an even number, and their chain-lengths range is from 12 to 19 of carbon atoms. Among the straight-chain fatty acids, the simplest are referred to as saturated fatty acids. They have no unsaturated linkages and cannot be altered by hydrogenation or halogenation. When double bonds are present, the fatty acids are said unsaturated. Table 2.1 shows fatty acid composition found in different vegetable oils.

**Table 2.1** Fatty acid composition of various vegetable oils [10-12]

| Vegetable oil | Composition (wt. %) | | | | | | | | |
|---|---|---|---|---|---|---|---|---|---|
| | 12:0 | 14:0 | 16:0 | 16:1 | 18:0 | 18:1 | 18:2 | 18:3 | Other |
| Peanut kernel | 0 | 0 | 11.4 | 0 | 2.4 | 48.3 | 32.0 | 0.9 | 4 |
| Poppy seed | 0 | 0 | 12.6 | 0.1 | 4.0 | 22.3 | 60.2 | 0.5 | 0 |
| Rapeseed | 0 | 0 | 3.5 | 0 | 0.9 | 64.1 | 22.3 | 8.2 | 0 |
| Safflower seed | 0 | 0 | 7.3 | 0 | 1.9 | 13.6 | 77.2 | 0 | 0 |
| Seasameseed | 0 | 0 | 13.1 | 0 | 3.9 | 52.8 | 30.2 | 0 | 0 |
| Soybean | 0 | 0 | 13.9 | 0.3 | 2.1 | 23.3 | 56.2 | 4.3 | 0 |
| Sunflowerseed | 0 | 0 | 6.4 | 0.1 | 2.9 | 17.7 | 72.9 | 0 | 0 |
| Walnut kernel | 0 | 0 | 7.2 | 0.2 | 1.9 | 18.5 | 56 | 16.2 | 0 |
| Wheat grain | 0 | 0.4 | 20.6 | 1.0 | 1.1 | 16.6 | 56 | 2.6 | 1.7 |

**Table 2.1** Fatty acid composition of various vegetable oils [10-12] (continued)

| Vegetable oil | Composition (wt. %) | | | | | | | | |
|---|---|---|---|---|---|---|---|---|---|
| | 12:0 | 14:0 | 16:0 | 16:1 | 18:0 | 18:1 | 18:2 | 18:3 | Other |
| Almond kernel | 0 | 0 | 6.5 | 0.5 | 1.4 | 70.7 | 20.0 | 0 | 0.9 |
| Bay laurel leaf | 26.5 | 4.5 | 25.9 | 0.3 | 3.1 | 10.8 | 11.3 | 17.6 | 0 |
| Canola | 0 | 0 | 4 | 0 | 2 | 61 | 22 | 10 | 1 |
| Castor[a] | 0 | 0 | 1.1 | 0 | 3.1 | 4.9 | 1.3 | 0 | 89.6 |
| Coconut | 0 | 0 | 9.7 | 0.1 | 3 | 6.9 | 2.2 | 0 | 65.7 |
| Corn | 0 | 0 | 6.5 | 0.6 | 1.4 | 65.6 | 25.2 | 0.1 | 0.6 |
| Corn marrow | 0 | 0 | 11.8 | 0 | 2 | 24.8 | 61.3 | 0 | 0.3 |
| Cottonseed | 0 | 0 | 28.7 | 0 | 0.9 | 13 | 57.4 | 0 | 0 |
| Linseed | 0 | 0 | 5.1 | 0.3 | 2.5 | 18.9 | 18.1 | 55.1 | 0 |
| Grape | 0 | 0.1 | 6.9 | 0.1 | 4 | 19 | 69.1 | 0.3 | 0.5 |
| Olive | 0 | 0 | 11.6 | 1 | 3.1 | 75.0 | 7.8 | 0.6 | 0.9 |
| Olive kernel | 0 | 0 | 5 | 0.3 | 1.6 | 74.7 | 17.6 | 0 | 0.8 |
| Palm | 0 | 0 | 42.6 | 0.3 | 4.4 | 40.5 | 10.1 | 0.2 | 1.1 |
| Peanut | 0 | 0.1 | 8 | 0 | 1.8 | 53.3 | 28.4 | 0.3 | 8.1 |

[a] *Castor oil contains 89.6% ricinoloic acid.*

### 2.1.2 Fuel properties of vegetable oils

Table 2.2 shows fuel properties of vegetable oils. The kinematic viscosity of vegetable oils varies in the range of 30-40 $mm^2 s^{-1}$ which is higher than that of diesel fuel. The high viscosity is resulted from their high molecular weight and chemical structure. The cetane number is in the range of 33-50. Vegetable oils have high flash point (above 200 °C). The heating value of vegetable oils (39-40 MJ $kg^{-1}$) is slightly lower than that of diesel fuel (50 MJ $kg^{-1}$). The presence of chemically bound oxygens in the triglyceride lowers the heating value of vegetable oils.

**Table 2.2** Fuel properties of various vegetable oils [12-13]

| Vegetable oil | Kinematic viscosity at 38 °C ($mm^2 s^{-1}$) | Cetane no. | Heating value (MJ $kg^{-1}$) | Cloud point (°C) | Pour point (°C) | Flash point (°C) | Density (kg $L^{-1}$) |
|---|---|---|---|---|---|---|---|
| Palm | 39.6 | 42.0 | - | 31.0 | - | 267 | 0.9180 |
| Peanut | 39.6 | 41.8 | 39.8 | 12.8 | -6.7 | 271 | 0.9236 |
| Rapeseed | 37.0 | 37.6 | 39.7 | -3.9 | -31.7 | 246 | 0.9115 |
| Safflower | 31.3 | 41.3 | 39.5 | 18.3 | -6.7 | 260 | 0.9144 |
| Wheat grain | 32.6 | 35.2 | 39.3 | - | - | - | - |
| Olive kernel | 29.4 | 49.3 | 39.7 | - | - | - | - |
| Almond kernel | 34.2 | 34.5 | 39.8 | - | - | - | - |

**Table 2.2** Fuel properties of various vegetable oils [12-13] (continued)

| Vegetable oil | Kinematic viscosity at 38 °C ($mm^2 s^{-1}$) | Cetane no. | Heating value ($MJ kg^{-1}$) | Cloud point (°C) | Pour point (°C) | Flash point (°C) | Density ($kg L^{-1}$) |
|---|---|---|---|---|---|---|---|
| Bay laurel leaf | 23.2 | 33.6 | 39.3 | - | - | - | - |
| Babassu | 30.3 | 38.0 | - | 20.0 | - | 150 | 0.9460 |
| Castor | 29.7 | 42.3 | 37.4 | - | - | - | - |
| Corn | 34.9 | 37.6 | 39.5 | -1.1 | -40.0 | 277 | 0.9095 |
| Cottonseed | 33.5 | 41.8 | 39.5 | 1.7 | -15.0 | 234 | 0.9148 |
| Crambe | 53.6 | 44.6 | 40.5 | 10.0 | -12.2 | 274 | 0.9048 |
| Linseed | 27.2 | 34.6 | 39.3 | 1.7 | -15.0 | 241 | 0.9236 |

### 2.1.3 Oil plants

Since raw material is the major factor affecting selling cost of biodiesel product, the suitable vegetable oil used as raw material for biodiesel production in each country depends on the availability and cost. Soybean oil is commonly used in the United States and China, while rapeseed oil is more abundant in the European countries. The Philippines, Malaysia, Indonesia and several other tropical island

countries are using coconut oil and palm oil as the major triglyceride sources. Currently, the potential raw material for biodiesel production in Thailand is palm oil due to its high crop yield, and the rapid expansion of the area for oil palm cultivation in Thailand.

#### 2.1.3.1 Palm oil

Palm oil is a potential raw material for biodiesel production. Palm tree is mainly growing in the South of Thailand. The major area for palm plantation are in five provinces; Krabi, Surat Thani, Chumphon, Trang and Satun. Table 2.3 shows the plantation area of palm oil, mature area of palm oil and fresh fruit bunch production between 2006 and 2011. The plantation area has steadily increased from 2.9 million rai in 2006 to 4.2 million in 2011 due to the policy of the Thai Government. In term of the fresh fruit bunch production, it increased from 6.7 million tons in 2006 to 9.1 tons in 2011.

**Table 2.3** Palm oil plantation and production in Thailand, year 2006-2011[14]

| Year | Plantation area (rai) | Mature area (rai) | FFB Production (Ton FFB) |
|---|---|---|---|
| 2006 | 2,953,924 | 2,374,202 | 6,715,036 |
| 2007 | 3,200,276 | 2,663,252 | 6,389,983 |
| 2008 | 3,676,096 | 2,884,720 | 9,270,510 |
| 2009 | 3,888,403 | 3,187,000 | 8,162,379 |
| 2010 | 4,077,000 | 3,553,000 | 8,223,000 |
| 2011 1/ | 4,285,000 | 3,754,740 1/ | 9,119,720 1/ |

Remark: 1/ is an estimation value of year 2011.

FFB = fresh fruit bunch

Palm oil is derived from the *Elaeis guineensis* palm tree that has long been recognized in West African countries. The palm fruit is oval shaped, about 3-cm long, and looks like a small red plum as shown in Figure 2.2a. The outer fleshy mesocarp gives the viscous orange palm oil while the kernel, which is inside a hard shell, gives

the clear white palm kernel oil (Figure 2.2b). Both oils from the same fruit have different fatty acid composition.

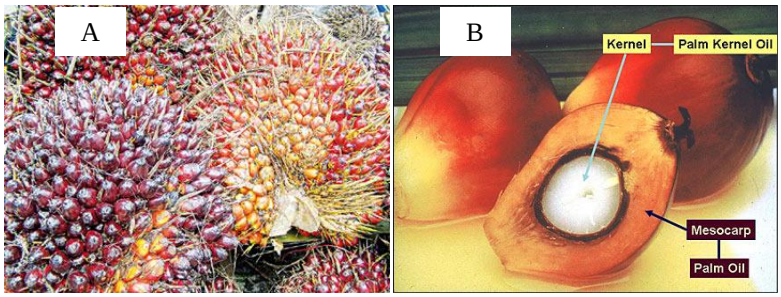


**Figure 2.2** Palm bunches (A) and palm fruits (B).

The main acid components containing in the palm oil are palmitic acid (C16:0) and oleic acid (C18:1). Others found with significant amount are linoleic acid (C18:2), stearic acid (C18:0) and myristic acid (C14:0).

## 2.2 Biodiesel and Biodiesel production

### 2.2.1 Biodiesel

Biodiesel is an alternative diesel fuel, which is made from renewable biological sources such as vegetable oils and animal fats. It can be used in any diesel engines without modifications. By using biodiesel, the engines run better and last longer. Biodiesel is good for the environment since it is biodegradable and nontoxic, and exhibits low emission profiles.

Biodiesel is a much cleaner fuel than conventional fossil-fuel petroleum diesel [15]

- Biodiesel burns up to 75% cleaner than petroleum diesel fuel.
- Biodiesel reduces unburned hydrocarbons, carbon monoxide and particulate matter in exhaust fumes. (US Environmental Protection Agency)
- Sulphur dioxide emissions are eliminated (biodiesel contains no sulphur).
- The ozone-forming (smog) potential of biodiesel emissions is nearly 50% less than petro-diesel emissions.
- Biodiesel exhaust is not offensive and doesn't cause eye irritation.
- Biodiesel is environmentally friendly which it is renewable and more biodegradable than sugar and less toxic than table salt.

- Biodiesel is a much better lubricant than petro-diesel and extends engine life.
- Biodiesel can be mixed with petro-diesel in any proportion, with no need for a mixing additive.
- Biodiesel has a higher cetane number than petroleum diesel because of its oxygen content. The higher the cetane number; the more efficient the fuel; the engine starts more easily, runs better and burns cleaner.

### 2.2.2 Biodiesel production [16]

There are three primary ways to make biodiesel, direct use and blending, thermal cracking (pyrolysis), and transesterification. The most commonly used method is the transesterification of vegetable oils and animal fats with small alcohols. The description of each production way is provided below.

#### 2.2.2.1 Direct use and blending

In 1980, Bartholomew has initiated the idea of using vegetable oil as a fuel. At that point, using 100% vegetable oil was not practical due to high viscosity, low cetane, and low flash point at low temperature. However, a mixture of 20% vegetable oil and 80% diesel fuel can replace diesel fuels without any adjustment of the engine. Direct use of vegetable oils and/or the use of blended oils have generally been considered to be not satisfactory and impractical for both direct and indirect diesel engines. The high viscosity, free fatty acid content, as well as gum formation due to oxidation and polymerization during storage and combustion, carbon deposit and lubricating oil thickening are obvious problems.

#### 2.2.2.2Thermal cracking (pyrolysis)

Pyrolysis is the conversion of one substance into another by means of heat. It involves heating in the absence of air or oxygen and cleavage of chemical bonds to yield small molecules. The pyrolyzed material can be vegetable oils, animal fats, natural fatty acids and methyl esters of fatty acids. The first pyrolysis of vegetable oil was conducted in an attempt to synthesize petroleum from vegetable oil. Since World War I, many investigators have studied the pyrolysis of vegetable oils to obtain products suitable for fuel. In 1947, Chang and Wan reported a large scale of thermal

cracking of tung oil calcium soaps. Tung oil was first saponified with lime and then thermally cracked to yield a crude oil, which was refined to produce diesel fuel and small amounts of gasoline and kerosene. The mechanism for the thermal decomposition of a triglyceride is given in Figure 2.3.

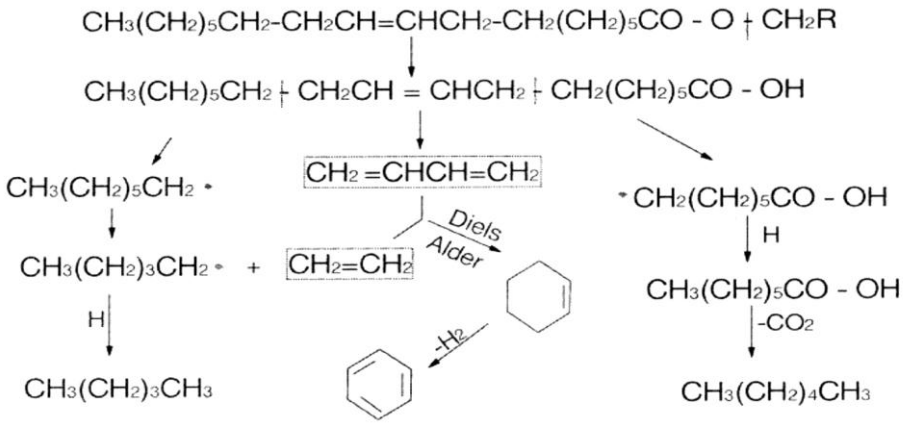


**Figure 2.3** Mechanism of thermal decomposition of triglycerides [16].

### 2.2.2.3 Transesterification (Alcoholysis)

Transesterification or alcoholysis is the reaction of vegetable oils or animal fats with small alcohols to form monoesters and glycerol as the main products and by-product, respectively. A catalyst is usually used to improve the reaction rate and the yield of the esters. The reaction is reversible, and an excess alcohol is needed to shift the equilibrium to the product side.

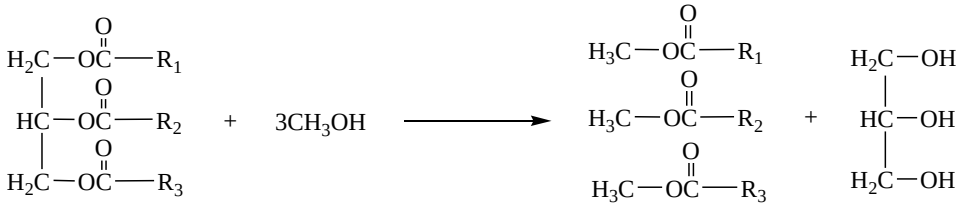


Triglyceride Methanol Methyl esters Glycerol (2.2)

Basically, the transesterification of triglyceride with methanol consists of a number of consecutive and reversible reactions as shown in (Eq.(2.2)). The first step is the conversion of the triglyceride to a diglyceride (Figure. 2.4a), followed by the successive conversion of the diglyceride to a monoglyceride (Figure. 2.4b), and

glycerol (Figure. 2.4c). In each step, a methyl ester is generated and thus three ester molecules are produced from one molecule of triglyceride. The conversion of the monoglyceride to methyl ester and glycerol is believed to be the rate determining step because monoglycerides are the most stable intermediates [17].

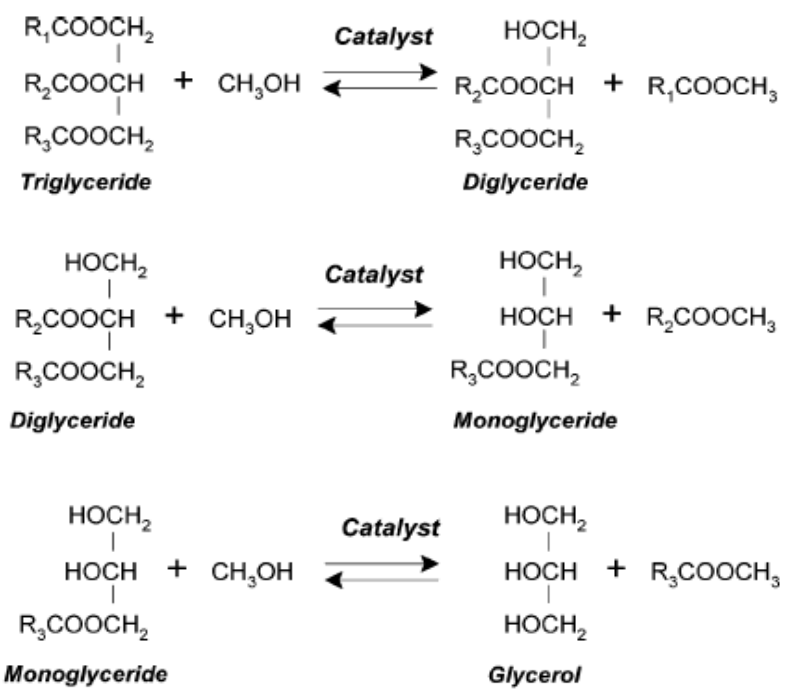


**Figure 2.4** Three-consecutive transesterification for methyl esters synthesis from triglyceride [17].

## 2.3 Biodiesel production technology [18-19]

### 2.3.1 Transesterification

As previously explained about the transesterification, the reaction can be catalyzed by alkaline, acid, or enzyme. Commonly, the alkaline used is NaOH and KOH due to their strong basicity. Sulfuric acid, sulfonic acid and hydrochloric acid are typical acid catalysts. Lipases also can be used as biocatalysts. The alkali-catalyzed transesterification is much faster than the acid-catalyzed one and is most often used commercially. In the alkali-catalyzed transesterification, triglycerides and alcohol must be substantially anhydrous (Wright et al., 1944) because the presence of

water makes the reaction partially change to saponification, which produces soap (Eq.(2.3)). The formation of soap lowers the yield of esters and renders the separation of esters and glycerol and the water washing difficult.

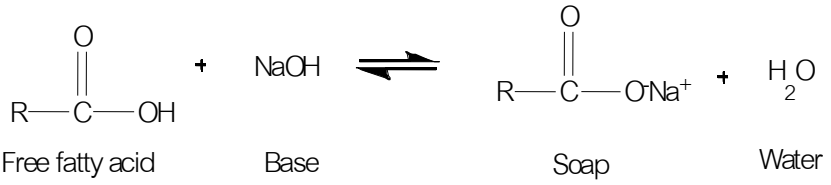


(2.3)

The choice of oils or fats being used for producing biodiesel is an important aspect of decision-making process. The process was exemplified as illustrated following.

#### 2.3.1.1 Batch processing

The simplest method for producing biodiesel is to use a batch, stirred tank reactor. The reactor may be equipped with a reflux condenser by operating temperature is usually about 65 °C. Alcohol-to-triglyceride ratios from 4:1 to 20:1 (mole:mole) have been reported, with the most common ratio of 6:1 . The most commonly used catalyst is sodium hydroxide, though potassium hydroxide also used. The typical catalyst loading is in the range from 0.3% to about 1.5%.

Figure 2.5 shows schematic diagram of biodiesel production with batch processing. In the transesterification, oil is firstly introduced into the system, followed by addition of solution of catalyst and methanol. The reaction mixture is stirred during the reaction progress, and then the stirring is decreased to give an initial separation of methyl esters and glycerol. Subsequently, the reaction mixture is pumped into a setting vessel or is put into a centrifuge in order to completely remove glycerol from the methyl esters. The alcohol remaining in both the methyl esters and glycerol phases is eliminated by using an evaporator or a flash unit. The esters phase is then neutralized, washed gently with deionized water, and dried. The purified biodiesel is finally transferred to storage, and crude glycerol is sent to a refining unit to increase concentration of glycerol.

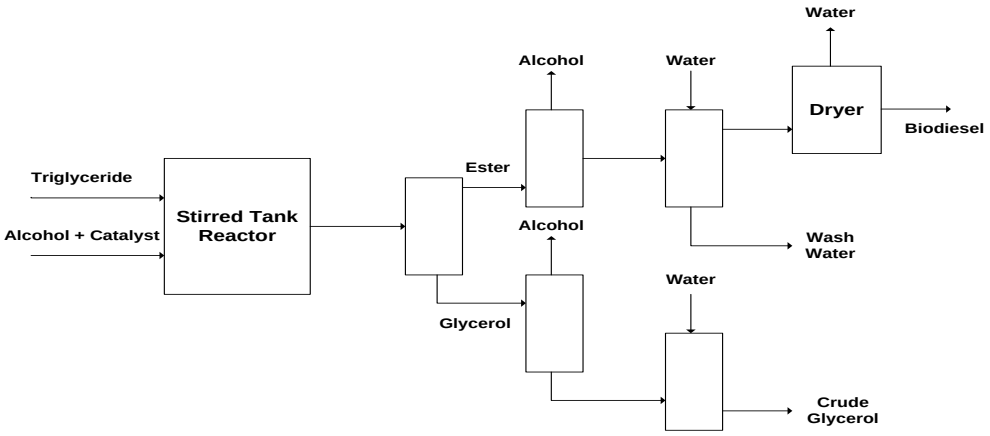


**Figure 2.5** Diagram of batch processing for biodiesel production [18].

### 2.3.1.2 Continuous process

The reaction mixture moves through reactor in a continuous plug with little mixing in the axial direction. A continuous system requires rather short residence times, as low as 6 to 10 min, for near completion of the reaction. In general, the separators of methanol and glycerol are placed to the reactor (Figure 2.6). The increase reaction rates have to operate at high temperature and pressure.

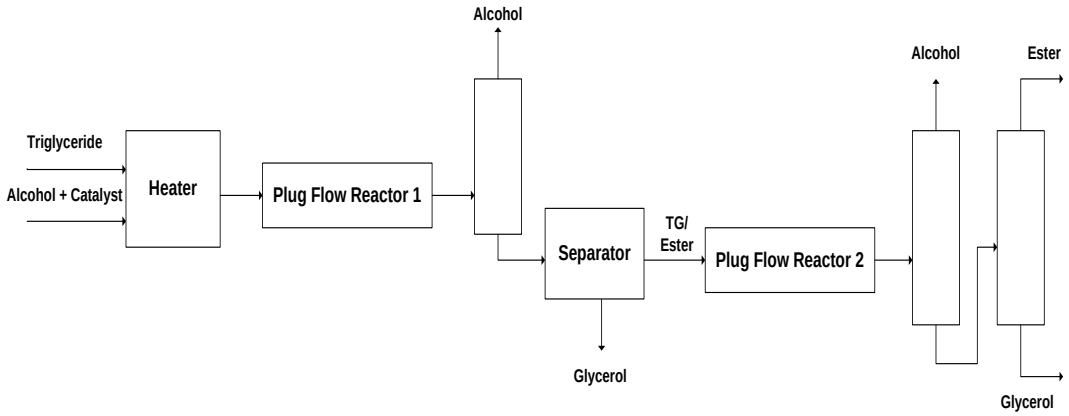


**Figure 2.6** Diagram of continuous processing for biodiesel production in plug flow reactor [18].

### 2.3.2 Esterification and transesterification

As a disadvantage, the transesterification over base catalysts is necessary to controlled free fatty acid content of triglycerides to prevent the formation of soap. If triglycerides with high content of water and free fatty acids are used, the reaction needs acid catalysts in which the carboxylic acids are converted to the methyl esters upon heating with alcohols (Eq.(2.4)).

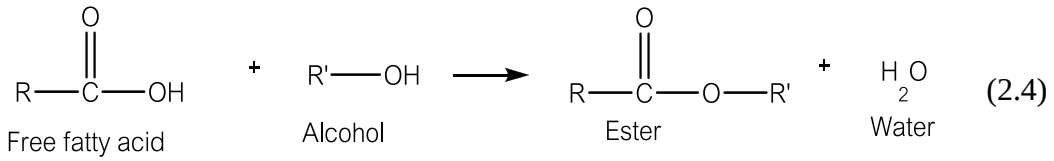


(2.4)

In general, high ratios of alcohol to free fatty acid and large amount of acid catalyst are required to complete the reaction in 10 minutes to 2 hours. The water generated as the by-product can combine with the catalyst at the bottom of reactor, lowering the yield of methyl esters. Therefore, evaporation must be used to separate the water from the reaction mixture after which the triglycerides remaining and the methyl esters produced are neutralized with base. In the last step, the triglycerides and the methyl esters are dried and moved to the transesterification reactor at which the base catalysts are used.

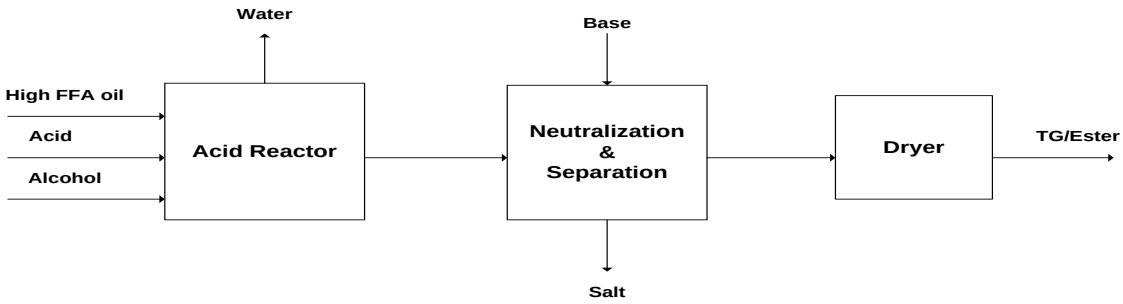


**Figure 2.7** Diagram of processing for eliminating free fatty acid in oil [18].

### 2.3.3 Hydrolysis and esterification

This process is suitable for the biodiesel production from very high free fatty acid oils. Firstly, the triglycerides are changed to fatty acid and glycerol by hydrolysis over acid catalysts as shown in Eq. 2.5.

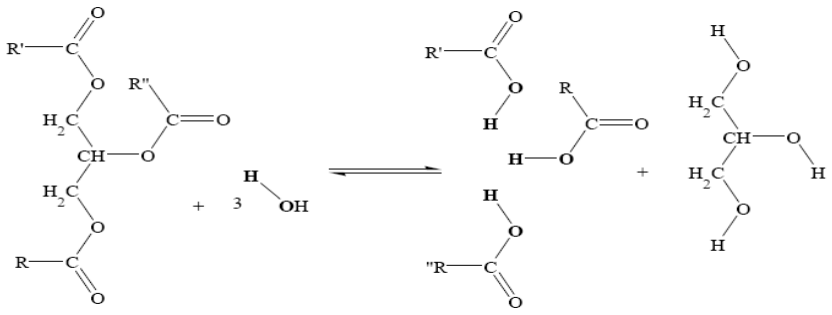

(2.5)

Technically, the reaction operates in a counter-current continuous flow reactor as shown in Figure 2.8. That is exactly what happens when esters are hydrolyzed by water or by dilute acids such as dilute hydrochloric acid. The products are composed with purified fatty acid and glycerol. The purified fatty acid is further moved to another counter-current continuous reactor in which it was esterified with acid catalyst to yield the methyl esters.

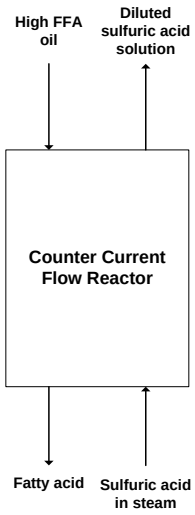


**Figure 2.8** Hydrolysis of high free fatty acid oil in counter-current continuous flow reactor [18].

The biodiesel production via the esterification of fatty acid with acid catalyst has been developing a decade ago but it encounters a decrease in the catalyst activity and the reaction rate due to dilution of the catalyst concentration by the water produced. The current commercial process for biodiesel production involves the use of alkali catalyst, followed by the removal of the soluble catalyst and the saponified products by water washing. In consequence, the other techniques, such as supercritical alcohol and heterogeneous catalysis, have been researched in the transesterification in order to overcome the problems caused by the existing processes .

Supercritical methanol is believed to solve the problems associated with the two-phase nature of normal methanol/oil mixtures by forming a single phase as a result of the dielectric constant of methanol in the supercritical state. Therefore, the reaction was found to be complete in very short time. In contrast to the catalytic processes under barometric pressure, the supercritical methanol process is non-catalytic, involves much simpler purification of products, has a lower reaction time, is more environmentally friendly, and requires higher energy use. However, the reaction requires temperature of 250 to 430 °C and pressures of 35 to 60 MPa by which scaling up for the large throughput is technically limited.

Calcium oxide is the single metal oxide catalyst most frequently applied to the study of biodiesel synthesis, probably due to its cheap price, minor toxicity and high availability. By comparing the heterogeneous catalysis using CaO with typical homogeneous catalysis, the reaction rate over the solid catalyst is much lower than the case of homogeneously catalyzed reaction. This phenomenon refers to mass transfer limitation of triglyceride molecules to the active surface of the solid oxide. Generally, a high reaction temperature (100–250 °C) and a large amount of methanol are required concomitantly with a proper process configuration to enhance the performance of the heterogeneous process, as evidenced in the commercialized Esterfip-H process (Figure 2.9).

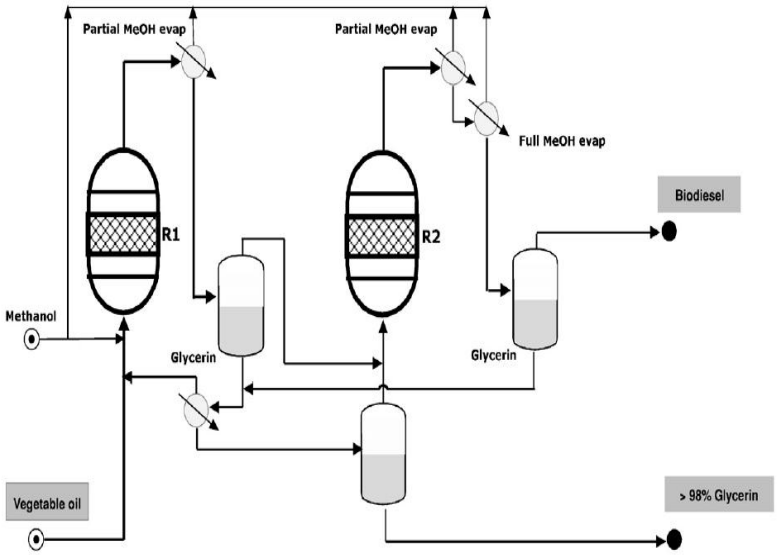


**Figure 2.9** Esterfip-H process developed by the French Institute of Petroleum (IFP) development [20].

## 2.4 Catalytic transesterification

Traditionally, catalysts are distinguished into 2 types, i.e. homogeneous and heterogeneous, this distinction is linked to the fact that the catalyst operates respectively in the same phase where the reaction occurs (homogeneous catalysts) or in a different phase (heterogeneous catalysts). In general, most of the processes using homogeneous catalysts occur in a liquid phase, whereas for the heterogeneous catalysts, the catalyst is usually in a solid form, and the reaction occurs either in the liquid or gaseous phase. The advantages/disadvantages of homogeneous and heterogeneous catalysis are compared in Table 2.4.

**Table 2.4** Comparison of homogeneously and heterogeneously catalyzed transesterification [21]

| Factors | Homogeneous catalysis | Heterogeneous catalysis |
|---|---|---|
| Reaction rate | Fast and high conversion | Moderate conversion |
| After treatment | Impossible or non-economic for recovery | Possible for recovery |
| Processing methodology | Limited use of continuous methodology | Continuous fixed bed operation possible |
| Presence of water/ free fatty acids | Sensitive | Less sensitive |
| Catalyst reuse | Not possible | Possible |
| Cost | Comparatively costly | Potentially cheaper |

Vegetable oils can be transesterified by heating them with a large excess of anhydrous methanol and a catalyst. The transesterification reaction can be catalyzed by acids, bases and enzyme.

### 2.4.1 Homogeneously acid-catalyzed transesterification

Sulfuric, hydrochloric and sulfonic acids are the most popular homogeneous catalyst in the acid-catalyzed transesterification. Generally, the reaction catalyzed by the acids are performed at high molar ratios of alcohol to oil, low to moderate temperatures and pressures, and high acid concentrations to obtain a high yield of methyl ester product. However, a large excess amount of alcohol makes the recovery of glycerol difficult. The transesterification pathway shown in Figure 2.10, for an acid-catalyzed reaction, indicates how in the catalyst-substrate interaction that the key

step is the protonation of the carbonyl oxygen. This in turn increases the electrophilicity of the adjoining carbon atom, making it more susceptible to nucleophilic attack by alcohol [21].

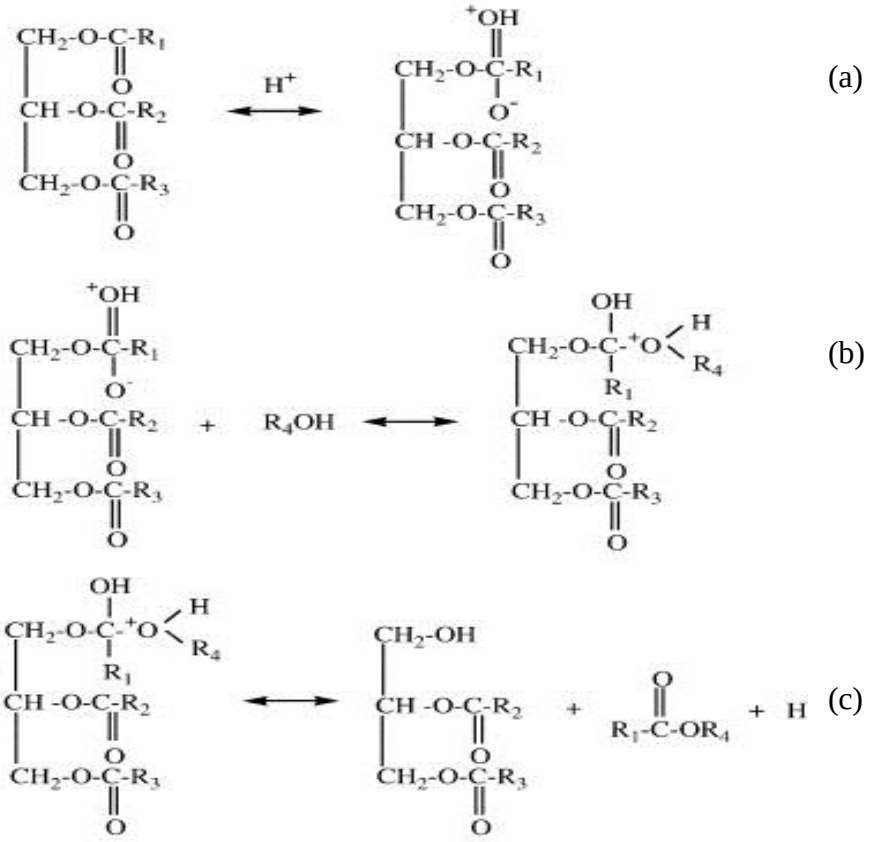


$R_1$, $R_2$, $R_3$: carbon chain of the fatty acids

$R_4$: alkyl group of the alcohol

**Figure 2.10** Mechanism of the transesterification of vegetable oils catalyzed by acid.

### 2.4.2 Homogeneously base-catalyzed transesterification

Currently, most of biodiesel is produced in the presence of alkaline catalysts, such as sodium hydroxide (NaOH), potassium hydroxide (KOH), sodium methoxide and potassium methoxide. Industrially, NaOH and KOH are preferred due to their wide availability and low cost [21]. In contrast, the base catalysis takes on a more direct route, creating first an alkoxide ion, which directly acts as a strong nucleophile, giving rise to a different reaction pathway (Figure 2.11)**.** Even though the

transesterification with homogeneous base catalysts is practical, the base-catalyzed process suffers from serious limitations that translate into high production costs for biodiesel. Strict feedstock specification is a main issue. In particular, the total FFA content associated with the lipid feedstock must not exceed 0.5 wt.%. Otherwise, soap formation seriously hinders the production of fuel grade biodiesel [22].

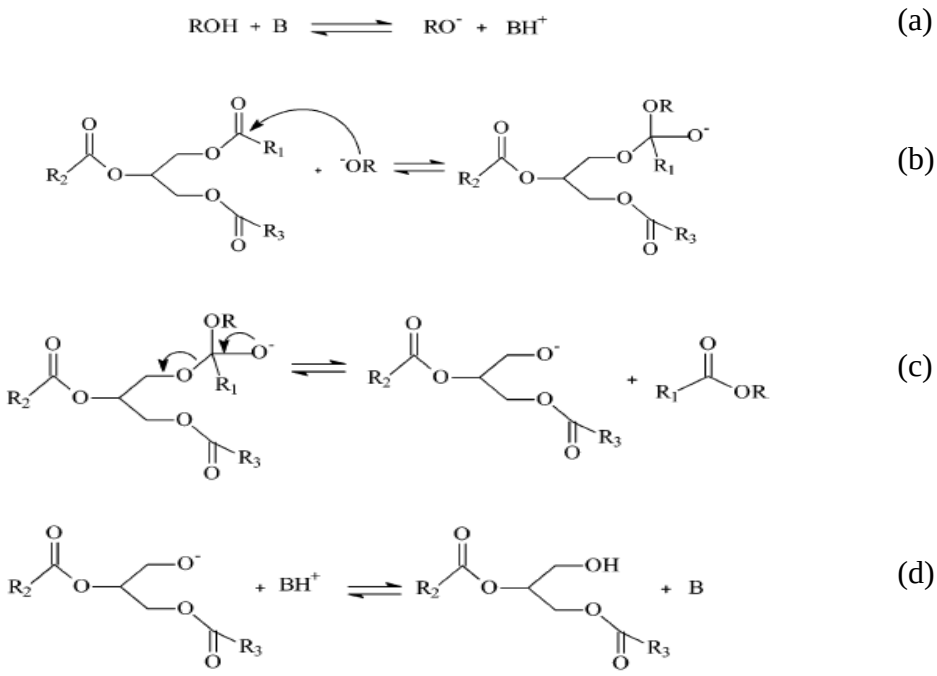


B: base catalyst

$R_1$, $R_2$, $R_3$: carbon chain of the fatty acids

$R_4$: alkyl group of the alcohol

**Figure 2.11** Mechanism of the transesterification of vegetable oils catalyzed by base.

### 2.4.3 Heterogeneously acid-catalyzed transesterification

Heterogeneous acid catalysts can simultaneously catalyze both esterification and transesterification, since they exhibit much higher tolerance to free fatty acids (FFAs) and water than the homogeneous counterparts. Similarly to the case of homogeneous system, heterogeneous acid catalysts perform less active than heterogeneous base ones, but they are favorable for low-qualified oil feedstocks with

high FFAs. The solid acids keep stably the catalytic activity in the conversion of low-qualified oils or fats to biodiesel. Currently, synthetic solid acids have already amounted to hundreds of species. Most of them can be used in both the esterification and the transesterification. The developed solid acid catalysts include such as Amberlyst-15 [23], zeolites [24], sulfated zirconia [25] and heteropoly acids [26].

### 2.4.4 Heterogeneously base-catalyzed transesterification

The transesterification of vegetable oils or animal fats to biodiesel by chemical catalysts, especially in the presence of a strong basic solution, such as sodium hydroxide and potassium hydroxide, has been widely used in industrial production of biodiesel. Such basic solutions can transform the triglycerides to their corresponding FAMEs with higher yield at lower temperature and shorter time than those by acid catalysts. However, separating the catalysts from the products is technically difficult. Moreover, the natural oils and fats usually contain small amounts of FFAs and water, which can have significantly negative effects on the transesterification of glycerides with alcohols, and also hinder the separation of FAMEs and glycerol due to the saponification of FFAs. Compared with the basic solutions, solid base catalyst is preferred due to easy separation. The heterogeneous base catalysis has a shorter history than the heterogeneous acid catalysis. The solid bases refer mainly to the solids with Brønsted basic and Lewis basic active centers, that supply electrons (or accept protons) for (or from) the reactants. The transesterification catalyzed by heterogeneous bases for the biodiesel synthesis has been studied intensively over the last decade. Low-qualified oil or fat with FFAs and water can be used under limited conditions. The catalytic efficiency of conventional heterogeneous base catalysts is relatively low and needs to be improved. Various types of solid bases have been studied to improve the transesterification of glycerides, such as hydrotalcites, metal oxides, metallic salts and supported base catalysts.

### 2.4.5 Enzyme-catalyzed transesterification

In general, the enzyme-catalyzed transesterification can be carried out at mild reaction conditions (temperature, 20-50 °C), with the oils from different sources,

including waste oils, refined and crude plant oils. Fats containing triglyceride and free fatty acid can be converted to alkyl esters in a one-step process because the lipases catalyze both transesterification and esterification reaction. In addition, the enzymatic process tolerates the water content in the starting oil and increases the biodiesel yield by avoiding soap formation. Another advantage of enzymatic biodiesel production is providing an easy recovery of glycerol without purification or chemical waste production.

In the recent work three different lipases (*Chromobacterium viscosum, Candida rugosa,* and Porcine pancreas) were screened for a transesterification reaction of jathopha oil in a solvent-free system to produce biodiesel; only lipase, (triglyceride hydrolases) from *Chromobacterium viscosum* was found to give appreciable yield. Immobilization of lipase on Celite-545 enhanced the biodiesel yield to 71% from 62% yield obtained by using free tuned enzyme preparation with a process time of 8 h at 160°C. Further addition of water tonthe free (1%, w v-1) and immobilized (0.5%, w v-1) enzyme preparations enhanced the yields to 73 and 92%, respectively. Immobilized *Chromobacterium viscosum* lipase can be used for ethanolysis of oil. It was seen that immobilization of lipases and optimization of transesterification conditions resulted in adequate yield of biodiesel in the case of the enzyme-based process [27].

Although the enzyme-catalyzed transesterification processes are not yet commercially developed because their high cost and low conformational stability restrict their industrial use, unless they can be irreversibly confined in porous material, allowing good accessibility and enhanced mass transport.

### 2.5 Preparation of heterogeneous catalyst

Heterogeneous catalysts are frequently defined as solids or mixtures of solids which accelerate chemical reaction without themselves undergoing changes. Even though the preparation procedures differ considerably from one catalyst to another, two broad categories can be introduced to classify the catalysts with respect to the preparation procedure: (i) bulk catalysts or supports and (ii) impregnated catalysts. On this basis the relative preparation methods are: (i) the catalytic active phase is

generated as a new solid phase and (ii) the active phase is introduced or fixed on a pre-existing solid by a process which intrinsically depends on the support surface [28].

### 2.5.1 Bulk catalysts and support preparation [29-30]

#### 2.5.1.1 Precipitation

Precipitation is one of the most widely employed preparation methods. Precipitation is the formation of a solid in a solution. In the precipitation of catalysts, the first step is mixing of two or more the sample solution, which the second phase is produced by adding a reagent so that certain components of the sample are more or less selectively precipitated. Calculation of the extent of precipitation of a trace component on the basis of tabulated solubility normally gives very inaccurate predictions. Solubility equilibria arise particularly at the trace level from a variety of side reactions, and interaction with sample components and container surfaces which normally would be considered inert. The rate of precipitation also greatly influences the efficiency of trace precipitation and, unless slow precipitation is achieved, distributions based on equilibrium calculations cannot be expected to be valid.

#### 2.5.1.2 Co-precipitation

Co-precipitation is the carrying down by a precipitate of substances normally soluble under the conditions employed that the synthesis of multi-component systems, the problems are even more complex. Co-precipitation allows one to obtain good macroscopic homogeneity. The composition of the precipitate depends on the differences in solubility between the components and the chemistry occurring during precipitation.

### 2.5.2 Supported catalysts preparation [28]

#### 2.5.2.1 Impregnation

Impregnation is the permanent solution to the porosity networks without impacting the functional or dimensional characteristics of the material. A certain volume of solution containing the metal precursor is contacted with the solid support,

and then it is aged, usually for a short time, dried and calcined. According to the volume of solution used, two types of impregnation can be distinguished: wet impregnation and incipient wetness impregnation.

In the wet impregnation technique (also called soaking or dipping), an excess of solution is used. After a certain time, the solid is separated from solution, and the excess solvent is removed by drying. The composition of the batch solution will change and the release of debris can form a mud which makes it difficult to completely use the solution.

In the incipient wetness impregnation is a commonly used technique for the synthesis of heterogeneous catalysts. Typically, the active metal precursor is dissolved in an aqueous or organic solution. Then, the metal-containing solution is added to a catalyst support containing the same pore volume as the volume of solution that was added. The solution added in excess of the support pore volume causes the solution transport to change from a capillary action process to a diffusion process, which is much slower. The catalyst can then be dried and calcined to drive off the volatile components within the solution, depositing the metal on the catalyst surface. The maximum loading is limited by the solubility of the precursor in the solution. The concentration profile of the impregnated compound depends in the mass transfer conditions within the pores during impregnation and drying.

#### 2.5.2.2 Ion exchange

Ion exchange is an exchange of ions between two electrolytes or an electrostatic interaction with the surface of a support by another ion species between an electrolyte solution and a complex. The support containing ions A is plunged into an excess volume (compared to the pore volume) of a solution containing ions B. Ions B gradually penetrate into the pore space of the support, while ions A pass into the solution, until equilibrium is established corresponding to a given distribution of the two ions between the solid and the solution.

#### 2.5.2.3 Adsorption

Adsorption allows the controlled anchorage of a precursor (in an aqueous solution) on the support. The adsorption is a process where ionic species from aqueous solutions are attracted electrostatically by charged sites on a solid surface. Often consideration is not given to the difference between true ion exchange processes and electrostatic adsorption at the charged surface of oxides. Catalyst systems, which need charge compensating ions are ideal materials for ion exchange (zeolites, cationic clays or layered double hydroxides). Instead most oxide supports, when placed in an aqueous solution, develop a pH-dependent surface charge.

#### 2.5.2.4 Dissolution- precipitation

Recently, ourgroup has developed a new method for preparation of heterogeneous catalysts from natural calcium source, i.e. waste shell [31]. The catalysts prepared exhibited a high activity and good stability. According to the preparation steps, it is called “dissolution- precipitation” method.

The dissolution-precipitation method is the process that an acid solution is used to partially dissolve an active metal precursor, usually solid state with low solubility, to give corresponding metal ion in the solution. A support material is subsequently added into the slurry in which the metal ion is precipitated. Then, excess water is evaporated to dryness, followed by calcination. Loading of metal precipitated on the support is determined by pH of the acid solution, the amount of metal precursor, and the temperature during the dissolution. In some cases, for example a promoter is required, the corresponding metal precursor can be simultaneously added in the acid solution.

### 2.6 Formulation of heterogeneous catalysts [32]

The usage of heterogeneous catalyst in powdery form in a fixed-bed reactor are not permitted due to the problems of reactor blockage and pressure drop. Therefore, the catalyst should be shaped in pellet, sphere or extrudate by formulation process. Paste extrusion is one of the most useful methods of size enlargement and now has the further advantage that a satisfactory theoretical basis to permit rational

and reliable design is emerging. There is significant scope for adjusting the properties of the solid and liquid components so that a product of desired quality can be made. In this case, a binder such as alumina, silica and clay, is used for maintaining the formulated shape and improving strength of the enlarged particle. Moreover, a plasticizer is sometimes required in small quantities to aid the formulation of catalyst and to increase its pore structure after thermal processing. However, the presence of binder results in lower activity of catalyst due to the reduction of surface area, pore volume and number of active sites.

### 2.6.1 Paste extrusion process

There are a number of unit processes that are necessary in order to prepare a catalyst, and the material made in extrusion may require several finishing steps in order to yield the required form of the product. The stages of forming a product by paste extrusion are illustrated in Table 2.5.

- Dry mixing

Dry mixing has a purpose to uniformly mix all of solid components. However, this is a difficult unit operation to achieve homogeneity but an addition of binder can help this mixing more distributed.

- Wet mixing

Wet mixing uniformly distributed particles in liquid. During this stage, the mixing of the solid components also continues stirring. If too high the viscosity of the mixture, achievable product may be inflective. Trouble can arise due to the adherence of wet powder to the rotors or due to the excessive entrapment of air. Addition of clay or powder polymer can avoid this problem.

- High- shear mixing

High-shear mixing is to break down the agglomerates forming a liquid layer around individual particles. It is pleasing to secure the formation of single particles with a liquid layer or film covering the whole surface of each particle. In this process the high liquid viscosity is important, so that liquid leakage does not occur giving regions of wetter and less wet solids, an effect also promoted by the imposition of high stresses.

**Table 2.5** Processing stages [33]

| Materials added | Unit processes | Materials removed | Nature of product |
|---|---|---|---|
| Powder | Dry mixing | | |
| Liquid | Wet mixing | | |
| Paste preparation: | High-shear mixing | Gas | |
| | Degassing | | |
| Forming: | Extrusion | | |
| | Extrudate handling | | Extrudate |
| Finishing: | Cutting | | Cut extrudate |
| | Drying | Vapour | Dried extrudate |
| | Thermal processing | Binder | |
| | | | Fried extrudate |

- Degassing

Degassing is to remove entrapped gas that prevents the creation of voids in the structure during later processing stages.

- Extrusion

Extrusion is then carried out to shape paste to profile desired by pressing the paste into and through a die of size and cross-section shape appropriate to that of the product.

- Extrudate handling and cutting

Extrudate handling and cutting are to remove the product and to form short units from the extrudate.

- Thermal processing

Thermal processing burns out any undesirable materials such as binder and organic material in the extrudate, and also develops mechanical strength of the extrudate. The strength can be controlled by the relationship between temperature and time settle during calcination process. The used temperature should be too high to generate crystallographic structure but must not high over that lead to sintering .

Normally, commercial catalysts are available in any form of pellets, spheres, granules, beads and extrudates that each form has suitable application to different types of reactor. Guideline is shown in Table 2.6.

**Table 2.6** Shapes of catalyst [33]

| Form of catalysts | Diameter | Reactor |
|---|---|---|
| Spheres | $d$ = 1-10 mm | Fluid bed reactor, moving bed reactor |
| Granules | $d$ = 1-20 mm | Fluid bed reactor |
| Beads | $d$ = 1-5 mm | Fluid bed reactor |
| Pellets | $d$ = 3-15 mm | Fluid bed reactor |
| Extrudates | $d$ = 1-50 mm | Fluid bed reactor |

### 2.6.2 Types of extruder [32]

When extrusion is deemed to be potentially useful technology, it is necessary to understand in detail methods of generating pressure, methods of describing the flow, and how these are dependent on the paste formulation. The various types of equipment are provided below.

### 2.6.2.1 Rotary extruders

This class of machine is often employed when the precise control of extrudate length and inessential hardness. This class of extruders lessens problems because the paste is governed to a high pressure for only a short time. There are a number of designs such as the Roll-Caster.

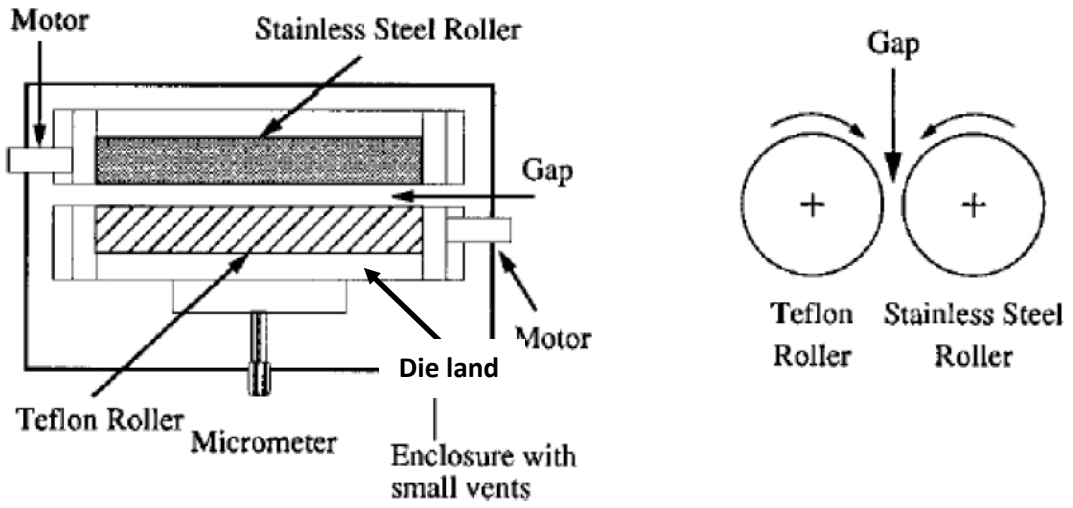


**Figure 2.12.** Left: Schematic plan view of the Roll-Caster. Two parallel rollers counter-rotate at a fixed separation controlled by a micrometer. Right: Cross-sectional view [34].

Figure 2.12 shows an extruder in which paste is applied between counter-rotating rolls, one of which is Teflon roller with the other being hollow and perforated. Rotation of the cylinders forces causes pressure generated in the nip which the paste down into die land to hollow. The extrusion process is controlled by shear informed by rotating of the cylinders to the paste held in the nip between cylinders.

### 2.6.2.2 Ram extruders

This class of extruder will be used when product specifics and sometimes complicated geometries are needed. The extrusion process requires very careful control of the extrusion process and refined extrudate handling. Ram extruders are widely used to elaborate shape components.

Figure 2.13 illustrates schematic drawing of a ram extruder that paste is fed in via container into the billet. In this process, the material move through the die entry into the die land by the ram force. The ram is either driven by a mechanical or hydraulic system. The extruded product can be cut by a blade or may fall off to form extrudate pieces of various types and then leaves the die land. The advantages of the ram extruder are accurate control of flow rate, and high pressures can be developed.

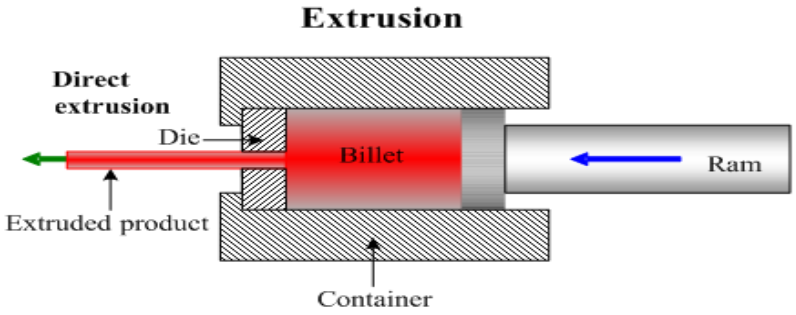


**Figure2.13** Ram extruder [35].

### 2.6.2.3 Screw extruders

A screw extruder is process for making large batches and for processing continuously. This extruder is suitable for soft pastes, whereas a ram extruder is better for firm materials that must use high extrusion pressures.

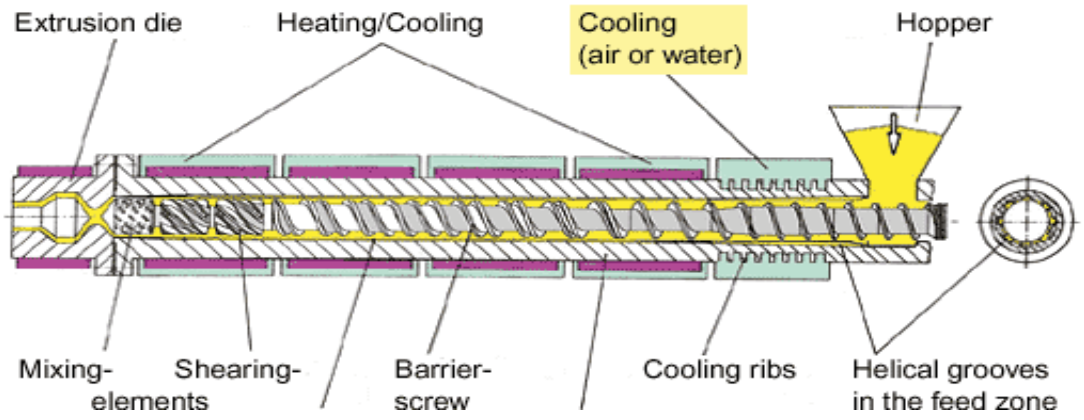


**Figure 2.14** A single screw extruder with barrier-screw with shearing and mixing parts [36].

Figure 2.14 shows a system of main extruder with a single screw in which a mixture of solid and liquid components is fed to hopper into the barrier-screw that the pressure developed to the paste moves towards the die.

#### 2.6.2.4 Manual extruder

This extruder is easy to operate and does not use high pressure. It matches with low batch size at least 50 grams of catalyst powder.

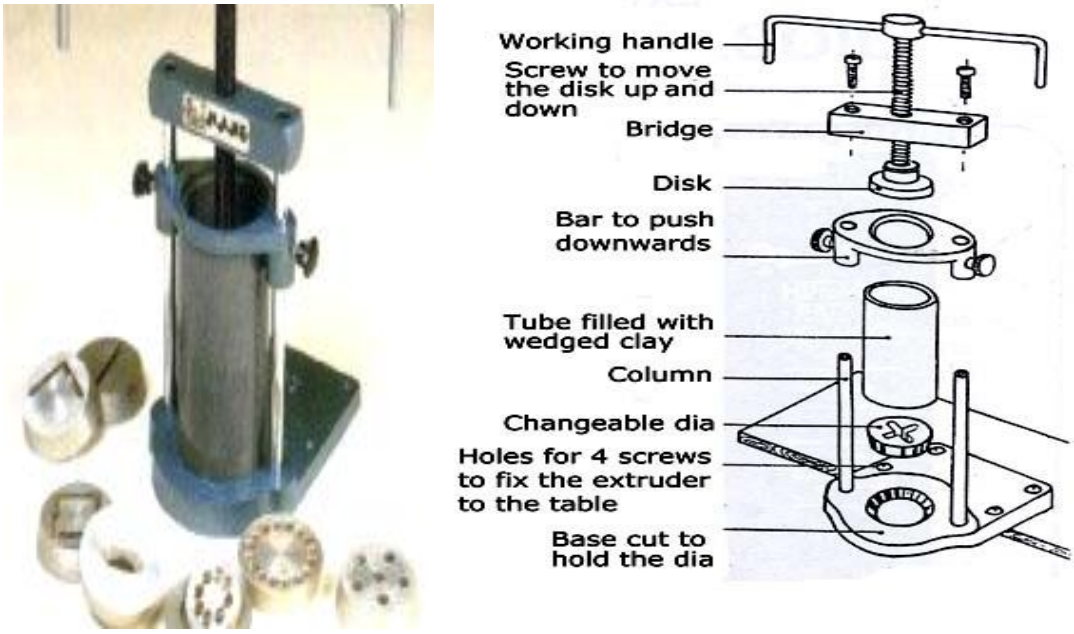


**Figure 2.15** Manual extruder [37].

Figure 2.15 shows the manual extruder that is a tool for passing paste through a tube to form coils. The pressure of closing the trigger pushes and turns the screw which moves the plunger down through the tube, making the paste comes out through the die. The dies which are metal disks with spaces cut out to extrude different shaped coils.

### 2.7 Calcium oxide (CaO) as heterogeneous base catalyst

At the present, CaO has been extensively investigated as a practical heterogeneous base catalyst for the transesterification of triglycerides because it has low cost, high basicity and low solubility in methanol. Commercially, CaO is

produced via a thermal decomposition of limestone and calcium-rich dolostone (dolomite) at high temperatures. Other $CaCO_3$-based materials, including coral, sea shells, and chalk, can be also used as the sources of CaO. Many reports have been published on the transesterification of vegetable oils with methanol catalyzed by CaO.

Gryglewicz *et al*. [38] compared the catalytic activity of CaO with that of typical homogeneous catalysts, including alkaline-earth metal hydroxides and alkoxides, in the transesterification of rapeseed oil with methanol at the boiling point of methanol. The order of activitie followed the order of Lewis basicity: $Ca(CH_3O)_2$> CaO > $Ca(OH_2)$. The reaction rate over the heterogeneous catalysts, however, was much lower than that over the homogeneous catalysts.

Demirbas *et al*. [39] has reported the biodiesel production from sunflower oil in the presence of supercritical methanol using CaO as the catalyst. The yield of fatty acid methyl esters (FAME) attained over CaO was heavily dependent on the reaction temperature and, especially, the methanol/oil molar ratio. The FAME yield increased from 65 to 99% as the methanol/oil molar ratio was increased from 6:1 to 41:1 and the catalyst amount of 3.3 wt.%. In the transesterification of soybean oil, a similar level of FAME yield (97%) was obtained at 300 °C with smaller amount of catalyst (0.58 wt.%) only when a large amount of methanol (methanol/oil ratio 39.3:1) was used.

Liu *et al*. [40] revealed that the catalysis rate over CaO was accelerated in the presence of water, because methoxide ions, which are believed to be the true catalytic agent for the transesterification, were increased through the hydrolysis of monoglyceride molecules. However, if too much water (more than 2.8% by weight of soybean oil) was added to methanol, FAME were hydrolyzed under basic conditions to generate fatty acid, which can react with CaO to form soap. The catalysis by CaO sometimes produces a lower FAME yield than expected from its high triglyceride conversion, which is usually attributed to the formation of $Ca(OCH_3)_2$ on the CaO surface. Some careful handling is required in order to use CaO as a base catalyst, because its active surface is chemisorbed very easily by $H_2O$ and $CO_2$ in the atmosphere. Therefore, the poisoning species must be removed at high temperature (more than 700 °C) and an exposure to the atmosphere should be strictly prevented before its use.

## 2.8 Dolomite [41]

One of naturally abundant carbonate mineral is dolomite that is composed of mixed Ca and Mg carbonate ($CaMg(CO_3)_2$). Dolomite is one of the few sedimentary rocks that undergo a significant mineralogical change after it is deposited. They are originally deposited as calcite/aragonite rich limestones, but during a process called diagenesis the calcite or aragonite is altered to dolomite.

### 2.8.1 Properties

Dolomite differs from calcite, $CaCO_3$, in the addition of $Mg^{2+}$ to make the formula, $CaMg(CO_3)_2$. The $Mg^{2+}$ are not the same size as Ca and the two ions seem incompatible in the same layer. In calcite, the structure is composed of alternating layers of $CO_3^{2-}$ and $Ca^{2+}$. In dolomite, the Mg occupy one layer by themselves followed by a carbonate layer which is followed by an exclusively calcite layer and so forth. It is probably the significant size difference between Ca and Mg and it is more stable to group the differing sized ions into the same sized layers.

#### 2.8.1.1Chemical properties

Dolomite does not rapidly dissolve in dilute hydrochloric acid unless it is scratched or in powdered form. Dolomite gives the basicity when it dissolves in water, the pH are in range of 9.0- 10.71.

#### 2.8.1.2 Physical properties

The mineral dolomite crystallizes in the trigonal-rhombohedral system. Dolomite can be several different colors, but colorless and white are very common. However, it is dolomite's pink color that sets another unique characteristic for dolomite. Crystals of dolomite are well known for their typical beautiful pink color, pearly luster and unusual crystal habit and it is these clusters that make very attractive specimens. The hardness of dolomite is 4 on the Moh’s hardness scale and specific gravity is 2.86.

### 2.8.2 Thermal decomposition of dolomite

Thermal analysis might offer the means of defining the fraction of each mineral lattice in such mixtures and the concentration of each cation in each lattice. The correlation of the thermal data with the structural pattern should provide a broader understanding of these minerals in their natural occurrence. Hashimoto et al. [42] proposed the mechanism of half decomposition of dolomite in which the reaction involved the direct formation of calcium carbonate via a 'magnesian' calcite with a gradual release of $Mg^{2+}$ ions to form calcite. At the beginning of the decomposition, $CO_2$ is released at defects on the surface of dolomite, leaving oxygen ions $O^{2-}$. Then, the $Mg^{2+}$ neighbors may move towards the oxygen ions, while $Ca^{2+}$ ions migrate in the opposite direction. $CaCO_3$ is formed in this zone. The higher temperature decomposition of calcite with the evolution of carbon dioxide. The phenomenon occurring during the thermal decomposition of fresh dolomite could be as follows:

$$MgCa(CO_3)_2 \rightarrow MgO{-}CaCO_3 + CO_2 \qquad (2.6)$$

$$MgO{-}CaCO_3 \rightarrow MgO{-}CaO + CO_2 \qquad (2.7)$$

### 2.8.3 Sources of dolomite in Thailand [41]

Dolomite appears to form in many different types of environment and can have varying structural, textural and chemical characteristics. Much modern dolomite differs significantly from the bulk of the dolomite found in the rock record, leading researchers to speculate that environments where dolomite formed in the geologic past differ significantly from those where it forms today. Dolomitization of calcite also occurs at certain depths of coral and atolls where water is undersaturated in calcium carbonate but saturated in dolomite. Convection created by tides and sea currents enhances this change. Hydrothermal currents created by volcanoes under the atoll may also play an important role.

Sources of dolomite have been generally found in every region of Thailand such as following.

| | |
|---|---|
| Northern Thailand | : Amphoe Umphang in Tak Province |
| | : Amphoe Rong Kwang in Phrae Province |
| Central Thailand | : Amphoe Tha Muang in Kanchanaburi Province |
| | : Amphoe Mueang, Chom Bueng and Photharam in Ratchaburi Province |
| | : Amphoe Pran Buri in Prachuapkhirikhan Province |
| Eastern Thailand | : Amphoe Ko Sichang in Chonburi Province |
| Southern Thailand | : Amphoe Donsak in Surat Thani Province |
| | : Amphoe Khanom in Nakhon Si Thammarat Province |

### 2.8.4 Applications of dolomite [43]

Dolomite is used in many construction and building product applications due to its increased hardness and density. Asphalt and concrete applications prefer dolomite as filler for its higher strength and hardness. Dolomite also finds use in a number of applications as a source of magnesium such as glass and ceramics manufacture, as well as a sintering agent in iron ore pelletization and as a flux agent in steel making. Farmers use dolomite for agricultural pH control. The chemical industry uses the mineral dolomite in making magnesium salts including magnesia, magnesium oxide (MgO), which is used in pharmaceuticals.

## 2.9 Literature review

Ngamcharussrivichai *et al*. [44] studied the transesterification of palm kernel oil (PKO) with methanol over various natural calciums, including calcite, cuttlebone, dolomite, hydroxyapatite, and dicalcium phosphate. The reaction was performed at 60

°C and 1 atm. The experimental showed that dolomite calcined at 800 °C, resulting in a formation of highly active mixed oxide, was the most active catalyst. Under the suitable reaction conditions, the amount of dolomite calcined at 800 °C = 6 wt.% based on the weight of oil, the methanol/oil molar ratio = 30, and the reaction time = 3 h, the methyl ester content of 98.0 wt.% can be achieved. The calcined dolomite can be reused many times.

Kouzu *et al*. [45] investigated different calcium-based catalysts for biodiesel production via the transesterification of edible soybean oil with refluxing methanol. The catalysts used were calcium oxide (CaO), calcium hydroxide ($Ca(OH)_2$) and calcium carbonate ($CaCO_3$). At 1 h of the reaction time, the yield of FAME was 93% for CaO, 12% for $Ca(OH)_2$, and 0% for $CaCO_3$. However, CaO was also rapidly poisoned by the moisture and carbon dioxide in the ambient atmosphere.

Yoosuk *et al*. [46] studied the hydration–dehydration technique for property and activity improvement of calcined natural dolomite in the heterogeneous biodiesel production. The results showed that a structural transformation had taken place during the modification and there was a structure–activity relation. Upon the calcination of dolomite, MgO grows on the surface of $MgCa(CO_3)_2$ in which $CaCO_3$ is progressively formed, followed by the decomposition to CaO. The transformation of oxide to hydroxide phase and the reverse occurred simultaneously during the hydration–dehydration step, resulting in a change in pore-size distribution, which is created by particle expansion in the formation of the hydroxide structure and the formation of more porosity and surface area. In the hydration–dehydration step, the number of strong basic sites significantly increased while the chemical nature of these sites did not changed. The resultant catalyst gave 93.3 wt.% of methyl esters in the transesterification of palm olein with methanol. This study provides an understanding regarding how this hydration–dehydration process influences the properties and activity of dolomite.

Cho *et al*. [47] carried out the transesterification of tributyrin with methanol over CaO catalysts prepared from various calcium precursors such as $CaCO_3$, $Ca(OAc)_2$, $Ca(NO)_3$, $Ca(OH)_2$ and $CaC_2O_4$. The precursors were transformed into CaO by calcination at different temperatures depending on the types of precursor. $Ca(OH)_2$ calcined at 600-800 °C showed the highest activity in the transesterification

among the prepared catalysts. The calcination at excessively high temperature caused a significant loss of basic sites due to a sintering. The CaO catalyst maintained its advantages as a heterogeneous catalyst in terms of its separation and repeated use.

Chandrasekar *et al*. [48] studied the extrusion of AlSBA-15 molecular sieves for an industrial use. The powdery AlSBA-15 with different nSi/nAl ratios (45, 136 and 215) were synthesized by hydrothermal technique. The powdered materials were extruded into cylindrical shape with the addition of bentonite as a binder. It was observed that the XRD intensities of higher angle reflections of AlSBA-15 extrudates were lower than those of the parent AlSBA-15. This was due to the presence of binder filling in between AlSBA-15 particles. The addition of binder also reduced the surface area, pore volume and pore diameter. Moreover, the surface acidity of AlSBA-15 was decreased after the extrusion processes were decrease due to a migration of alkali/alkali earth metal cations from binder to AlSBA-15 protonic sites of AlSBA-15. The *t*-butylation of phenol was carried out to test the catalytic activity of AlSBA-15 extrudates by which the phenol conversion of 62.9% was attained.

Serrano *et al*. [49] prepared the catalyst extrudates of TS-1 zeolites for their application to propylene epoxidation. Three different methods for the paste preparation were investigated. Method I was consisted of dry mixing of TS-1 powder with clay (sepiolite), methylcellulose, and distilled water (200 wt.% of solid). In method II, clay was added over a suspension of TS-1 powder in water (200 wt.% of solid), and method III was analogous to method II but using ultrasound and larger amount of water (240 wt.% of solid). The optimal extrusion procedure was according to method III by which the formation of aggregates could be avoided when using the weight proportion of TS-1/sepiolite of 60/40. Moreover, this method provided the catalysts with mechanical strength for its use in a fixed bed reactor. The evaluation of catalytic activity indicated that the conversion and the selectivity were close to 97% and 80%, respectively, which just decreased slightly along the reaction time.

Ngamcharussrivichai *et al*. [50] investigated the effects of binder addition on the preparation of catalyst extrudates from limestone. CaO derived from the thermal decomposition of limestone was the major catalytically active sites. The hydroxide and the oxide of Mg acted as solid lubricants that helped the extrusion of the catalyst pastes smoothly. Combining these Mg precursors with the Al precursors generated the

spinel $MgAl_2O_4$ as the new active phase, which promoted the transesterification and improved the strength of the catalyst extrudates. The suitable Mg/Al ratio in the mixed catalyst precursors was 3. The transesterification activity and the extrudate strength were optimized through the thermal treatment of the limestone at 600 °C, followed by the calcination of the mixed precursors at 800 °C. The addition of $NaAlO_2$ was a key to attain the dense and hard extrudates by inducing the formation of the mixed Ca and Al phases. The catalyst can be regenerated and used repeatedly. The catalytic test in the transesterification of various oils with methanol and ethanol in the continuous-flow fixed bed reactor suggested the good activity and stability of the catalyst extrudates.

Kasture *et al*. [51] reported the influences of binder on the catalytic performance of H-beta (H/β) zeolites synthesized by using fly ash as a source of silica and alumina. The influences of the different percentages of alumina binder and formulations on the catalytic performance in isopropylation of benzene were investigated. Acetic acid (3%) was added to the catalyst mixture to form a homogeneous paste. It was then subjected to extrusion using hand extrusion machine with 1.2-mm diameter disc. The extrudates were dried and then calcined at 550 °C for 10 h in air atmosphere. It was demonstrated that fly ash can improve the catalyst activity and stability. The addition of 40% of alumina binder was observed to be superior on account of its stable benzene conversion (around 18.5%) and cumene selectivity (ca. 92.5%) due to an increase in both tetra- and octa-hedral coordinated aluminum.

Coetzee *et al*. [52] developed the solid phosphoric acid catalyst for the oligomerization of $C_3$–$C_5$ alkenes, an important reaction for the refining of Fischer-Tropsch products. The catalyst was prepared in 500-g batches in which Celite FB kieselguhr was impregnated with 115% phosphoric acid at 200 °C, followed by mixing for 5 min in a Kenwood processor equipped with a stainless steel mixing bowl. The quantities were controlled in order to obtain a mixture with the acid to kieselguhr mass ratio of 2.7:1, giving paste with a dry sandy texture that exhibited satisfactory extrusion. It was then passed through a laboratory extruder to produce extrudates of 6 mm in diameter and approximately 10 mm in length. The calcination was set at 400 °C for 25 min with an air flow of 1 mL/min before the testing of

crushing strength and catalyst lifetime. The XRD study showed that the new phases of silicon pyrophosphate ($SiP_2O_7$) and silicon orthophosphate ($Si_5(PO_4)O_6$) which were generated from the reaction of silica with phosphoric acid. Amount of silicon pyrophosphate phase associated with mechanical strength and lifetime of extrudates. Based on this finding, a new commercial catalyst was formulated which required no any additional binders.

Müller *et al*. [53] studied the formulation of Cu/ZnO extrudates for the single-stage gas-phase processing of dimethyl maleate to tetrahydrofuran. To produce the catalyst paste for extrusion, the dried copper/zinc carbonate precursor was mixed with boehmite and 22% (m/m) water in a rheo-kneader at a constant temperature of 293 K and a rotor speed of 40 $min^{-1}$. The paste was transferred to a piston extruder at which the cylindrical greenbodies with a diameter of 2 mm and a length of about 400 mm were formed. The greenbodies were dried at room temperature and cut into pieces of about 5 mm length. The particles were calcined in air for 3 h at 550 °C. At this stage, the metal carbonates were transformed into the oxides, and the binder particles built a strong matrix of $\gamma$ -alumina. The mercury porosimetry analysis of extrudates indicated the presence of mesopores that are voids in between the catalyst particles and binders. Moreover, increasing of boehmite improved mechanical strength of extrudates conversely with a decrease in the active surface area and the catalytic activity of Cu.

Bournay *et al*. [54] reported about new heterogeneous process for biodiesel production that had been developed by French Institute of Petroleum (IFP). In this process, the transesterification of vegetable oils was continuously carried out in two-consecutive columns packed with heterogeneous catalyst. The catalyst was a mixed oxide of zinc and aluminum, which promoted the reaction without an activity loss. However, the reaction must be performed at temperature and pressure higher than the conventional homogeneous catalysis processes. A large amount of methanol was needed to promote the glycerides conversion after which the excess methanol was evaporized and recovered into the reaction. The major advantage of this process is that glycerin produced has high purity (at least 98%) and is exempt from any salt contaminants. With all these features, this process can be considered as a green process.

Maćias *et al*. [55] studied the effects of different catalyst particle shapes (sphere, pellet, cylinder, 2-lobe, 3-lobe, and 4-lobe) on the characteristics and behavior of hydrodesulfurization catalyst and reactor. The analysis was based on the experimental information obtained in a small hydrodesulfurization reactor using straight-run gas oil as the feed and a tri-lobular commercial catalyst sample at typical commercial operating conditions. The shape and the size of catalyst particles will influence properties such as activity, bulk density, pressure drop, strength, and liquid distribution during commercial operation. The amount of sulfurs eliminated was associated with the external area by which the hydrodesulfurization activity was increased following the trend: 4-lobe >3-lobe> 2-lobe>cylinder >pellet >sphere. The impact of particle size (volume to external area of the catalyst particle (Vp/Sp)) on the sulfur content in the product was observed that a reduction in the particle size gave higher sulfur conversion due to high effectiveness of the small particles.

Lange *et al*. [56] studied the mass transport limitation in zeolite catalysts used in the dehydration of 1-phenyl-ethanol to styrene under $N_2$ stream at 220-300 °C. The catalysts applied in life-test experiments were based on various commercial H-ZSM-5 powders that were extruded with various amounts of silica precursors (Sipernat 50) into tri-lobes of 1.6mm diameter. The extrudates showed an average mesopore diameter of 10-20 nm, as measured by Hg-porosimetry. Short and preliminary experiments confirmed this for various molecular sieve powders, namely for the large-pore H-Beta, for various medium-pore H-ZSM-5 and even for the narrow-pore SAPO-34. All these zeolites exhibited a high activity at 250–290 °C and high styrene selectivity up to high phenyl-ethanol conversion. The lack of influence of micro-pores size indicates that the dehydration reaction proceeds mainly at the external surface of the zeolites and not inside the micro-pores. The preliminary tests were then followed-up by life-tests with various ZSM-5 extrudates bound with $SiO_2$. These tests revealed clear improvements in the catalyst selectivity and stability under operation at lower temperature (220 °C) combined with lower WHSV with extrudates of lower zeolite content and with crushed catalyst particles. All these results are consistent with the presence of strong internal diffusion limitations inside the mesopores of the extrudates that favour the consecutive oligomerisation of the styrene intermediate.

Freiding *et al*. [57] investigated the extrusion of zeolite catalysts with a help of novel aluminium phosphate sinter matrix. The preparation of $AlPO_4$-bound extrudates of ZSM-5 used a solution of 8.5% (w/w) hydroxyethyl cellulose (HEC) as a plasticizer. Mixing of solids and HEC solution was always carried out at room temperature for 20 min in a rheo-kneader at a constant rotor speed of 40 $min^{-1}$. HEC solution was first poured into the mixing chamber of the kneader, and then the powder of thoroughly pre-mixed solids was added. After mixing, the paste was extruded through the nozzle of a piston extruder at a constant piston speed of 0.5 cm/min to obtain cylindrical strings with a diameter of 2 mm and a length of approximately 30 cm. After drying for 24 h at room temperature, they were broken into pieces of 5 mm length. The resulting green body particles were then transferred to calcination at 550 °C for 3 h. Generally, the calcination of extruded greenbodies has be combusted and removed together with residual water, be it physisorbed or chemically bound. In addition, the binder is transformed into a matrix with enhanced mechanical stability. In the case of conventional particulate binders like alumina or silica, the mechanical strength evolves through adhesive forces and cross-linking of terminal hydroxyl groups between neighboring binder particles. Finally, the matrix is mesoporous and represents a network of more or less strongly interconnected particles with voids in-between.

# CHAPTER III

# EXPERIMENTALS

## 3.1 Chemicals

### 3.1.1 Chemicals for synthesis of catalysts

1. Dolomite (P&S DOLO-LIME Company Limited)
2. Aluminum oxide ($Al_2O_3$, 95%) (AR grade, Ajax Finechem)
3. Hydroxyethyl cellulose (HEC) (Commercial grade, A.H.A International Company and Thai Specialty Chemical Company and AR grade, Fluka)
4. Sodium sulfate (AR grade, Ajax Finechem)
5. Nitric acid ($HNO_3$, 50-70%) (JT.baker)

### 3.1.2 Chemicals for transesterification

1. Refined bleach deodorized palm kernel oil (The Patum Vegetable Oil Company Limited)
2. Methanol ($CH_3OH$, 99.5%) (Commercial grade)
3. Sodium sulfate ($Na_2SO_4$, 99%) (Riedel-deHaën)

### 3.1.3 Chemicals for reaction products analysis

1. Methyl heptadecanoate ($C_{18}H_{36}O_2$, 99.5%) (Fluka)
2. *n*- Heptane (n-$C_7H_6$, 99.8%) (Riedel- deHaën)

### 3.1.4 Chemicals for quantitative analysis of monoglycerides, diglycerides and triglycerides in FAME layer

1. Tricaprin ($C_{33}H_{62}O_6$, 99%) (Sigma Aldrich)
2. α -Monopalmitin ($C_{19}H_{38}O_4$, 99%) (Sigma Aldrich)
3. Dipalmitin ($C_{35}H_{68}O_5$, 99%) (Sigma Aldrich)
4. Tripalmitin ($C_{51}H_{98}O_{6,}$ 99%) (Sigma Aldrich)
5. Monoolein ($C_{21}H_{40}O_4$, 99%) (Sigma Aldrich)
6. Diolein ($C_{39}H_{72}O_5$, 99%) (Sigma Aldrich)
7. Triolein ($C_{57}H_{104}O_6$, 99%) (Sigma Aldrich)

## 3.2 Instruments and Equipments

### 3.2.1 Instruments and equipments for catalyst preparation

1. Beaker 100 and 1000 mL
2. Crucible
3. Muffle furnace
4. Desiccator
5. pH meter
6. Stirrer
7. Magnetic bar
8. Overhead stirrer
9. Oven

10. Dropper

11. Balance

12. Manual extruder (Figure 3.1)

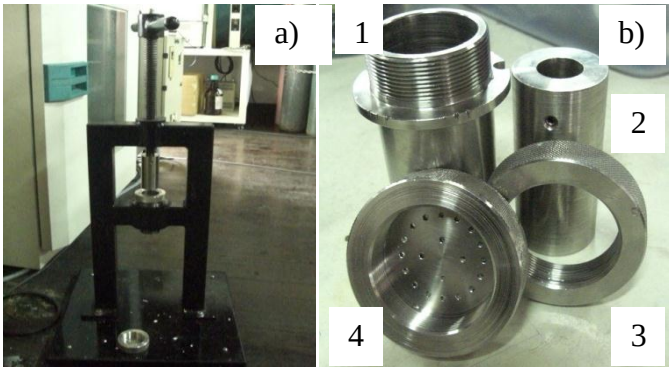


**Figure 3.1** Manual extruder used for formulation of catalyst: a) extruder and b) extruder components made of stainless steel (1= sample container, 2 = pressing rod, 3= ring for locking the container, 4= die with 2- mm holes)

### 3.2.2 Instruments and equipments for transesterification

1. Round bottom flask 100 mL

2. Condenser

3. Glass column (30- cm height and 3- cm diameter)

4. Thermometer

5. Water bath

6. Heater equipped with stirrer

7. Band heater

8. Temperature controller

9. Centrifuge

10. Rotary evaporator

## 3.3 Instruments and Equipments for Characterization of Catalyst

### 3.3.1 X-ray fluorescence spectrometer (XRF) [58]

Elemental analysis of a catalyst was performed on an Oxford ED-2000 X-ray fluorescence spectrometer at the Scientific and Technological Research Equipment Centre of Chulalongkorn University. X-ray fluorescence is an x-ray instrument used for routine, relatively non-destructive chemical analyses of materials. The analysis of major and trace elements in materials by X-ray fluorescence is made possible by the behavior of atoms when they interact with radiation. When materials are excited with high-energy, short wavelength radiation (e.g., X-rays, gamma ray), they can become ionized. If the energy of the radiation is sufficient to eject an inner electron, the atom becomes unstable and an outer electron replaces the missing inner electron. When this happens, energy is released due to the decreased binding energy of the inner electron orbital compared with an outer one. The emitted radiation is of lower energy than the primary incident X-rays and is termed fluorescent radiation. Because the energy of the emitted photon is characteristic of a transition between specific electron orbitals in a particular element, the resulting fluorescent X-rays can be used to detect the abundances of elements that are present in the sample.

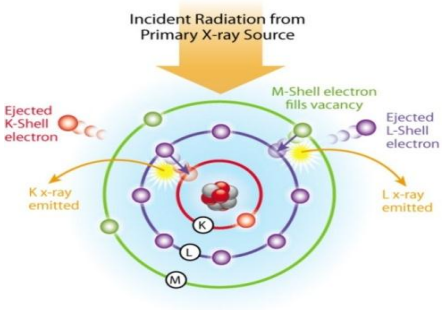


**Figure 3.2** Schematic of the XRF principle. Incident X-ray knocks out an inner shell electron, higher shell electron fills the empty vacancy and excess energy given up as an X-ray (photon).

### 3.3.2 X-ray diffractometer (XRD) [59]

Structure of a catalyst was determined by a technique of powder XRD using a Bruker D8 Discover equipped with Cu Kα radiation. X-ray diffraction is a family of non-destructive analytical techniques which display information about the crystal structure, chemical composition, and physical properties of materials. The X-ray diffraction is now a common technique for the study of crystal structures and atomic spacing that crystalline substances act as three-dimensional diffraction gratings for X-ray wavelengths similar to the spacing of planes in a crystal lattice. X-ray diffraction is based on constructive interference of monochromatic X-rays and a crystalline sample. These X-rays are generated by a cathode ray tube, filtered to produce monochromatic radiation, collimated to concentrate, and directed toward the sample. The interaction of the incident rays with the sample produces constructive interference and a diffracted ray when conditions satisfy Bragg's Law ($n\lambda = 2d \sin \theta$, Where $n$ = an integer, $d$ = interplanar distance of the crystal (Å; 1 Å= $10^{-10}$ m), $\theta$ = angle between X-ray and crystal planes (degree, $\lambda$ = wavelength (Å). This law relates the wavelength of electromagnetic radiation to the diffraction angle and the lattice spacing in a crystalline sample. These diffracted X-rays are then detected, processed and counted. By scanning the sample through a range of $2\theta$ angles, all possible diffraction directions of the lattice should be attained due to the random orientation of the powdered material. Conversion of the diffraction peaks to $d$-spacings allows identification of the mineral because each mineral has a set of unique $d$-spacings. The diffraction of X-rays by a crystal is shown in Figure 3.4.

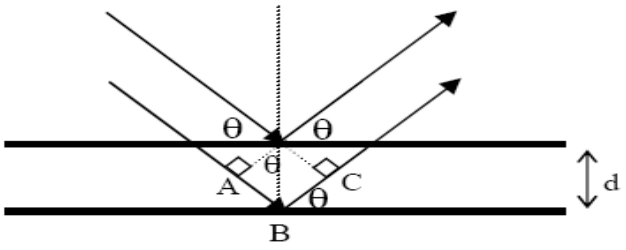


**Figure 3.3** Diffraction of X-ray by a crystal.

### 3.3.3 Thermogravimetric/differential thermal analyzer (TG/DTA) [60]

Thermogravimetric analysis (TGA) was carried out by using a Perkin Elmer Pyris Diamond thermogravimetric/differential thermal analyzer. Typically, 10 mg of a sample was placed in a platinum pan and heated from 40 to 1,000 °C at a ramping rate of 8 °C $min^{-1}$ with air flow rate of 50 mL $min^{-1}$.


**Figure 3.4** Thermogravimetric/differential thermal analyzer.

A type of testing that is performed on samples to determine changes in weight in relation to change in temperature. This analysis relies on a high degree of accuracy in three measurements: weight, temperature, and temperature change. Thermal gravimetric analysis is the act of heating a mixture to a high enough temperature so that one of the components decomposes into a gas, which separates into the air. Heat and stoichiometric ratios are used to determine the percent by mass ratio of solute. If we are known of the compounds in the mixture, then the percentage by mass can be determined by taking the weight of what is left in the mixture and subdividing it by the initial mass. Knowing the mass of the first mixture and the total mass of impurities releasing upon heating the stoichiometric ratio can be used to calculate the percent mass of the substance in a sample. TGA is commonly employed in research and testing to determine characteristics of materials such as polymers, to determine degradation temperatures, absorbed moisture content of materials, the level of inorganic and organic components in materials, decomposition points of explosives, and solvent residues. It is also often used to estimate the corrosion kinetics in high temperature oxidation.

Differential thermal analysis (or DTA) is a thermoanalytic technique, similar to differential scanning calorimetry. In DTA, the material under study and an inert reference are made to undergo identical thermal cycles, while recording any temperature difference between sample and reference. This differential temperature is then plotted against time, or against temperature (DTA curve). Changes in the sample, either exothermic or endothermic, can be detected relative to the inert reference. Thus, a DTA curve provides data on the transformations that have occurred, such as glass transitions, crystallization, melting and sublimation. The area under a DTA peak is the enthalpy change and is not affected by the heat capacity of the sample.

### 3.3.4 Chemisorption analyzer

Chemisorption analysis of a catalysts was performed by the temperature-programmed desorption (TPD) method, using an AutoChemII 2920 of Micromeritics equipped with a thermal conductivity detector (TCD) (Figure 3.5). In case of basicity measurement, $CO_2$ was used as a probe molecule. The experimental procedure for $CO_2$-chemisorption measurements starts from pretreatment of a sample under Ar flow at 300 °C (50 mL $min^{-1}$) for 1 h. After that, $CO_2$ was allowed to contact the clean sample at 100 °C for 1 h (10 mL $min^{-1}$). Subsequently, the signal of $CO_2$ was collected upon elevating the sample temperature to 800 °C.


**Figure 3.5** Chemisorption analyzer.

Chemisorption is a fundamental process in heterogeneous catalysis. The chemisorptions process associated with an interaction of catalyst surface and reactant.

Therefore, the temperature at which gases are desorbed from a surface is demonstrative for describing the strength of bonds between the gas molecules and the catalyst surface. The adsorption of a probe molecule at low temperature followed by monitoring of its desorption characteristics with temperature elevated can be characterize the surface properties of catalysts and absorbents. This is the basis of temperature-programmed analysis methods in which, for a linear increase in temperature, the concentration of the reacting/desorbing molecules is recorded as a function of temperature.

Pulse chemisorption, a flowing gas technique, is regularly performed at ambient pressure. After a sample was cleaned at a certain temperature, an adsorbate is injected until the sample is saturated. A calibrated thermal conductivity detector (TCD) is used to determine the quantity of adsorptive molecules taken up by active sites. Initial injections may be total adsorption until the injection gives none of significant adsorption that indicates the saturation. The number of molecules of gas adsorbed is directly related to the exposed surface area of active material.

### 3.3.5 Scanning electron microscope (SEM) [61]

Morphological study of a catalyst was carried out with a JEOL JSM-5410 LV electron microscope (SEM). The sample was sputter-coated with gold before the observation. The SEM micrographs were taken by using a 15 kV electron beam with a magnification of 15 - 35,000.

SEM was built and incorporated a fine beam of electron about 200 angstroms across to scan the specimen much like the "single spot of light that passes across the face of a television screen to build an entire picture". The interactions with the electron beam and the "specimen surface causes several types of energetic emissions, including backscattered electrons, secondary electrons, Auger electrons (a special form of secondary electrons), continuous X-rays, and characteristics X-rays" (Reed-Hill and Abbaschiam, 1994). The image displayed on the cathode ray tube comes from the secondary and backscattered electrons. The secondary electrons are the

excited electrons emitted from the specimen by being bombarded by the electron beam. A simple schematic diagram of the SEM can be seen in Figure 3.6.

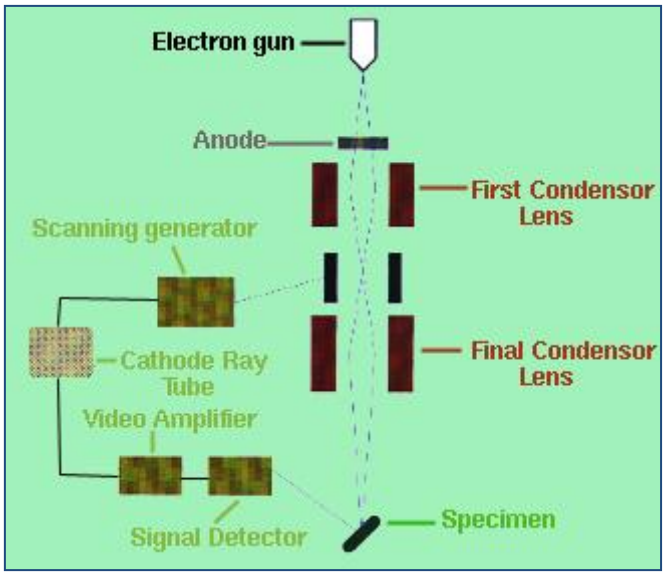


**Figure 3.6** Schematic diagram of scanning electron microscope [61].

Phases within a material are distinguished by the backscattering electrons. The backscattered electrons are affected by the atomic number of the atom in a way that causes the electrons scattered by the atom with the lowest atomic number to not reach the detector. These electrons will therefore appear dark in the image. As the atomic number increases, the corresponding region will appear lighter

### 3.3.6 Surface area and porosity analyzer

Specific surface area of a calcined catalyst was determined by $N_2$ adsorption-desorption measurement using a Micromeritics ASAP 2020 surface area and porosity analyzer (Figure 3.7).


**Figure 3.7** Surface area and porosity analyzer.

BET surface area analysis is a technique used to determine the specific surface area of powders, solids and granules, the values are expressed in meter square per gram. Clean solid surfaces adsorb surrounding gas molecules and Brunauer, Emmett and Teller theory (BET) provides a mathematical model for the process of gas sorption. This physical adsorption of a gas over the entire exposed surface of a material and the filling of pores is called physisorption and is used to measure total surface area and pore size analysis of nanopores, micropores and mesopores. The BET surface area measurement is crucial in understanding the behaviour of a material, as material reacts with its surroundings via its surface, a higher surface area material is more likely to react faster, dissolve faster and adsorb more gas than a similar material with a lower surface area.

### 3.4 Reaction Products Analysis

FAME composition was determined by a Shimadzu GC-14B gas chromatograph (GC) equipped with a 30-m DB-Wax capillary column and a flame ionization detector (FID) (Figure 3.8). The GC conditions for determination of FAME composition are shown in Table 3.1.

**Table 3.1** GC conditions for determination of methyl esters composition

| Condition | Value |
|---|---|
| Carrier gas (He) flow rate | 1.0 mL $min^{-1}$ |
| Make up gas (He) pressure | 100 kPa |
| Hydrogen pressure (for FID) | 60 kPa |
| Air pressure (for FID) | 30 kPa |
| Detector temperature | 250 °C |
| Split ratio | 1 : 100 |
| Injection port temperature | 250 °C |
| Inject volume | 0.1 μL |
| Initial column temperature | 180 °C |
| Ramp rate | 8 °C $min^{-1}$ |
| Final column temperature | 200 °C |

**Figure 3.8** Gas chromatograph.

The quantitative analysis of FAME was based on an external standardization method according to EN 14103. Methyl heptadecanoate ($C_{18}H_{36}O_2$) was used as the reference standard and *n*- heptane ($n$-$C_7H_{16}$) was used as the solvent. The calculation of the FAME yield followed the equation below:

$$\text{FAME yield (wt.\%)} = \frac{\text{Weight of FAME attained by GC}}{\text{Theoretical weight of FAME}} \times 100 \quad (3.1)$$

### 3.5 Preparation of catalyst from natural dolomite by dissolution-precipitation method

Firstly, dolomite was calcined in a muffle furnace at 600-800 °C. The calcined dolomite was then mixed with a solution of nitric acid with pH ranging from 1-3 under vigorous stirring at room temperature for 2 h. Subsequently, aluminium oxide ($Al_2O_3$) as a binder was added and the mixture was stirred for 1 h. After that, the resulting slurry was sonicated for 4 h and then dried at 100 °C overnight. The dried solid was crushed by a mortar and calcined in a muffle furnace at 500-800 °C. Hereafter, the catalyst is designated as DM x00+$Al_2O_3$+Y where DM x00, $Al_2O_3$ and Y represent type of calcined temperature of dolomite, aluminium oxide and hydroxyethyl cellulose (HEC) or $NaAlO_2$, respectively.

### 3.6 Formulation of catalyst from natural dolomite by dissolution-precipitation method

A solution of nitric acid with pH ranging from 1-3 was prepared. A dolomite calcined at 800 °C was added into the solution, followed by stirring at room temperature for 2 h. $Al_2O_3$ was then added into the mixture. After stirring at room temperature for 1 h, HEC was mixed with the slurry at room temperature for 1 h. The resulting mixture was further vigorously stirred at 100 °C until an uniform paste was formed. Finally, the paste was shaped into continuous rod with cross-sectional diameter of 2 mm by using a manual extruder. The solid extrudated was dried at 100 °C, cut into 5-mm length followed by calcination in muffle furnace at 500-800 °C.

### 3.7 Transesterification of RBD palm oil with methanol in a batch reactor

A 100-mL three-neck round bottom flask equipped with a water-cooled condenser and a magnetic stirrer was used as a batch reactor for transesterification of palm oil with methanol. According to the previous study, the suitable molar ratio of methanol/oil was fixed at 30 [31]. A calcined catalyst (1g) was suspended in methanol and temperature of the slurry was controlled at 60 ºC by using a water bath. Palm oil

(10 g) was added into the flask under vigorous stirring. After the course of reaction (3 h), the catalyst was separated from the reaction mixture by centrifugetion and the excess methanol was removed by using a rotary evaporation. FAME layer was subsequently washed with deionized water and dried with $Na_2SO_4$. The FAME, equivalent to FAME yield, was determined by a gas chromatograph (GC).

### 3.8 Transesterification of RBD palm oil with methanol in a fix-bed reactor

Transesterification of palm oil with methanol in a fix-bed reactor was carried out in a glass column (30-cm height and 3-cm diameter) packed with about 100 g of calcined catalyst extrudates. Glass bead with diameter of ca. 3 mm (30 g ) was used as the bed supporter. The glass bead was also added to the top of extrudate bed in order to prevent the catalyst overflowing with the product from the top of the column. Typically, oil and methanol were separately fed upward into the column by peristaltic pumps with a LHSV of 0.96 $h^{-1}$ (Figure 3.9), total flow rate 2.0 ml $min^{-1}$ and the methanol/oil molar ratio inside the reactor was maintained at 30. The column temperature was controlled at 65 °C by using a band heater equipped with a thermocouple connected to a temperature controller. The product mixture was collected in a 50-mL glass bottle at every hour. The excess methanol was removed by a rotary evaporator and the layer of ester phase was recovered without any washing. The analysis of the ester phase was carried out with a Shimadzu 14B gas chromatograph (GC) equipped with a FID detector and a 30-m DB- Wax capillary column.

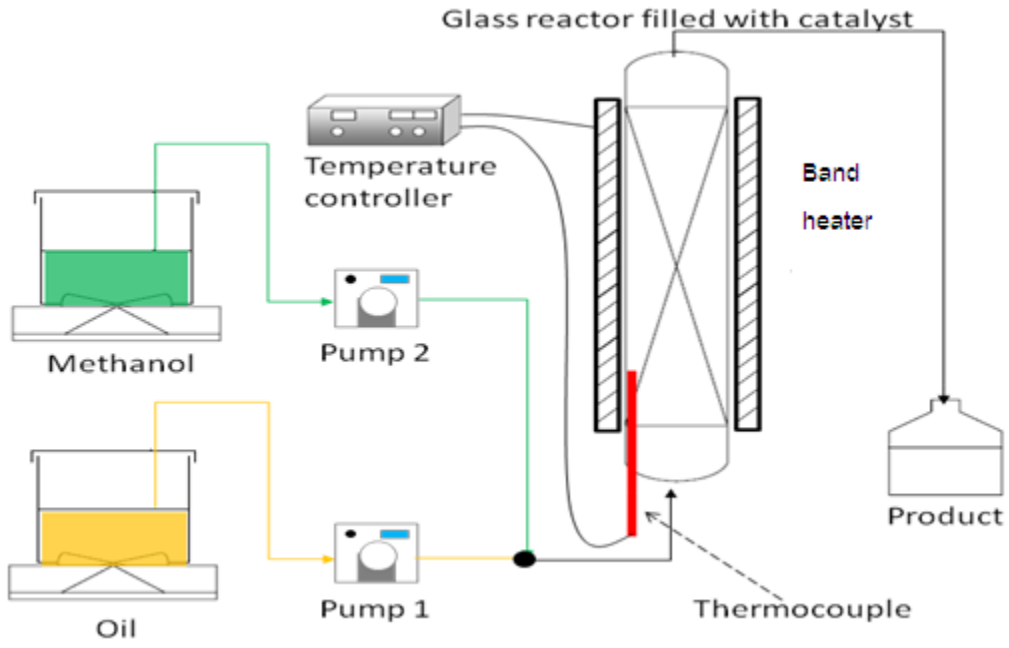


**Figure 3.9** Experimental setup for transesterification of vegetable oil under fixed bed conditions.

### 3.9 Quantitative analysis of monoglycerides, diglycerides and triglycerides on FAME

An Agilent 7890A gas chromatograph (GC) equipped with a FID detector and a 15-m DB-5ht capillary column was applied to the quantification of glycerides remaining. The analysis method was carried out according to the standard method of EN 14105 using tricaprin as the reference standard. *N*-methyl-*N*-(trimethylsilyl)trifluoroacetamide (MSTFA, > 99%, Fluka) was used to convert monoglycerides and diglycerides to more volatile derivatives. A small amount of sample (about 0.1 g) was dissolved in about 100 µL of 99% *N*-methyl-*N*(trimethylsilyl)trifluoroacetamide. The solution was shaked and placed at room temperature for 25 min. Subsequently, 100 µL of tricapin (5 mg $mL^{-1}$) and 100 µl of methyl heptadecanoate (30 mg $mL^{-1}$) were added into the solution. Finally, the volume of the solution was adjusted to 1.5 mL with *n*-heptane.

# CHAPTER IV
# RESULTS AND DISCUSSION

## 4.1 Dolomite as a heterogeneous base catalyst for transesterification of vegetable oil

### 4.1.1 Physical properties of dolomite

**Table 4.1** Elemental composition of natural dolomite analyzed by XRF spectroscopy

| Catalyst | Composition (wt.%) | | | | | |
|---|---|---|---|---|---|---|
| | CaO | MgO | $Al_2O_3$ | $SiO_2$ | Other[a] | Total |
| Dolomite | 32.42 | 19.88 | 0.12 | 0.27 | 47.31 | 99.97 |

[a]Carbon dioxide as the major component.

The elemental analysis of natural dolomite determined by means of XRF is shown in Table 4.1. The natural dolomite composed of Ca and Mg as the main metals with a trace amount of Al and Si. It was expected that Ca and Mg were present in the form of mixed carbonate compounds as $CaMg(CO_3)_2$ since other elements found were C and O.

The XRD patterns of non-calcined dolomite (as-received), dolomite calcined at 600 °C (DM-600) and dolomite calcined at 800 °C (DM-800) are shown in Figure 4.1. It can be seen that the parent dolomite consisted of $CaMg(CO_3)_2$ and $CaCO_3$ both of which were rhombohedral structure of calcite (Figure 4.1(a)). The decomposition of the carbonate species started from 600 °C at which $MgCO_3$ in $CaMg(CO_3)_2$ was transformed to MgO, whereas $CaCO_3$ was transformed to CaO at 800 °C. The presence of $Ca(OH)_2$ peaks should be related to a rapid reaction of CaO with moisture in the atmosphere during the sample preparation for the XRD analysis (Figure 4.1(c)).

The TGA result indicated that the decarbonation of the mixed metal carbonates occur particularly at 780 °C (Figure 4.2). Therefore, the calcination of dolomite at 800 °C is enough to convert the carbonates into the basic metal oxides.

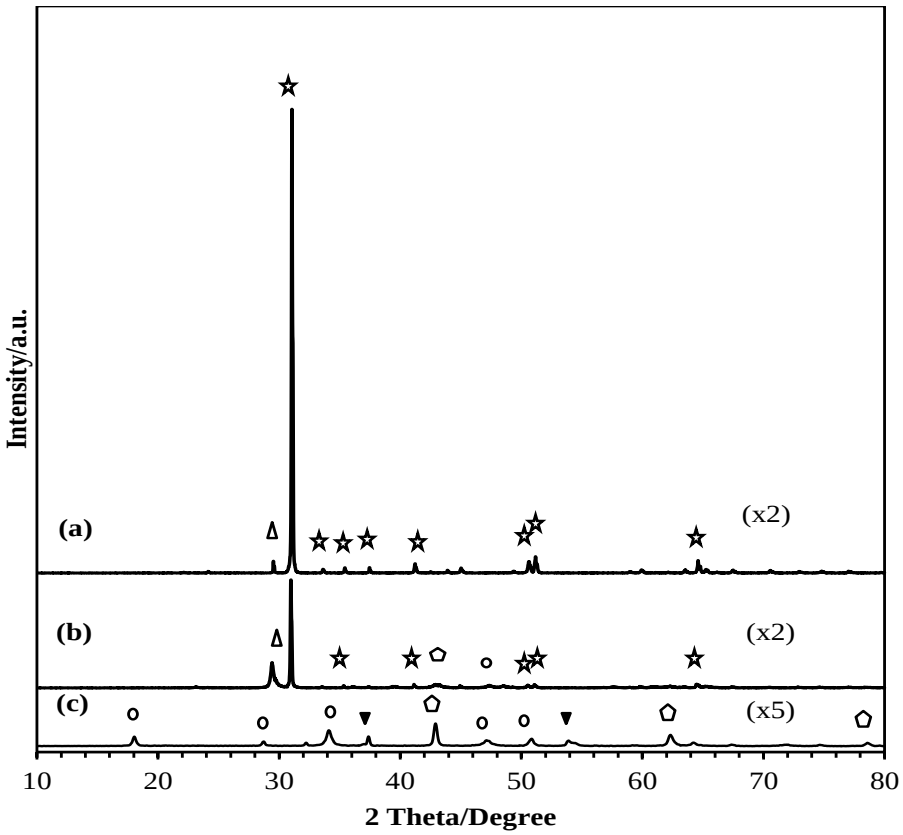


**Figure 4.1** XRD patterns of non-calcined dolomite (a), and dolomite calcined at 600 °C (b) and 800 °C (c). (Symbols: (☆) $CaMg(CO_3)_2$, (Δ) $CaCO_3$, (○) $Ca(OH)_2$, (▼) CaO and (⌂) MgO )

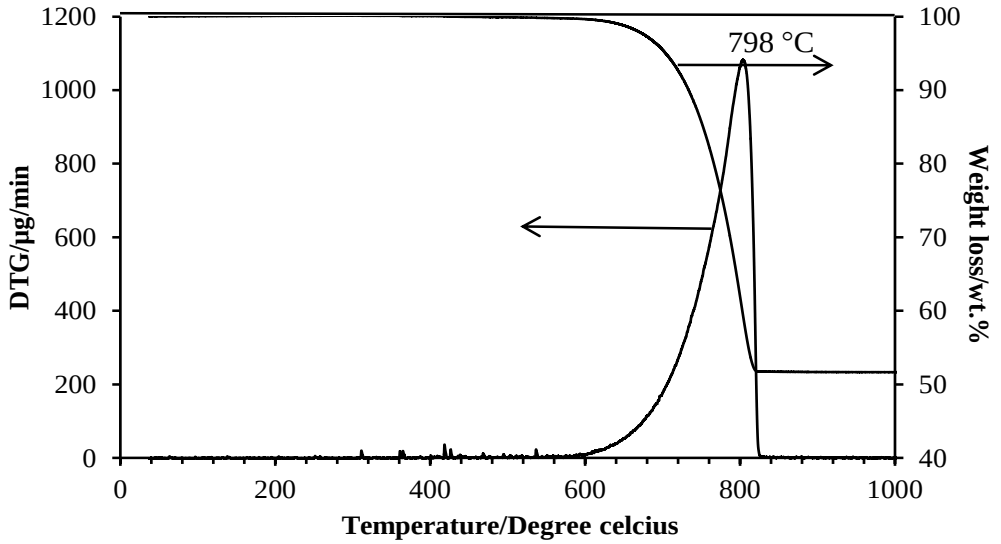


**Figure 4. 2** Weight loss and DTG curves of natural dolomite.

### 4.1.2 Transesterification of vegetable oil over natural dolomite calcined at different temperatures

Effects of calcination temperature of natural dolomite on the transesterification of RBD palm oil with methanol are summarized in Table 4.2. The as-received dolomite and the dolomite calcined at 600 °C did not catalyze the transesterification. The FAME yield of 89.4% was achieved when the calcination of dolomite was performed at 800 °C. These results should be related to the extensive degree of decarbonation of dolomite at 800 °C, providing the active basic sites for the transesterification. Taking into account these reaction results and the data from XRD (Figure 4.1), it was suggested that CaO was the catalytically active sites.

**Table 4.2** Effects of calcination temperature of natural dolomite on FAME yield attained from transesterification[a] of palm oil with methanol in batch reactor

| Catalyst | Calcination temperature (°C) | FAME yield (wt.%) |
|---|---|---|
| Dolomite | None | 0 |
| | 600 | 0 |
| | 800 | 89.4 |

[a]Reaction conditions: Methanol/oil molar ratio, 30; catalyst amount, 10 wt.%; temperature, 60 °C; time, 3 h.

## 4.2 Preparation of heterogeneous base catalysts from dolomite by dissolution-precipitation method

### 4.2.1 Effects of pH of nitric acid solution

The XRD patterns of DM800 merged in nitric acid solution with pH of 1, 2 and 3 are shown in Figure 4.3. It can be seen that the major phases presenting in the dried samples were $Ca(OH)_2$ and $Mg(OH)_2$. $CaCO_3$ at 2 Theta about 30 degree observed that increased intensity when decreasing the solution acidity from pH 1 to pH 3. It can be indicated that the active metal precursor was less dissolved. $CaCO_3$ should be restored from adsorption of $CO_2$ in the atmosphere onto CaO during the catalyst preparation. After the calcination at 800 °C, the transformation of the

hydroxide and the carbonate structures to the corresponding oxides occurred, as shown in Figure 4.4.

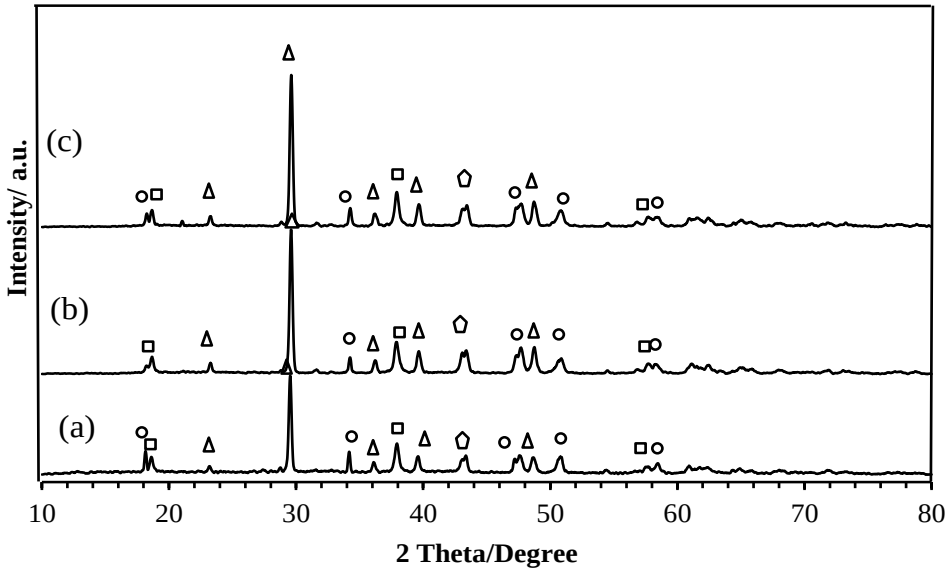


**Figure 4.3** XRD patterns of DM800 merged in nitric acid solution with pH of 1 (a), 2 (b) and 3 (c). The samples were dried at 100 °C prior to the analysis. (Symbols: (Δ) $CaCO_3$, (○) $Ca(OH)_2$, (□) $Mg(OH)_2$, (▼) CaO and (⌓) MgO )

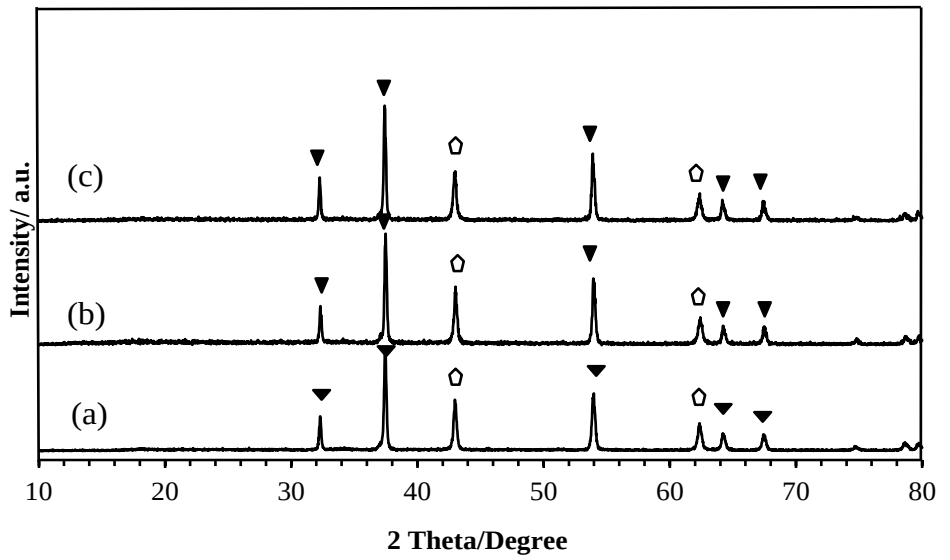


**Figure 4.4** XRD patterns of DM800 merged in nitric acid solution with pH of 1 (a), 2 (b) and 3 (c), followed by calcination at 800 °C for 2 h. (Symbols: (Δ) $CaCO_3$, (○) $Ca(OH)_2$, (□) $Mg(OH)_2$, (▼) CaO and (⌓) MgO )

**Table 4.3** Effects of pH of nitric acid solution used in preparation of dolomite catalyst on FAME yield attained from transesterification of palm oil with methanol in batch reactor

| Catalyst[a] | pH | FAME yield[b] (wt.%) |
|---|---|---|
| Dolomite | 1 | 94.9 |
| | 2 | 86.4 |
| | 3 | 80.2 |

[a]Catalyst was calcined at 800 °C.
[b]Reaction conditions: Methanol/oil molar ratio, 30; catalyst amount, 10 wt.%; temperature, 60 ºC; time, 3 h.

Effects of pH of nitric acid solution for the preparation of catalyst on the transesterification of palm oil with methanol are summarized in Table 4.3. An enhancement of the FAME yield from 80.2 to 95% was observed when increasing the solution acidity from pH 3 to pH 1. The high acidity of the solution should dissolve better an active metal precursor from the calcined dolomite. The dehydration of $Ca(OH)_2$ into CaO generates a new oxide structure with higher surface area and basicity [46].

### 4.2.2 Effect of adding binder ($Al_2O_3$)

The XRD patterns of the catalysts prepared from dolomite calcined at 800 °C, with adding $Al_2O_3$ (DM800+$Al_2O_3$) before and after the calcination at 500 °C, 600 °C, 700 °C, and 800 °C are shown in Figure 4.5. Before the calcination (Figure 4.5 (a)), the major phases presenting in the catalyst were $Ca(OH)_2$ and $Mg(OH)_2$. The presence of $CaCO_3$ should be derived from the reaction of CaO and $CO_2$ existing in the ambient during the catalyst preparation. After the calcination (Figure 4.5 (b)-(e)), the catalysts exhibited a gradual increase in the amount of CaO and MgO phases concomitantly with decreasing of other phases. The largest amount of the oxide phases was attained at 800 °C (Figure 4.5 (e)). The peaks of $Ca(OH)_2$ appeared on the XRD patterns of the catalysts calcined at 500-800 °C (Figure 4.5(b)- (e)) should be due to the hydrolysis of CaO by moisture in the ambient air.

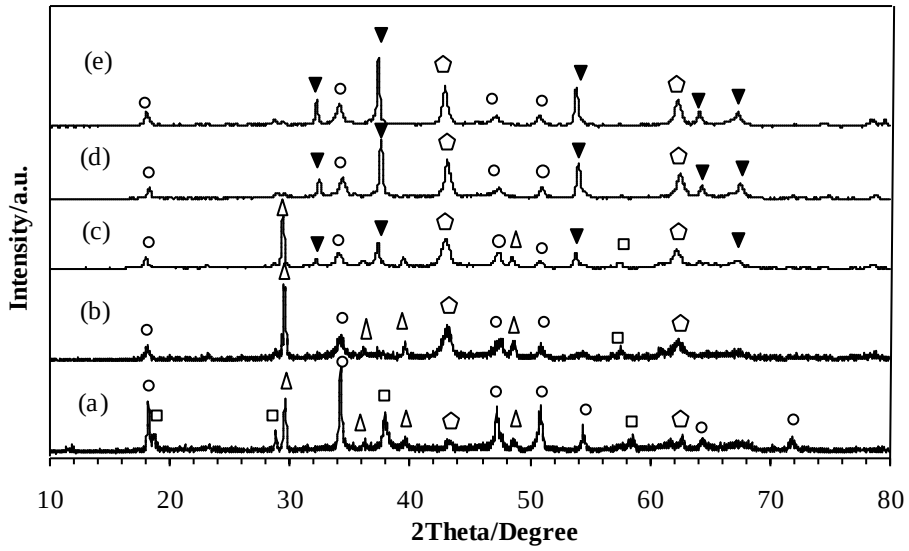


**Figure 4.5** XRD patterns of non-calcined DM800+$Al_2O_3$ (a), and DM800+$Al_2O_3$ calcined at 500 °C (b), 600 °C (c), 700 °C (d) and 800 °C (e). (Symbols: (Δ) $CaCO_3$, (○) $Ca(OH)_2$, (□) $Mg(OH)_2$ (▼) CaO and (⌂) MgO)

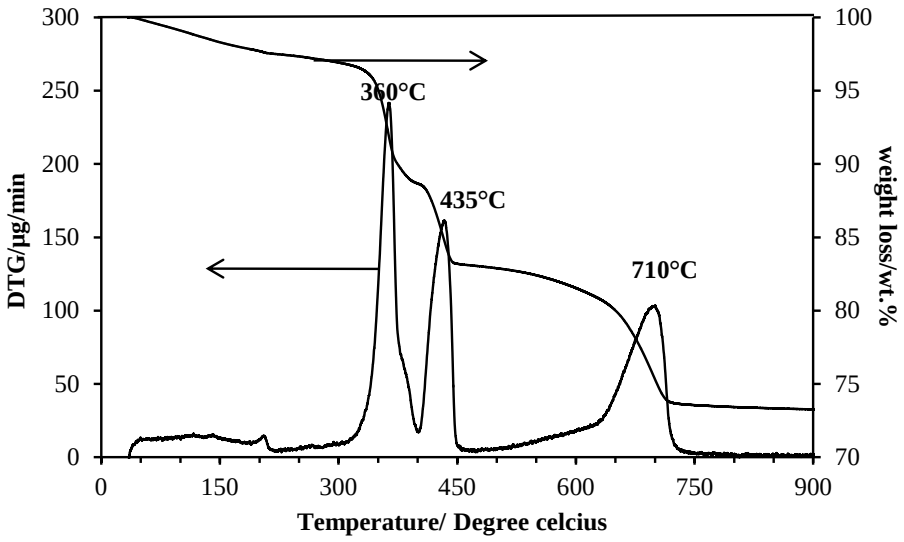


**Figure 4.6** Weight loss and DTG curves of as-synthesized DM800+$Al_2O_3$ catalyst.

Figure 4.6 reveals the weight loss and DTG curves of the as-synthesized DM800+$Al_2O_3$ catalyst. The decomposition pattern of DM800+$Al_2O_3$ catalyst exhibited a three-step weight loss. The weight loss at 360 ºC should be attributed to the decomposition of $Mg(OH)_2$ (8.3%), while the loss appearing at 435 ºC

corresponded to the water derived from the dehydration of $Ca(OH)_2$ (5.5%). The high temperature step at 710 ºC was related to the decomposition of $CaCO_3$ (10.2%), which was generated during the catalyst preparation as evidenced by the XRD results (Figure 4.5).

**Table 4.4** Effects of adding $Al_2O_3$ and calcination temperature of DM800+$Al_2O_3$ catalyst on FAME yield attained from transesterification of palm oil and methanol in batch reactor

| Catalyst[a] | Calcination temperature (°C) | Extrudate characteristics | | FAME yield[b] (wt.%) |
|---|---|---|---|---|
| | | after drying at 100°C | after calcination | |
| DM800 | 800 | Brittle | Very brittle | 95.1 |
| DM800+$Al_2O_3$ | None | Brittle | - | 13.5 |
| | 500 | Brittle | Very brittle | 47.3 |
| | 600 | Brittle | Very brittle | 60.4 |
| | 700 | Brittle | Very brittle | 80.2 |
| | 800 | Brittle | Very brittle | 92.4 |

[a]Catalyst was prepared in the nitric acid solution with pH of 1 and ratio of water/total solid = 1.5.
[b]Reaction conditions: Methanol/oil molar ratio, 30; catalyst amount, 10 wt.%; temperature, 60 ºC; time, 3 h.

In the presence of binder, the catalysts formulated gave the FAME yield lower than the pure dolomite prepared in the nitric acid solution with pH of 1 (Table 4.4).

The effects of calcination temperature for the preparation of DM800+$Al_2O_3$ extrudates on the transesterification of palm oil with methanol are summarized in Table 4.4. An enhancement of the FAME yield was observed when the calcination temperature was increased from 500 to 800 ºC. It should be due to an increase in the amount of CaO in the DM800+$Al_2O_3$ catalyst as informed by the XRD analysis (Figure 4.5). However, the extrudates attained after drying at 100 °C and calcining

were brittle by which the application of these catalysts in a fixed bed reactor was neglected.

### 4.2.3 Effects of adding plasticizer (HEC)

#### 4.2.3.1 Effects of HEC grade

HEC was used as plasticizer to improve characteristics of catalyst paste and extrudates. The HEC available are diversities by molecular weight, purity and cost. The molecular weight of HEC is reflected by viscosity of its aqueous solution, while the cost strongly depends on the HEC purity. Here, three different HEC from different companies were used for the comparison. The AR grade has much higher cost than the commercial grade (Table 4.5). Figure 4.7 and 4.8 show physical appearance of paste mixture and extruded catalyst, respectively. HEC with high viscosity, from Thai Specialty Chemical and A.H.A International neatly homogenized the catalyst paste (Figure 4.7(b) and (c)), whereas the mixture with HEC from Fluka was less homogeneous as shown in Figure 4.7(a). The extrusion of catalyst in the presence of HEC was easier performed and found that the mixture with HEC from A.H.A International passed the die gave the longer extrudates as shown in Figure 4.8(c).

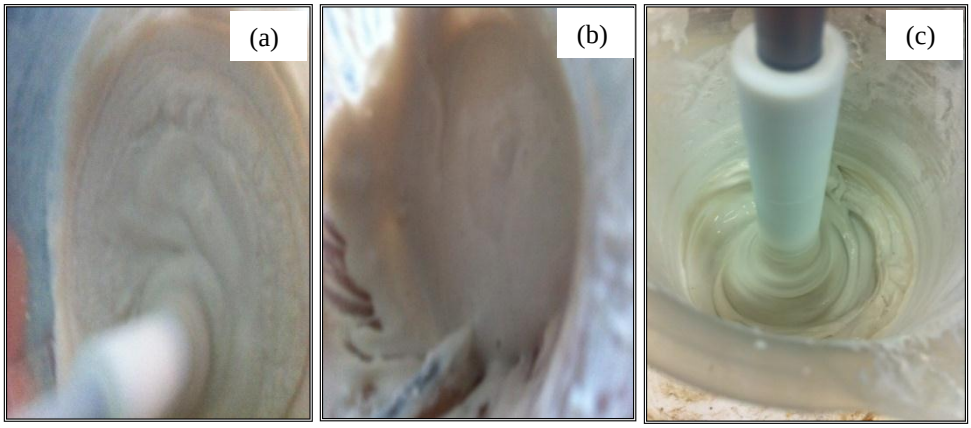


**Figure 4.7** Pastes of DM800+$Al_2O_3$+3%HEC catalyst containing different HEC; (a) Fluka, (b) Thai Specialty Chemical and (c) A.H.A International.

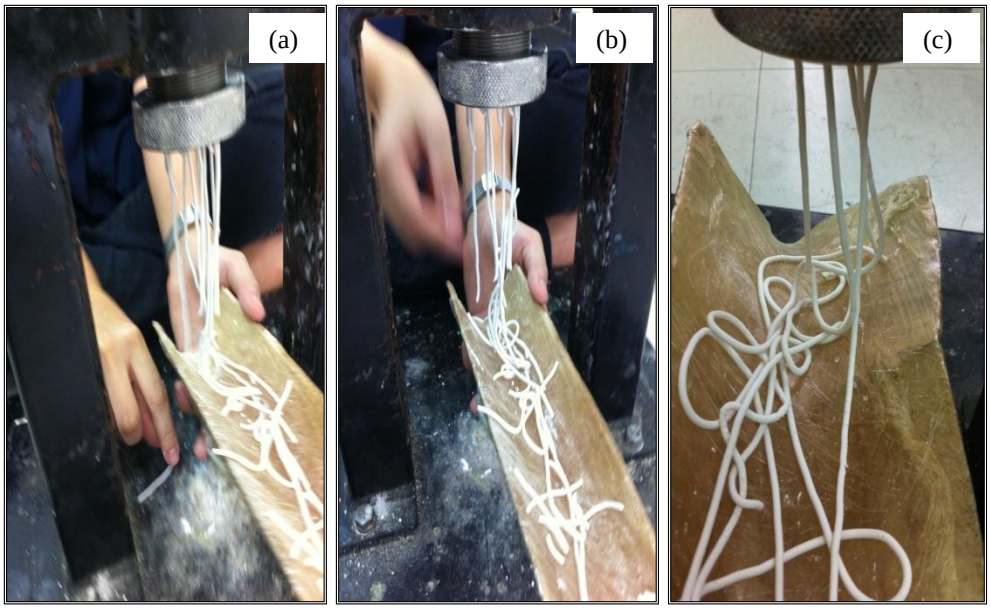


**Figure 4.8** Extrusion of DM800+$Al_2O_3$+3%HEC catalyst containing different HEC; (a) Fluka, (b) Thai Specialty Chemical and (c) A.H.A International.

**Table 4.5** Effects of HEC grade used in the preparation of DM800+$Al_2O_3$+3%HEC extrudates on FAME yield attained from transesterification of palm oil and methanol in batch reactor

| Catalyst[a] | HEC grade | Viscosity as aqueous solution (mPa.s) | Company | Cost (Baht/kg) | FAME yield[b] (wt.%) |
|---|---|---|---|---|---|
| DM800+$Al_2O_3$ + 3%HEC | AR | 113-150 at 5% | Fluka | 25,000 | 85.1 |
| | Commercial | 145 at 1% | Thai Specialty Chemical | 355 | 84.5 |
| | Commercial | 2,960 at 1% | A.H.A International | 320 | 86.6 |

[a]Catalyst was prepared in the nitric acid solution with pH of 1 and ratio of water/total solid = 1.5. The catalyst was calcined at 800 °C before being used.

[b]Reaction conditions: Methanol/oil molar ratio, 30; catalyst amount, 10 wt.%; temperature, 60 ºC; time, 3 h.

Table 4.5 shows the effects of HEC grade used in the preparation of DM800 +$Al_2O_3$+3%HEC extrudates on the FAME yield attained from the transesterification of palm oil and methanol. It is likely that the grade of HEC did not affect the FAME yield due to the calcination of catalyst extrudates at 800 °C, the HEC was completely decomposed. Therefore, the HEC from A.H.A International was used in the next study.

#### 4.2.3.2 Effect of drying temperature

The catalyst extrudates left at room temperature (Figure 4.9(a)), followed by the calcination at 800 °C were more brittle than the extrudates dried at 100 and 130°C (Figure 4.9(b) and 4.9(c)), respectively. This result may be related to the amount of water remaining in the catalyst extrudates before the calcination. The loss of water, both the physisorbed water and the water from the dehydration of the metal hydroxides, at once would damage the extrudate structure.

The bulk density of catalyst extrudates left at room temperature was observed that it was higher than the extrudates dried at 100 and 130°C due to the amount of water remaining in the catalyst extrudates as shown in Table 4.6.

**Table 4.6** Effects of drying temperature of DM800+$Al_2O_3$+3%HEC on extrudates characteristics

| Catalyst[a] | Drying temperature (°C) | Bulk density[b] (g/mL) | Extrudates characteristics | |
|---|---|---|---|---|
| | | | Drying | After calcining at 800 °C |
| DM800+$Al_2O_3$ | Room temp. | 0.72 | Hard | Very brittle |
| +3%HEC | 100 | 0.63 | Hard | Brittle |
| | 130 | 0.60 | Hard | Brittle |

[a]Catalyst was prepared in the nitric acid solution with pH of 1 and ratio of water/total solid = 1.5.
[b]Bulk density was determined from ratio of weight to volume of extrudates packed in a 500-mL cylinder.

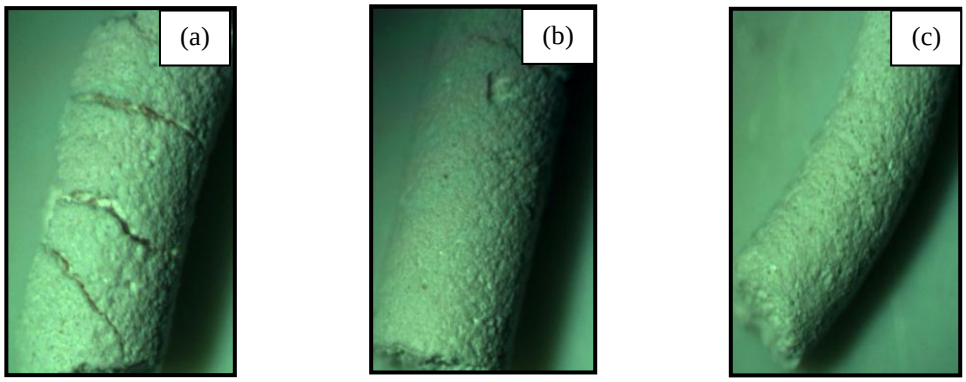


**Figure 4.9** Images of DM800+$Al_2O_3$+3%HEC extrudates dried at room temperature (a)**,** 100°C (b) and 130°C (c), followed by the calcination at 800°C.

#### 4.2.3.3 Effects of calcination temperature of catalyst extrudates

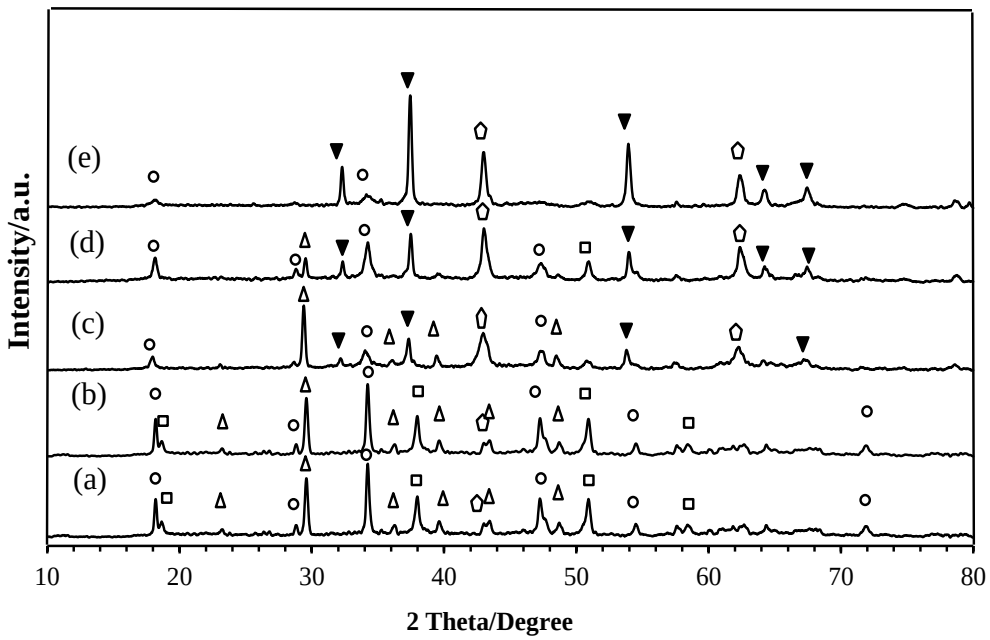


**Figure 4.10** XRD patterns of non-calcined DM800+$Al_2O_3$+3%HEC catalyst (a), and DM800+$Al_2O_3$+3%HEC calcined at 500 °C (b) , 600 °C (c), 700 °C (d) and 800 °C (e). (Symbols: (Δ) $CaCO_3$, (○) $Ca(OH)_2$, (□) $Mg(OH)_2$), (▼) CaO and (⌂) MgO)

Figure 4.10 shows XRD patterns of the catalysts prepared from dolomite calcined at 800 °C, with adding $Al_2O_3$ and 3%HEC (DM800+$Al_2O_3$+3%HEC) before and after the calcination at 500 °C, 600 °C, 700 °C and 800 °C. The major phases

presenting in the catalyst before the calcination (Figure 4.10 (a)) were $Ca(OH)_2$ and $Mg(OH)_2$. The presence of $CaCO_3$ should be derived from the reaction of CaO and $CO_2$ existing in the ambient during the catalyst preparation. After the calcination (Figure 4.10 (b)-(e)), the catalysts exhibited a gradual increase in the amount of CaO and MgO phases concomitantly with decreasing of other phases. The largest amount of the oxide phases was attained at 800 °C (Figure 4.10 (e)). The peaks of $Ca(OH)_2$ appeared on the XRD patterns of the catalysts calcined at 500-800 °C (Figure 4.10(b)-(e)) should be due to the hydrolysis of CaO by moisture in the ambient air.

The basicity of DM800+$Al_2O_3$+3%HEC catalyst calcined at 800 °C was higher than DM800 as shown in Table 4.7. The catalyst preparation by dissolution-precipitation method would bring about not loss of number of basic sites due to binder blockage. Furthermore, the enhancement of basicity of DM800+$Al_2O_3$+3%HEC catalyst from 18.7 to 35.0 μmol/g was observed when increasing the calcination temperature from 500 to 800 °C. Since the calcination at 500 °C, the major phase is $CaCO_3$ and $Ca(OH)_2$ and increased calcination temperatures were generated CaO phase as shown in XRD result (Figure 4.10).

**Table 4.7** Total basicity of DM800+$Al_2O_3$+3%HEC extrudates calcined at different temperatures

| Catalyst [a] | Calcined temperature of extrudates (˚C) | Number of basic site[b] (μmol/g) |
|---|---|---|
| DM800 | - | 29.2 |
| DM800+$Al_2O_3$+3%HEC | 500 | 18.7 |
| | 600 | 24.0 |
| | 700 | 26.1 |
| | 800 | 35.0 |

[a]Catalyst was prepared in the nitric acid solution with pH of 1 and ratio of water/total solid = 1.5.
[b]Measured by $CO_2$-pluse chemisorption technique.

Table 4.8 shows the effects of calcination temperature of DM800+$Al_2O_3$+3%HEC on the extrudates characteristics and the transesterification activity. All extrudates attained after drying at 100 °C were hard, but after calcining at

different temperatures they became brittle. Before the calcination, the catalyst gave FAME yield of 10.2%, suggesting that $Ca(OH)_2$ was not active in the transesterification. An enhancement of the FAME yield was observed when the calcination temperature was increased from 500 to 800 °C. It should be due to an increase in the amount of CaO and the number of basic sites in the catalysts as evidenced by the XRD results (Figure 4.10) and the chemisorption study (Table 4.7), respectively.

**Table 4.8** Effects of calcination temperature of DM800+$Al_2O_3$+3%HEC on extrudates characteristics and transesterification activity

| Catalyst[a] | Calcination temperature (°C) | Extrudate characteristics | | FAME yield[b] (wt.%) |
|---|---|---|---|---|
| | | Drying at 100 °C | After calcining | |
| DM800+$Al_2O_3$+3%HEC | None | Hard | - | 10.2 |
| | 500 | Hard | Brittle | 48.7 |
| | 600 | Hard | Brittle | 51.5 |
| | 700 | Hard | Brittle | 76.5 |
| | 800 | Hard | Brittle | 91.3 |

[a]Catalyst was prepared in the nitric acid solution with pH of 1 and ratio of water/total solid = 1.5.

[b]Reaction conditions: Batch reactor; methanol/oil molar ratio, 30; catalyst amount, 10 wt.%; temperature, 60 ºC; time, 3 h.

#### 4.2.3.4 Effects of water amount

A disadvantage of the dissolution-precipitation method is to spend a long time for evaporation of water after the mixing process. The amount of water remaining in the paste affects the formulation process. Here, the amount of water used in the paste preparation was varied in order to achieve the paste with an acceptable degree of formulation. Obviously, the decrease of water content could reduce half of time spent for the water evaporation. When the extruded paste left the die, surface fracture

(Figure 4.11a) was more found when used an equivalent weight of water to solid. The surface fracture enhances attrition of the extrudates.

**Table 4.9** Effects of water amount on extrudate characteristics

| Catalyst | Amount of water (times of total solid) | Extrudates characteristics | | |
|---|---|---|---|---|
| | | Surface fracture | Hardness | |
| | | | Drying at 100 °C | Calcined at 800 °C |
| DM800+$Al_2O_3$+4%HEC | 1 | Many | Hard | Brittle |
| | 1.5 | Little | Dense and hard | Brittle |

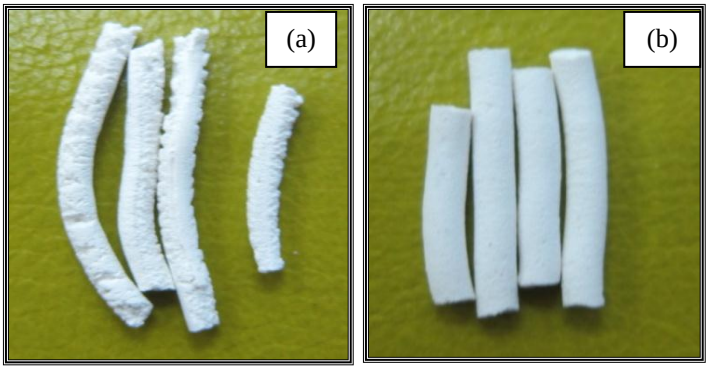


**Figure 4.11** Effect of water content on surface fracture of extrudates; (a) 1 and (b) 1.5 times.

Figure 4.12, shows the effect of water amount in the paste preparation on the FAME yield achieved from the transesterification in the fixed- bed reactor. The extrudates prepared by using the mass ratio of water/solid of 1 gave slightly lower FAME yield. It should be due to a large amount of surface fracture, resulting in a loss of the catalytic activity.

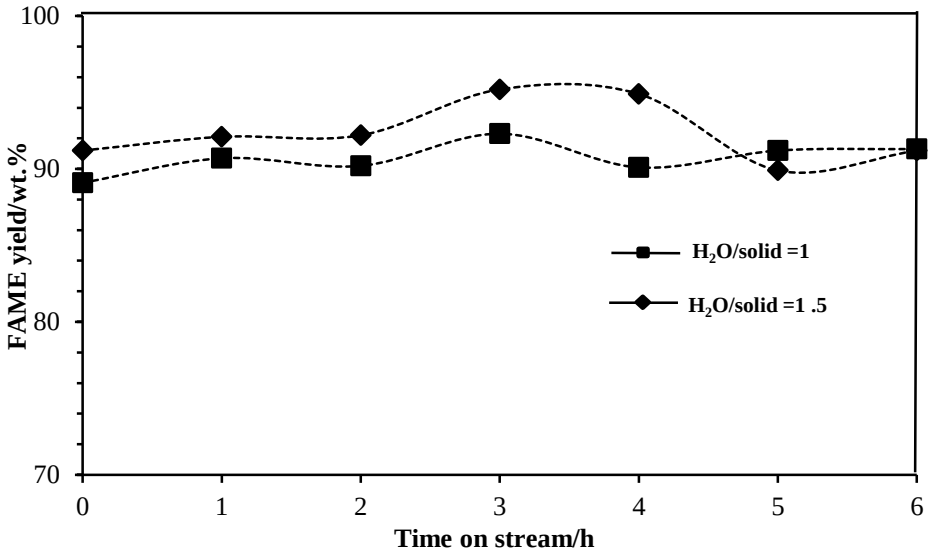


**Figure 4.12** Effect of water amount on FAME yield attained from transesterification of palm oil with methanol over DM800+$Al_2O_3$+4%HEC extrudates in a fixed-bed reactor. Reaction conditions: Methanol/oil ratio, 30; total flow rate, 2 mL/min; LHSV, 1.18 $h^{-1}$ ; temperature, 65 °C.

#### 4.2.3.5 Effects of amount of HEC

**Table 4.10** Effects of amount of HEC on textural properties of DM800+$Al_2O_3$+HEC extrudates

| Catalyst | Amount of HEC (wt.%) | $S_{BET}$[a] ($m^2/g$) | $V_p$[b] ($cm^3/g$) | $d_p$[c] (nm) |
|---|---|---|---|---|
| DM800+$Al_2O_3$ | 0 | 30.3 | 0.155 | 20.4 |
| +HEC | 1 | 18.4 | 0.071 | 15.6 |
| | 3 | 24.1 | 0.239 | 39.8 |
| | 4 | 24.8 | 0.208 | 33.4 |

[a]BET surface area.
[b]Average pore volume.
[c]Average pore diameter.

The textural properties of DM800+$Al_2O_3$+HEC extrudates with different HEC amounts, determined from the $N_2$ adsorption- desorption measurement (Table 4.10)

indicated a decrease in the BET surface area when adding HEC whereas the average pore volume and the average pore size were increased. The amount of 1% HEC added did not give the homogeneous paste. Consequently, the results of DM800+$Al_2O_3$ +HEC with 1%HEC were out of trend.

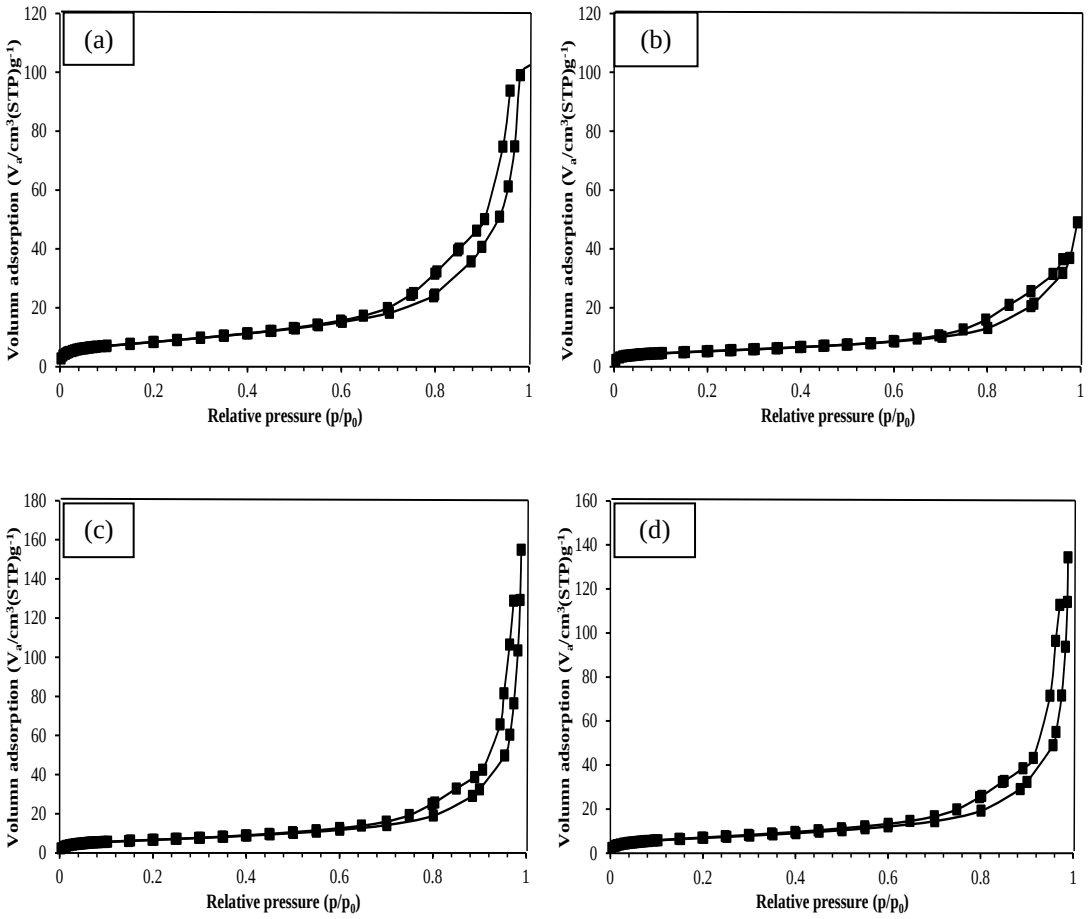


**Figure 4.13** $N_2$ adsorption-desorption isotherms of DM800+$Al_2O_3$+HEC extrudates prepared with different amounts of HEC; 0% HEC (a), 1%HEC (b), 3%HEC (c) and 4%HEC (d). The extrudates were calcined at 800 °C before the measurement.

As shown in Figure 4.13, all isotherms of DM800+$Al_2O_3$+HEC extrudates prepared with different amounts of HEC exhibited type III of the IUPAC classification. A hysteresis loop observed at high relative pressures ($P/P_0$ = 0.7–1.0) is associated with filling and emptying of mesopores via capillary condensation. The loop can be classified as type H3 profile which is ascribed to the presence of slit-shaped pores (or plate-like particles).

The pore size distribution determined from the BJH plot indicated that the major part of the catalyst particles exhibited a mean diameter of 12 nm (Figure 4.14(a)-(d)). Using HEC in the catalyst formulation shifted the pore size distribution towards larger diameters and generated new pores with the sizes around 50-60 nm except for DM800+$Al_2O_3$+1%HEC. The results indicated that adding HEC can increase the porosity of the extrudates.

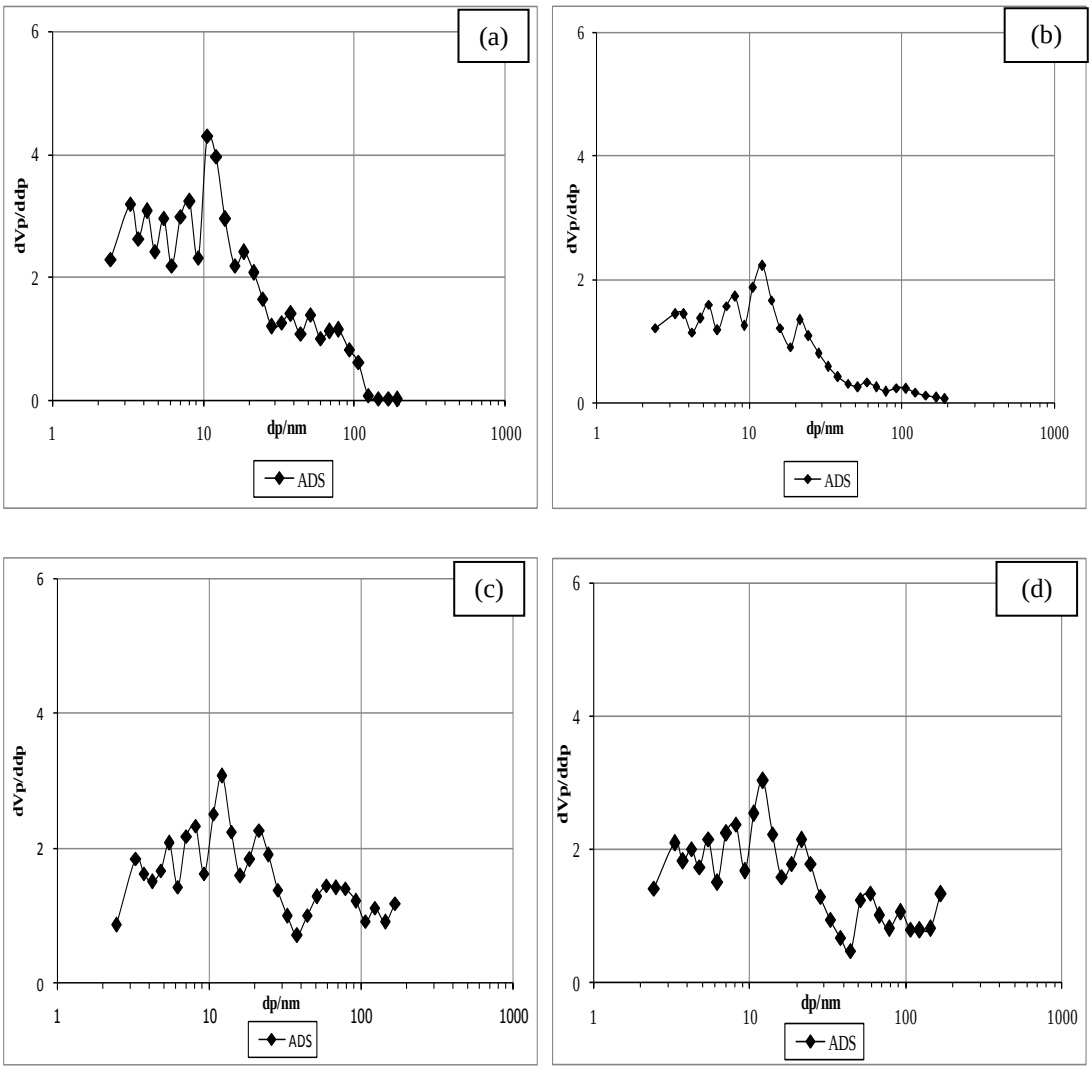


**Figure 4.14** BJH plots of DM800+$Al_2O_3$+HEC extrudates prepared with different amounts of HEC; 0% HEC (a), 1%HEC (b), 3%HEC (c) and 4%HEC (d). The extrudates were calcined at 800 °C before the measurement.

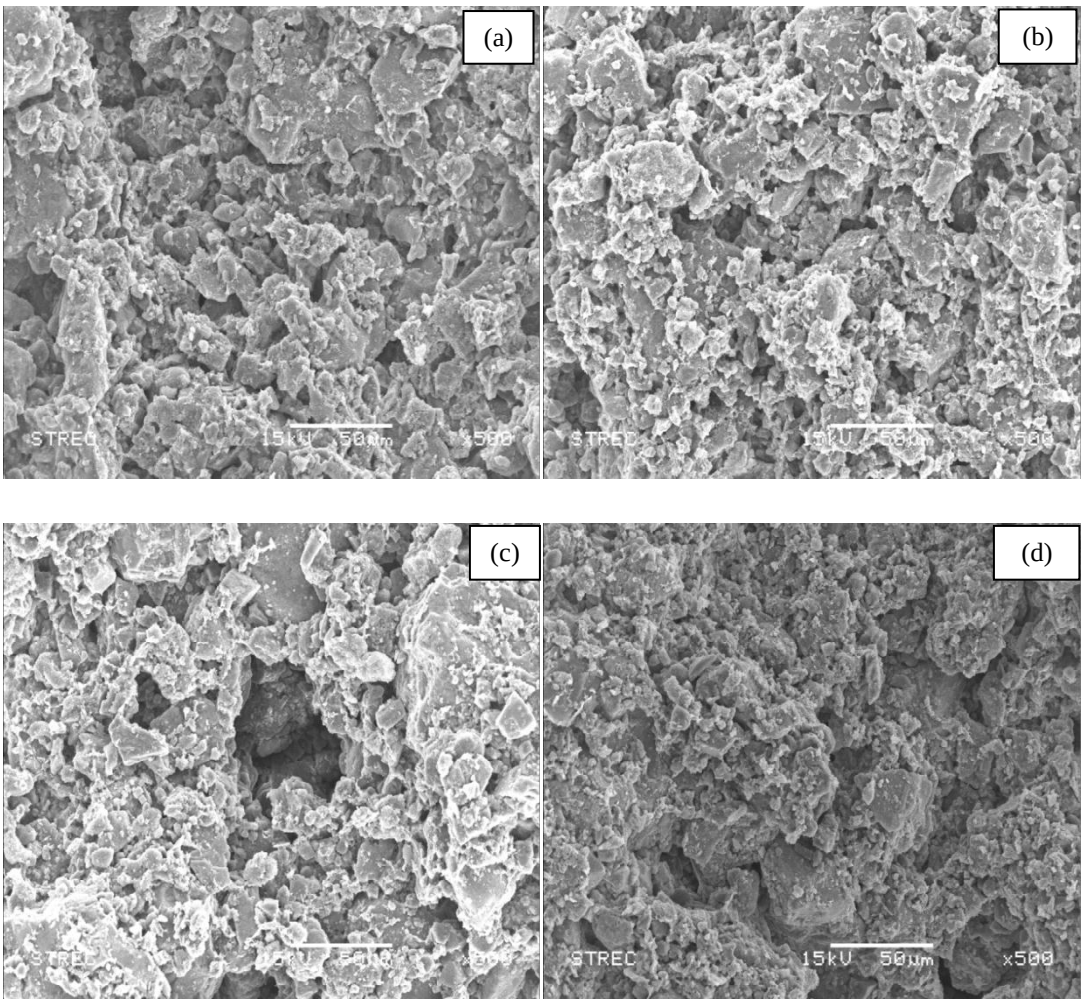


**Figure 4.15** SEM images of cross-sectional area of non-calcined DM800+$Al_2O_3$ +HEC extrudates prepared with different amounts of HEC; 0% HEC (a), 1% HEC (b), 3%HEC (c) and 4%HEC (d).

The cross-sectional area images of the catalyst extrudates prepared with different amounts of HEC after drying at 100 °C are shown in Figure 4.15. The bigger pores with average diameter of 18.4 µm appeared in the extrudates containing 3% and 4% HEC (Figure 4.15(c) and (d), respectively). Since HEC is a water-soluble polymer, the observed porous structure should be derived from a loss of water bound to HEC molecules. Without the HEC addition, the smaller pores with the average diameter of 10.7 µm were generated (Figure 4.15(a)).

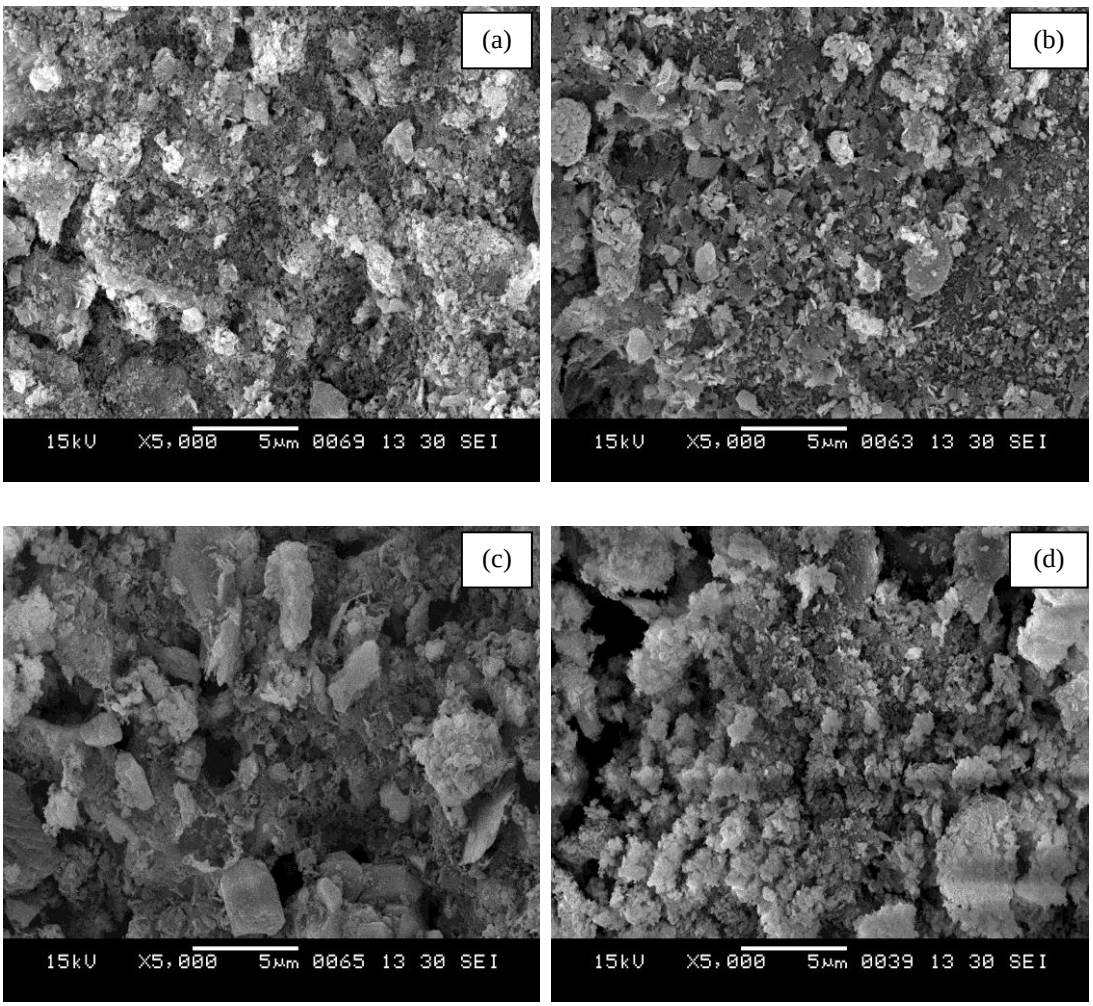


**Figure 4.16** SEM images of side area of calcined DM800+$Al_2O_3$+HEC extrudates prepared with different amount of HEC; 0% HEC (a), 1% HEC (b), 3%HEC (c) and 4%HEC (d).

The side area of the extrudates without the HEC addition exhibited a number of small pores with the average diameter of 1.07 μm (Figure 4.16a). They should be generated from the loss of water as both physisorbed one and dehydroxylation by-product. After adding HEC, the larger pore sizes were found (Figure 4.16(b)-4.16(d)). The average pore diameter was increased with increasing the HEC amount. These pores should not be only derived from the liberation of water, but also $CO_2$ that produced by the combustion of HEC during the calcination.

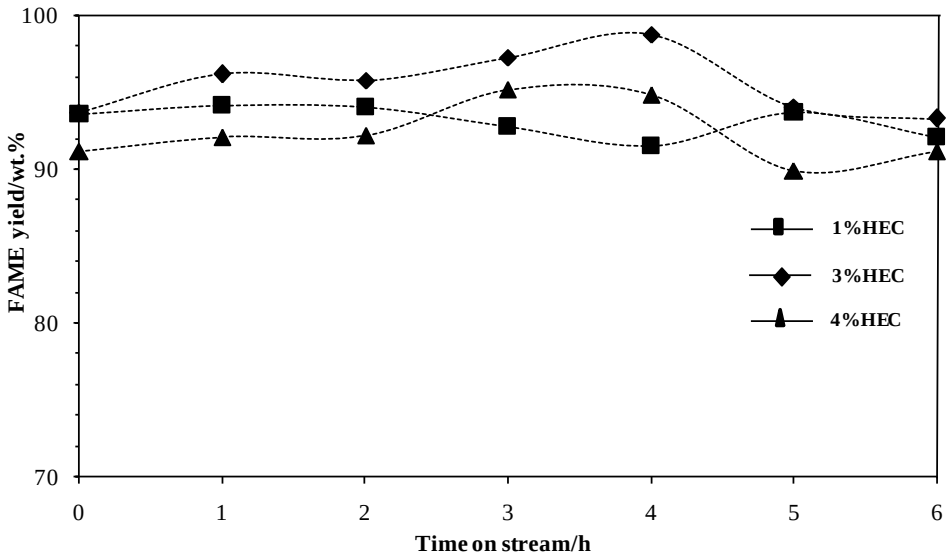


**Figure 4.17** Effect of HEC amount on FAME yield attained from transesterification of palm oil with methanol over DM800+$Al_2O_3$+HEC in a fixed-bed reactor. Reaction conditions: Methanol/oil ratio, 30; total flow rate, 2 mL/min; LHSV, 1.18 $h^{-1}$; temperature, 65 °C.

The effect of HEC amount on the FAME yield attained from the transesterification of palm oil with methanol over DM800+$Al_2O_3$+HEC in the fixed-bed reactor is shown in Figure 4.17. The highest FAME yield was achieved when using the extrudates with 3%HEC. This result may be related to the highest pore volume (Table 4.10) and the higher number of large pore sizes (Figure 4.16(c)) by which an efficient transport of the reactants to the active sites of catalyst extrudates can be ensured. After 3h of the reaction, all of the extrudates, however, were broken, especially, one in the middle of the reactor column, resulting a strange trend of the reaction results.

### 4.2.4 Effects of addition of sodium aluminate

From the physical appearance, the addition of $NaAlO_2$ in the catalyst paste remarkably improved the hardness of the resulting extrudates. In the present case, the amount of the sodium salt added was tuned to avoid the formation of soap.

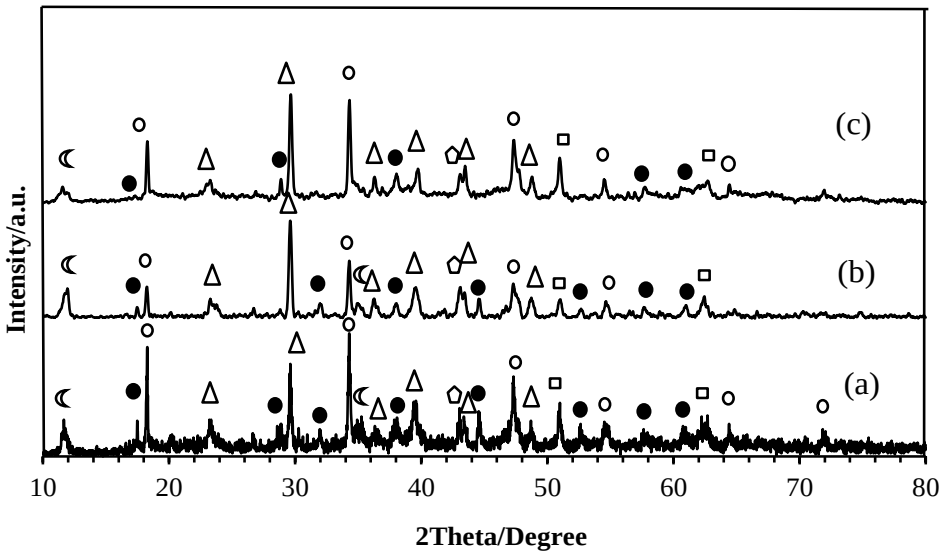


**Figure 4.18** XRD patterns of non-calcined DM800+$Al_2O_3$+$NaAlO_2$ catalysts: DM800 +$Al_2O_3$+$NaAlO_2$ (70:10:20) (a), DM800+$Al_2O_3$+$NaAlO_2$(70:10:20)+3%HEC (b) and DM800+$Al_2O_3$+$NaAlO_2$(70:20:10)+3%HEC (c). (Symbols: (Δ) $CaCO_3$, (○) $Ca(OH)_2$ , (□) $Mg(OH)_2$, (⌂) MgO, (≪) $Mg_2Al(OH)_7$, (●) $(CaO)_3Al_2O_3(H_2O)_6$)

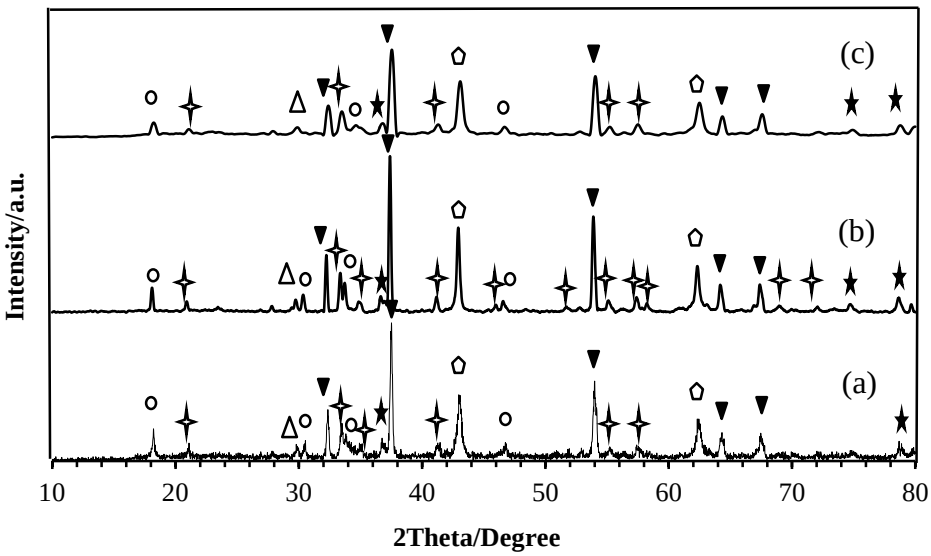


**Figure 4.19** XRD patterns of calcined DM800+$Al_2O_3$+$NaAlO_2$ catalysts: DM800 +$Al_2O_3$+$NaAlO_2$ (70:10:20) (a), DM800+$Al_2O_3$+$NaAlO_2$(70:10:20)+3%HEC (b) and DM800+$Al_2O_3$+$NaAlO_2$(70:20:10)+3%HEC (c). (Symbols: (Δ) $CaCO_3$, (○) $Ca(OH)_2$ , (▼) CaO, (⌂) MgO, (★) $MgAl_2O_4$, (✧) $Ca_{12}Al_{14}O_{33}$)

Figure 4.18 shows the XRD patterns of as-synthesized DM800+$Al_2O_3$+ $NaAlO_2$(70:10:20), DM800+$Al_2O_3$+$NaAlO_2$(70:10:20)+3%HEC and DM800+$Al_2O_3$ +$NaAlO_2$(70:20:10)+3%HEC. It can be seen that the major phases presenting in the catalyst extrudates were mixed hydroxides of Ca, Mg and Al such as $Mg_2Al(OH)_7$ and $(CaO)_3Al_2O_3(H_2O)_6$. The presence of $CaCO_3$ should be due to the reaction of CaO and $CO_2$ existing in the ambient during the catalyst preparation. After the calcination (Figure 4.19), the hydroxide phases were converted to the corresponding oxides. It was suggested by the XRD analysis that the dense and hard characteristics of the extrudates should be related to the formation of $MgAl_2O_4$ and $Ca_{12}Al_{14}O_{33}$. Adding smaller amount of $NaAlO_2$ resulted in less forming of the mixed oxides of Ca and Al as indicated in Figure 4.19 (c)).

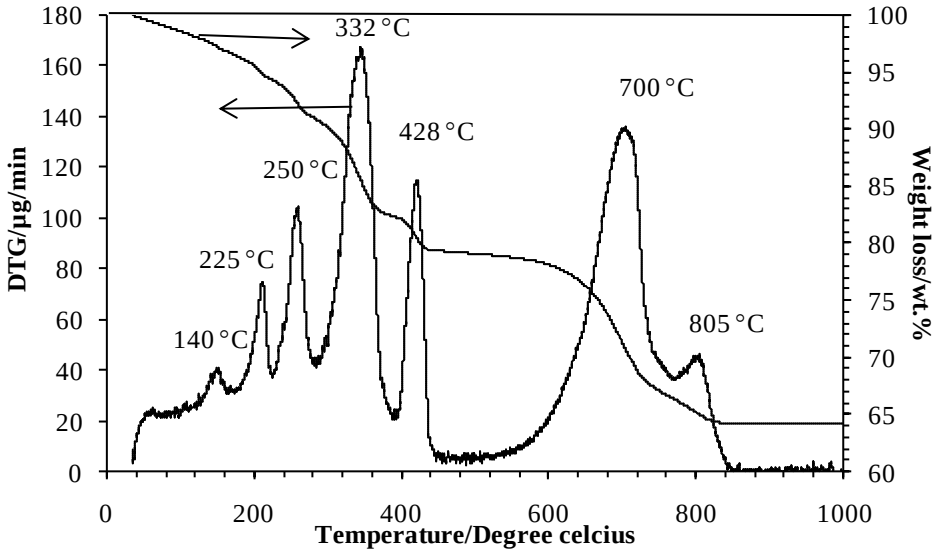


**Figure 4.20** Weight loss and DTG curves of DM800+$Al_2O_3$+$NaAlO_2$ (70:10:20) +3%HEC.

Figure 4.20 reveals the weight loss and DTG curves of the as-synthesized DM800+$Al_2O_3$+$NaAlO_2$(70:10:20)+3%HEC catalyst. The decomposition pattern of this catalyst showed a six-step weight loss. The weight loss at 145 °C should be attributed to the decomposition of $Al(OH)_3$ (3%), while the losses appearing at 225 °C and 250 °C should be ascribed to the dehydration of $Al(OH)_3$ presenting in $Mg_2Al(OH)_7$ (3%) and $(CaO)_3Al_2O_3(H_2O)_6$) (4%) structures, respectively. The weight losses at 332 °C and 428 °C were related to the dehydration of $Mg(OH)_2$ (7.5%) and

$Ca(OH)_2$ (3.7%), respectively. The weight loss at 700 °C corresponded to the decomposition of $CaCO_3$ (12%). The high temperature step at 805 °C should be related to the desorption of $CO_2$ from $NaAlO_2$.

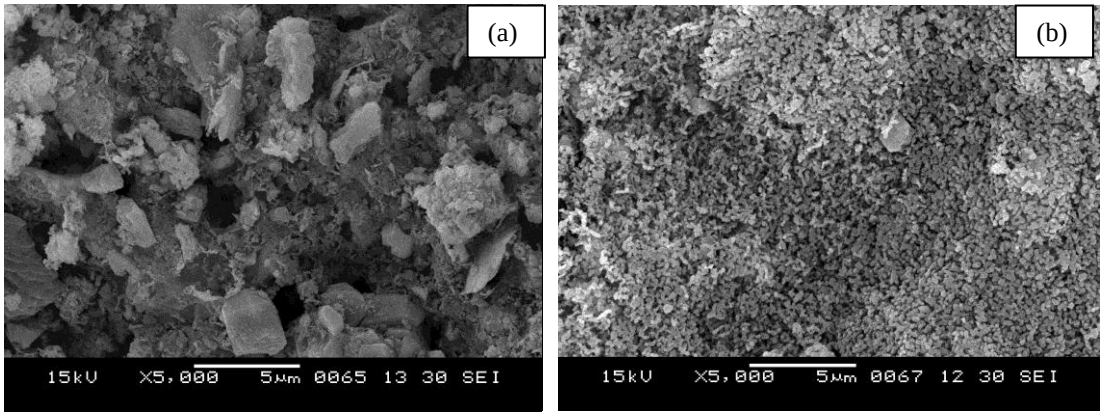


**Figure 4.21** SEM images of side area of calcined DM800+$Al_2O_3$+3%HEC extrudates prepared with and without $NaAlO_2$ addition; DM800+$Al_2O_3$+3%HEC (a) and DM800+$Al_2O_3$+$NaAlO_2$(70:10:20)+3%HEC (b).

The side area images of the DM800+$Al_2O_3$+3%HEC extrudates with and without $NaAlO_2$ addition are shown in Figure 4.21. After the calcination, the large pores appeared on the catalyst extrudates without the $NaAlO_2$ addition (Figure 4.21(a)) whereas these pore disappeared by adding $NaAlO_2$ (Figure 4.21(b)). It should be related to the generating of new phases, mixed oxides of Mg, Ca and Al, that transformed the large oxide/hydroxide particles into the smaller one. The homogeneous distribution of the small particles reduced the pore sizes and made the catalyst extrudates dense and hard.

The comparison of basic strength of calcined DM800+$Al_2O_3$+$NaAlO_2$ (70:10:20), DM800+$Al_2O_3$+$NaAlO_2$(70:10:20)+3%HEC and DM800+$Al_2O_3$+$NaAlO_2$ (70:20:10)+3% HEC by using $CO_2$-TPD technique is shown in Figure 4.22. The results indicated that DM800+$Al_2O_3$+$NaAlO_2$(70:20:10)+3%HEC (Figure 4.22(c)) had the highest basic strength since the desorption of $CO_2$ from its basic sites was found at highest temperature (790 °C).

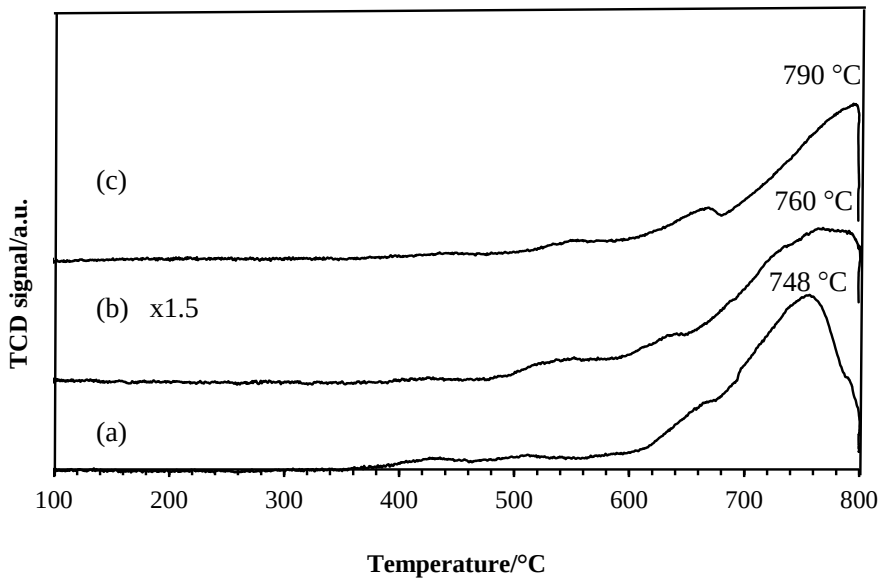


**Figure 4.22** $CO_2$-TPD profiles of calcined DM800+$Al_2O_3$+$NaAlO_2$(70:10:20) (a), DM800+$Al_2O_3$+$NaAlO_2$(70:10:20)+3%HEC (b) and DM800+$Al_2O_3$+$NaAlO_2$(70:20:10)+3%HEC (c).

**Table 4.11** Total number of basic sites of calcined DM800+$Al_2O_3$+$NaAlO_2$ extrudates determined by $CO_2$-pulse chemisorption

| Catalyst [a] | Number of basic sites (μmol/g) |
|---|---|
| DM800+$Al_2O_3$+$NaAlO_2$(70:10:20) | 14.3 |
| DM800+$Al_2O_3$+$NaAlO_2$(70:10:20)+3%HEC | 14.8 |
| DM800+$Al_2O_3$+$NaAlO_2$(70:20:10)+3%HEC | 21.9 |

[a]Catalyst was prepared in the nitric acid solution with pH of 1 and ratio of water/total solid = 1.5.The catalysts were calcined at 800 °C before the measurement.

The results in Table 4.11 show that the total number of basic sites of DM800+$Al_2O_3$+$NaAlO_2$(70:20:10)+3%HEC prepared with smaller amount of $NaAlO_2$ was highest. It should be related to the smaller extents of the formation of $Ca_{12}Al_{14}O_{33}$, when compared to DM800+$Al_2O_3$+$NaAlO_2$(70:10:20) and DM800+ $Al_2O_3$+$NaAlO_2$(70:10:20)+3%HEC, as indicated by the XRD analysis (Figure 4.19).

Although the formation of the mixed oxide of Ca and Al enhanced the extrudates hardness, it brought about a loss of number of CaO active sites.

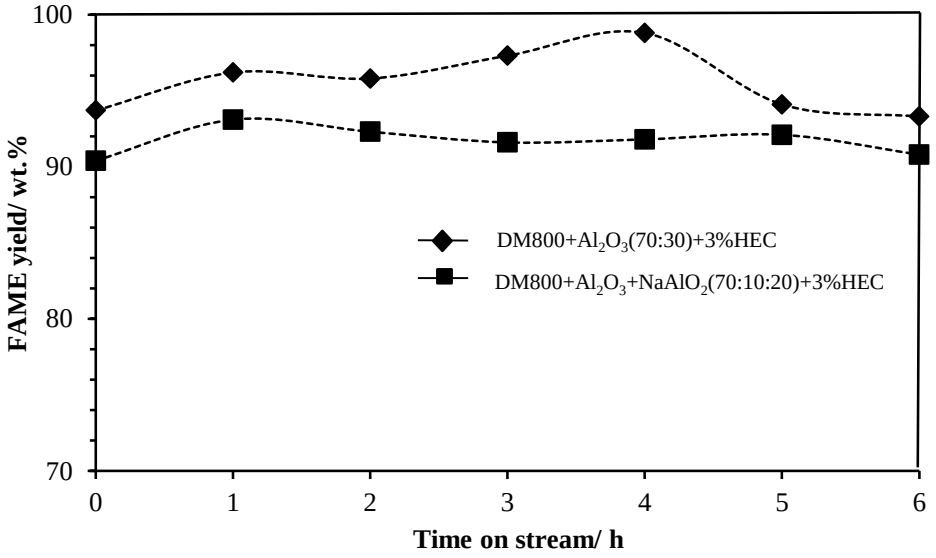


**Figure 4.23** FAME yield attained from transesterification of palm oil with methanol over DM800+$Al_2O_3$+3%HEC catalyst extrudates prepared with and without $NaAlO_2$ addition in a fixed-bed reactor. Reaction conditions: Methanol/oil ratio, 30; total flow rate, 2 mL/min; LHSV, 1.18 $h^{-1}$; temperature, 65 °C .

Figure 4.23 shows the FAME yield attained from the transesterification of palm oil and methanol over DM800+$Al_2O_3$+3%HEC extrudates prepared with and without $NaAlO_2$ addition in the fixed-bed reactor. The higher FAME yield was achieved from the catalyst without adding $NaAlO_2$. However, the breaking of this catalyst extrudates occurred in the middle of the column reactor after 2h of the reaction. As mentioned above that the adding of $NaAlO_2$ reduced the total number of basic sites due to the formation of $(CaO)_3Al_2O_3(H_2O)_6$ and $Ca_{12}Al_{14}O_{33}$, the FAME yield was decreased consequently. Nevertheless, these phases enhanced dense and hard characteristics of the extrudates. Therefore, the FAME yield produced over DM800+$Al_2O_3$+$NaAlO_2$(70:10:20)+3%HEC was stable along 6 h of the reaction, and the catalyst extrudates were not broken after use.

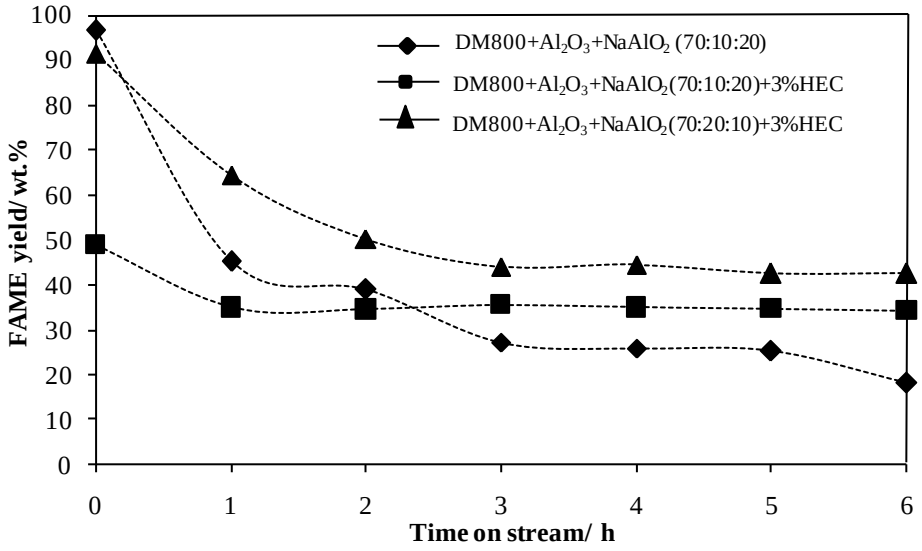


**Figure 4.24** FAME yield attained from transesterification of palm oil with methanol over various DM800+$Al_2O_3$+$NaAlO_2$ extrudates in a fixed-bed reactor. The catalyst bed height was reduced to 15 cm. Reaction conditions: Methanol/oil ratio, 30; total flow rate, 2 mL/min; LHSV, 1.09 $h^{-1}$; temperature, 65 °C .

Figure 4.24 shows the FAME yield attained from the transesterification of palm oil and methanol over DM800+$Al_2O_3$+$NaAlO_2$ extrudates with different compositions in the fixed-bed reactor. Using DM800+$Al_2O_3$+$NaAlO_2$(70:20:10)+3% HEC gave the highest FAME yield. It should be due to its highest number of basic sites (Table 4.11). Both DM800+$Al_2O_3$+$NaAlO_2$ with adding HEC exhibited more stable FAME yield than that without the HEC addition, which a severe drop of the FAME yield was observed through the reaction course. These results should be related to the generation of larger porous structure derived from the loss of HEC during the calcination. The large pore size provided less mass transfer limitation for the reactants to reach the active sites in the pore of the catalyst extrudates, and also mitigated the catalyst deactivation caused by an adsorption of large molecules.

## 4.3 Dependence of product distribution on reaction time in the transesterification of palm oil and methanol

As illustrated in Table 4.12, the conversion of triglycerides formerly presenting in palm oil with methanol over DM800+$Al_2O_3$+$NaAlO_2$(70:10:20)+3%

HEC extrudates in the fixed-bed reactor was stably high within the studied reaction course. Unexpectedly, the amount of monoglycerides and diglycerides observed was very low, suggesting a fast rate of reaction. According to the Thailand biodiesel standard issued by the Ministry of Energy, the upper limits of mono-, di- and triglycerides content of biodiesel fuel are 0.8, 0.2 and 0.2 wt.%, respectively. All produced glycerides were slightly over the standard limits. Further adjustment of operating conditions, such as the methanol/oil molar ratio and LSHV, may lower the glycerides content.

**Table 4.12** Dependence of product distribution on reaction time in transesterification[b] of palm oil with methanol over DM800+$Al_2O_3$+$NaAlO_2$(70:10:20)+3%HEC extrudates in a fixed-bed reactor

| Catalyst[a] | Time (h) | FAME yield (wt.%) | Glycerides yield (wt.%) | | |
|---|---|---|---|---|---|
| | | | Mono- | Di- | Tri- |
| DM800+$Al_2O_3$+$NaAlO_2$ | 0 | 0 | 0 | 0 | 100 |
| (70:10:20)+3%HEC | 1 | 90.4 | 1.0 | 0.5 | 1.9 |
| | 2 | 93.1 | 0.9 | 0.5 | 1.3 |
| | 3 | 92.3 | 0.8 | 1.0 | 1.5 |

[a]Catalyst was prepared in the nitric acid solution with pH of 1 and ratio of water/total solid = 1.5. The catalyst was calcined at 800 °C before being used.

[b]Reaction conditions: Methanol/oil ratio, 30; total flow rate, 2 mL/min; LHSV, 1.18 $h^{-1}$; temperature, 65 °C.

## 4.4 Mechanical testing of DM800+$Al_2O_3$+$NaAlO_2$(70:10:20) +3%HEC catalyst extrudates

Crushing strength of DM800+$Al_2O_3$+$NaAlO_2$(70:10:20)+3%HEC catalyst extrudates was evaluated according to ASTM D-4179-82. The result is shown in Table 4.13. It was found that the crushing strength was 0.01 MPa only, while that of

the commercial catalyst is around 1.5-2.1 MPa. The small crushing strength should be due to the formulation of the catalyst by using the manual extruder that applies low pressure on the catalyst paste. However, the catalyst extrudates developed in this study can be practically used in the fixed-bed reactor in laboratory scale.

**Table 4.13** Crushing strength of DM800+$Al_2O_3$+$NaAlO_2$(70:10:20)+3%HEC catalyst extrudates

| Catalyst[a] | Crushing strength (MPa) | | |
|---|---|---|---|
| | Repeat number | | Average |
| | I | II | |
| DM800+$Al_2O_3$+$NaAlO_2$(70:10:20)+3%HEC | 0.01 | 0.01 | 0.01 |

[a]Catalyst was prepared in the nitric acid solution with pH of 1 and ratio of water/total solid = 1.5.The extrudates were calcined at 800 °C before the measurement.

# CHAPTER V

# CONCLUSIONS AND RECOMMENDATIONS

## 5.1 Conclusions

From the present study on the preparation of the heterogeneous base catalysts from natural dolomite by the dissolution-precipitation method, the following conclusions can be made:

- The pH of nitric acid solution of 1 dissolved better the active metal precursor from the calcined dolomite, resulting in the catalysts with high activities.

- In the presence of binder, the catalysts formulated gave the FAME yield lower than the pure dolomite prepared in the nitric acid solution with pH of 1. However, the extrudates attained after drying at 100 °C and calcining were brittle by which the application of these catalysts in a fixed bed reactor was neglected.

- HEC was used as the plasticizer to improve characteristics of catalyst paste and extrudates. HEC with high viscosity neatly homogenized the catalyst paste. The HEC addition can increase the porosity of the extrudates. The enhancement of basicity of DM800+$Al_2O_3$+3%HEC catalyst from 18.7 to 35.0 µmol/g was observed when increasing the calcination temperature from 500 to 800 °C. The highest FAME yield (95.6%) was achieved when using the extrudates with 3%HEC. After 3 h of the reaction, the extrudates were broken, especially, one in the middle of the column reactor, resulting the drop of the FAME yield.

- The addition of $NaAlO_2$ in the catalyst paste remarkably improved the hardness of the resulting extrudates. The dense and hard characteristics of the extrudates should be related to the formation of $MgAl_2O_4$ and

$Ca_{12}Al_{14}O_{33}$ after the calcination at 800 °C. However, the FAME yield was decreased due to the contraction of porous structure. DM800+ $Al_2O_3$+$NaAlO_2$(70:20:10)+3% HEC had the highest basic strength and the total number of basic sites, and gave the highest FAME yield. DM800+$Al_2O_3$+$NaAlO_2$ with adding HEC exhibited more stable FAME yield than that without the HEC addition, which a severe drop of FAME yield was observed through the reaction course.

- Crushing strength of DM800+$Al_2O_3$+$NaAlO_2$(70:10:20)+3%HEC catalyst extrudates was evaluated according to ASTM D-4179-82. The result demonstrated that the crushing strength was only 0.01 MPa. The small crushing strength should be due to the formulation of the catalyst by using the manual extruder that applies low pressure on the catalyst paste.

## 5.2 Recommendations

1) Since CaO rapidly reacts with moisture and $CO_2$ in the atmosphere, after the calcination of catalyst an exposure to air must be avoided in order to minimize the generation of $Ca(OH)_2$ and $CaCO_3$, respectively.

2) To achieve the Thailand standard specification of biodiesel, the content of mono-, di- and triglycerides must be reduced. Adjustment of the operating conditions, such as the methanol/oil molar ratio and LHSV, should be performed as a future study.

3) To improve the crushing strength of the catalyst extrudates, the formulation process should be done by using a single or twin screw extruder.

## REFERENCES


[1] Dennis, Y.C., Xuan, W., and Leung, M.K.H. A review on biodiesel production using catalyzed transesterification. Applied Energy 89 (2010): 1083-1095.

[2] Kim, M.J., Park, S.M., Chang, D.R., and Seo, G. Transesterification of triacetin, tributyrin, and soybean oil with methanol over hydrotalcites with different water contents. Fuel Processing Technology 91 (2010): 618-624.

[3] Kouzu, M., Kasuno, T., Tajika, M., Sugimoto, Y., Yammaka S., and Hidaka, J. Calcium oxide as a solid base catalyst for transesterification of soybean oil and its application to biodiesel production. Fuel 87 (2008): 2798-2806.

[4] Reddy, C.R.V., Oshel R., and Verkade, J.G. Room- temperature conversion of soybean oil and poultry fat to biodiesel catalyzed by nanocrystalline calcium oxides. Energy fuels 20 (2006): 1310-1314.

[5] Hashimoto, H., Komaki, E., Hayashi, F., and Uematsu, T. The mechanism of thermal decomposition of dolomite: New insights from 2D-XRD and TEM analyses. Solid State Chemistry 33(1980): 81-188.

[6] Kouzu, M., Hidaka, J., Komichi, Y., Nakano, H., and Yamamoto, M. A process to transesterify vegetable oil with methanol in the presence of quick lime bit functioning as solid base catalyst. Fuel 88 (2009): 1983-1990.

[7] Kwon, S., and Messing, G.L. Constrained densification in boehmite-alumina mixtures for the fabrication of porous alumina ceramics. Journal of Materials Science 33 (1998): 913-921.

[8] Bartholomew, C.H., and Farrauto, R.J. Fundamentals of Industrial Catalytic Processes, 2nd edition. John Wiley& Sons New Jersey, 2006.

[9] Formo, M.W., Jungerman, E., Norris, F.A., and Sonntag, N.O.V. Bailey's industrial oil and fat products. 4thedition. John Wiley& Sons New York, 1979.

[10] Ramos, M.J., Fernandez,C.M., Casas, A., Rodriquez, L., and Perez, A. Influence of fatty acid composition of raw materials on biodiesel properties. Bioresource Technology 100 (2009): 261-268.

[11] Moser, B.R. Biodiesel production, properties and feedstocks. In Vitro Cellular & Developmental Biology- Plant. 45 (2009): 229-266.

[12] Demirbas, A. Biodiesel fuels from vegetable oils via catalytic and non catalytic supercritical alcohol transesterifications and other methods: a survey. Energy Conversion and Management 45 (2003): 2093-2109.

[13] Barnwal, B.K., and Sharma, M.P. Prospects of biodiesel production from vegetable oils in India. Renewable and Sustainable Energy Reviews 9 (2005): 14-34.

[14] Chavananand, K. Future of the Thai palm oil industry. Palm oil Industry inThailand [Online]. 2011. Available from: http:// www.thaipalmoil.com [2011, June]

[15] Biodiesel [Online].1999. Available from: http://journeytoforever.org/biodiesel. html [2010, April]

[16] Ma, F., and Hanna, M.A. Biodiesel production: review. Bioresource Technology 70 (1999): 1-15.

[17] Demirbas, A. Progress and recent trends in biodiesel fuels. Energy Conversion and Management 50 (2009): 14-34.

[18] Ngamcharussrivichai, C. Technology and development of biodiesel [Online]. 2008. Available from: http://www.vcharkarn.com/varticle/37458.html [2010, June]

[19] Knothe, G., Dunn, R.O., and Bagby, M.O. Biodiesel: the use of vegetable oils and their derivatives as alternative diesel fuels [Online]. 1977. Available from: http://www.oupusa.org/j778/isbn/ 0841235082.html [2011, March]

[20] Bournay, L., Casanave, D., Delfort, B., Hillion, G., and Chodorge, J.A. New heterogeneous process for biodiesel production: A way to improve the quality and the value of the crude glycerin produced by biodiesel plants. Catalysis Today 106 (2005): 190-192.

[21] Helwani, Z., Othman, M.R., and Vargas, R.M. Solid heterogeneous catalysts for transesterification of triglycerides with methanol: A review. Applied Catalysis A: General 363 (2009): 1-10.

[22] Schuchardi, U., Sercheli, R., and Vargas, R.M. Transesterification of vegetable oils: A review. Journal of the Brazilian Chemical Society 9 (1998):199-210.

[23] Pappu, VK., Yanez, AJ., Peereboom, L., Muller, E., Lira, CT., and Miller, DJ. A kinetic model of the Amberlyst-15 catalyzed transesterification of methyl stearate with n-butanol. Bioresource Technology 102 (2011): 1270-1272.

[24] Brito, A., Borges, M.E., and Otero, N. Zeolite Y as a heterogeneous catalyst in biodiesel fuel production from used vegetable oil. Energy Fuels 21 (2007) : 3280-3283.

[25] Jitputti, J., Kitiyanan, B., Rangsunvigit, P., Bunyakiat, K., Attanatho, L., and Jenvanitpanjakul, P. Transesterification of crude palm kernel oil and crude coconut oil by different solid. Chemical Engineering Journal 116 (2006): 61-66.

[26] Kulkarni, M.G., Gopinath,R., Mecher L.C., and Dalai, A.K. Solid acid catalyzed biodiesel production by simultaneous esterification and transesterification. Green Chemistry 8 (2006): 1056-1062.

[27] Shah, S., Sharma, S., and Gupta, M.N. Biodiesel preparation by lipase-catalyzed transesterification of *Jathopha oil*. Energy Fuels 18 (2004): 154-159.

[28] Campanati, M., Fornasari, G., and Vaccari, A. Fundamental in the preparation of heterogeneous catalysts. Catalysis Today 77 (2003): 299-314.

[29] Schwarz, J.A., Contescu, C., and Contescu, A. Methods for preparation of catalytic materials. Chemical Reviews. 95 (1995): 477-510.

[30] Etrl, G., Knözinger, H., and Weitkamp, J. Preparation of solid catalysts. New York: Wiley VCH, 1999.

[31] Jaiyen, S. Preparation of heterogeneous base catalysts from shell for transesteerification. Master's Thesis, Department of Chemical Technology, Faculty of Science, Chulalongkorn University, 2010.

[32] Benbow, J., and Bridgwater, J. Paste flow and extrusion. New York: Oxford University, 1993.

[33] Banerjee, D., Nagaishi, N., and Yoshida, T. Hydropyrolysis of Alberta coal and petroleum residue using calcium oxide catalyst and toluene additive. Catalysis Today 45 (1998): 385-391.

[34] Cheolmin, P., Jongseung Y., and Edwin, L.T. Enabling nanotechnology with self-assembled block copolymer patterns. Polymer 44 (2003): 6725-6760.

[35] Kopeliovich, D. Aluminum extrusion [Online]. 2012. Available from: http://www.substech.com [2012, June]

[36] Lim, L.T., Auras, R., and Rubino, M. Processing technologies for poly (lactic acid). Progress in Polymer Science 33 (2008): 820-852.

[37] Mussi, S. Ceramic Dictionary [Online]. 2006. Available from: http://ceramicdictionary.com/manual extruder [2011, July]

[38] Gryglewicz, S. Rapeseed oil methyl esters preparation using heterogeneous catalysts. Bioresource Technology 70 (1999): 249-253.

[39] Demirbas, A. Biodiesel from sunflower oil in supercritical methanol with calcium oxide. Energy Conversion Manage 48 (2007): 937-941.

[40] Liu, X., Piao, X., Wang, Y., Zhu, S., and He, H. Calcium methoxide as a solid base catalyst for the transesterification of soybean oil to biodiesel with methanol. Fuel 87 (2008): 1076-1082.

[41] DMR Technical Reports Dolomite [Online]. 2010. Available from: www.dmr.go.th/dolomite/ [2010, November]

[42] Hashimoto, H., Komaki, E., Hayashi, F., and Uematsu, T. Partial decomposition of dolomite in $CO_2$. Journal of Solid State Chemistry 33 (1980): 181-188.

[43] Natural environment research council [Online]. 2006. Available from: www.brunnings.com.au/ products /dolomite [2011, January]

[44] Ngamcharussrivichai, C., Nunthasanti, P., Tanachai, S., and Bunyakiat, K. Biodiesel production through transesterification over natural calciums. Fuel Processing Technology 91 (2010): 1409-1415.

[45] Kouzu, M., Kasuno T., Tajika, M., Sugimoto, Y., Yamanaka, S., and Hidaka, J. Calcium oxide as a solid base catalyst for transesterification of soybean oil and its application to biodiesel production. Fuel 87 (2008): 2798-2806.

[46] Yoosuk, B., Udomsap, P., and Puttasawat, B. Hydration-dehydration technique for property and activity improvement of calcined natural dolomite in heterogeneous biodiesel production: Structural transformation aspect. Applied Catalysis A: General 395 (2011): 87-94.

[47] Cho, B., Seo, Y., Rae, G., and Chang, D. Transesterification of tributyrin with methanol over calcium oxide catalysts prepared from various precursors. Fuel Processsing Technology 90 (2009): 1252-1258.

[48] Chandrasekar, G., Hartmann, M., Palanichamy, M., and Murugesan. V. Extrusion of AlSBA-15 molecular sieves: An industrial point of view. Catalysis Communications 8 (2007): 457-461.

[49] Serrano, D.P., Sanz, R., Pizarro., Moreno, I., de Frutos, P., and Blázquez, S. Preparation of extruded catalysts based on TS-1 zeolite for their application in propylene epoxide. Catalysis Today 143 (2009): 151-157.

[50] Ngamcharussrivichai, C., Meechan, W., Ketcong, A., Kangwansaichon, K., and Butnark. S. Preparation of heterogeneous catalysts from limestone for transesterification of vegetable oils- Effect of binder addition. Journal of Industrial and Engineering Chemistry (2011): DOI:10.1016/j.jiec.2011.05.

[51] Kasture, M.W., Niphadkar, P.S., Bokade, V.V., and Joshi, P.N. On the catalytic performance in isopropylation of benzene over H-zeolite catalysts: Influence of binder. Catalysis Communication 8 (2007): 1003-1010.

[52] Coetzee, J.H., Mashapa, T.N., Prinsloo, N.M., and Rademan, J.D. An improved solid phosphoric acid catalyst for alkene oligomerization in a Fischer-Tropsch refinery. Applied Catalysis A 308 (2006): 204-212.

[53] Müller, S.P., Kucher, M., Ohlinger, C., and Kraushaar-Czarnetzki, B. Extrusion of Cu/ZnO catalysts for the single-stage gas-phase processing of dimethyl maleate to tetrahydrofuran. Journal of Catalysis 218 (2003): 419-428.

[54] Bournay, L., Casanave, D., Delfort, B., Hillion, G., and Chodorge, J.A. New heterogeneous process for biodiesel production: A way to improve the quality and the value of the crude glycerin produced by biodiesel plants. Catalysis Today 106 (2005): 190-201.

[55] Macas, M.J., and Ancheyta, J. Simulation of an isothermal hydrodesulfurization small reactor with different catalyst particle shapes. Catalysis Today 98 (2004): 243-256.

[56] Lange, J.P., and Mesters, C.M.A.M. Mass transport limitations in zeolite catalysts: The dehydration of 1-phenyl-ethanol to styrene. Applied Catalysis A 210 (2001): 247-255.

[57] Freiding, J., Patcas, F.C., and Kraushaar-Czarnetzki, B. Extrusion of zeolites: Properties of catalysts with a novel aluminium phosphate sintermatrix. Applied Catalysis A 328 (2007): 210-221.

[58] Basic Theory of X- ray Fluorescence [Online]. 2006. Available from: http://serc.carleton.edu/research/geochemsheets/techniques/XRF.html [2010, August]

[59] Basic Theory of X-ray diffractometer [Online]. 2004. Available from: http://serc.carleton.edu/research/geochemsheets/techniques/XRD.html [2010, August]

[60] Thermogravimetric analysis [Online]. 2009. Available from: http://en.Wikipedia.Org /wiki/Thermogravimetric analysis [2010, July]

[61] scanning electron microscope [Online]. 2005. Available from: http://www.sv.vt.edu/classes/MSE2094_NoteBook/experimental/electron.html [2010, August]

# APPENDICES

# Appendix A
## Calculation for Catalyst Preparation

**Example** Preparation of DM800+$Al_2O_3$+$NaAlO_2$+3%HEC with the percent by mass ratio of DM800/$Al_2O_3$/$NaAlO_2$ = 70:20:10 and using the amount of deionized water of 1.5 times.

Percent composition (by mass) calculation from equation following

$$\textbf{Percent by mass} = \frac{\textbf{Mass of A}}{\textbf{Mass of A+B+C}} \times \textbf{100}$$

Percent by mass of dolomite = 70

$$70 = \frac{\text{Mass of dolomite}}{1} \times 100$$

Percent by mass of $Al_2O_3$ = 20

$$20 = \frac{\text{Mass of Al2O3}}{1} \times 100$$

Percent by mass of $NaAlO_2$ = 10

$$10 = \frac{\text{Mass of NaAlO2}}{1} \times 100$$

Using dolomite 0.7 g mixing with $Al_2O_3$ 0.2 g and $NaAlO_2$ 0.1 g

Using 3%HEC

Catalyst 100 g using HEC 3 g

Therefore, Catalyst 1 g using HEC (3x1)/100 = 0.03g

DM800+$Al_2O_3$+$NaAlO_2$+3%HEC = 0.7+0.2+0.1+0.03 = 1.03 g

Therefore, adding water 1.5 times, 1.5x 1.03 =1.545 g

## Appendix B

## Calculation of Liquid Hourly Space Velocity

Liquid Hourly Space Velocity, which is defined in the equation below:

$$LHSV = \frac{T \times 60\ (min)}{V_{void} \times 1\ (h)} \qquad (A\text{-}1)$$

where;

LHSV = Liquid Hourly Space Velocity ($h^{-1}$)

T = Total flow rate of reactant (mL/min)

$V_{void}$= Volume of liquid in packed column (ml)

$$V_{void} = V_{void\ of\ Cat\ in} + V_{void\ of\ Cat\ out} + V_{void\ of\ bead} \qquad (A\text{-}2)$$

where; $V_{void}$ = Volume of liquid in packed column

$V_{void\ of\ Cat\ in}$ = Volume of inner catalyst

$V_{void\ of\ Cat\ out}$ = Volume of outer catalyst

$V_{void\ of\ bead}$ = Volume of glass bead

## Appendix C

## Calculation of Methanol to Oil Molar Ratio

**Example** Calculation of methanol to oil molar ratio of 30

Molecular weight of palm oil = 847 g $mol^{-1}$

Density of palm oil = 1 g $ml^{-1}$

Molecular weight of methanol = 32.04 g $mol^{-1}$

Density of methanol = 0.792 g $ml^{-1}$

For 10 g of palm oil

From molecular weight of palm oil = 847 g

So, 10 g of palm oil = 10/ 847 = 0.0118 mol

From methanol to oil molar ratio of 30

So, mol of methanol = 30x 0.0118 = 0.354 mol

From molecular weight of methanol = 32.04 g $mol^{-1}$

So, methanol = 0.354x 32.04 = 11.34 g

From density of methanol = 0.792 g $ml^{-1}$

So, methanol = 11.34/ 0.792 = 14.32 ml

Therefore, the desired amount of methanol was 14.32 g

# Appendix D

## Calculation of Methyl Ester Content

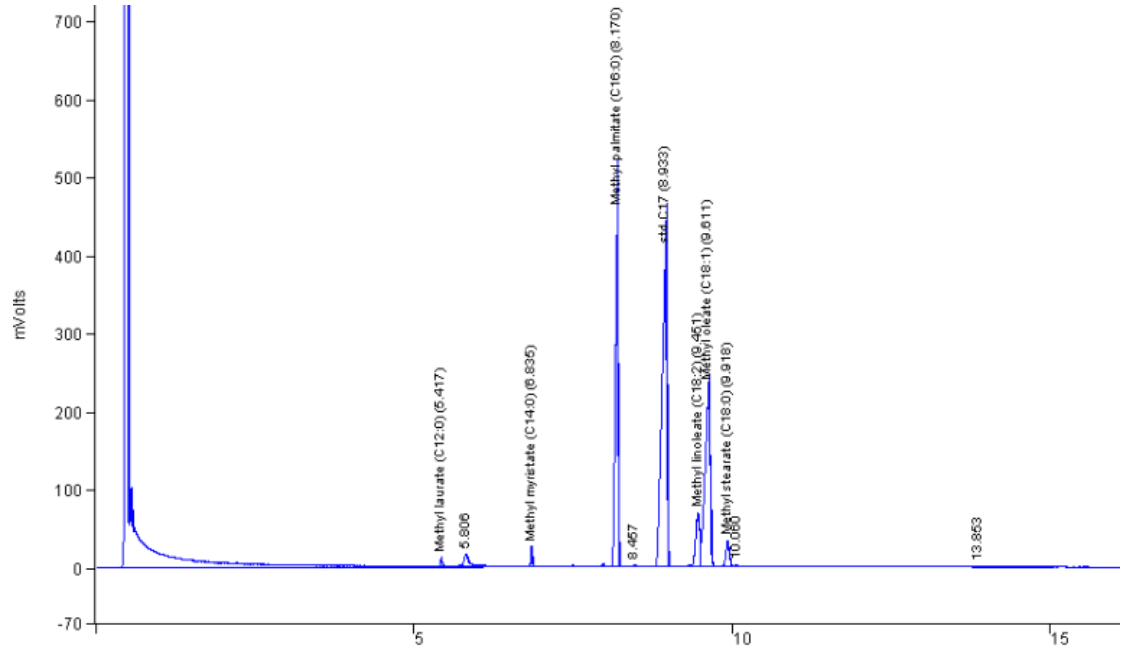


**Figure D-1** The chromatograms of methyl ester product

The methyl ester content (wt.%) was calculate from the formula

$$Wt.\% = (\sum A_i \times W_{std}) / A_{std} \times Ws)$$

Where $\sum A_i$ = The total area from methyl ester, from methyl caprylate (C8:0) to methyl stearate (C18:0)

$W_{std}$ = The weight of methyl undecanoate

$A_{std}$ = The area of methyl undecanoate

$W_s$ = The weight of the sample

## Appendix E

## Standard curve of product distribution

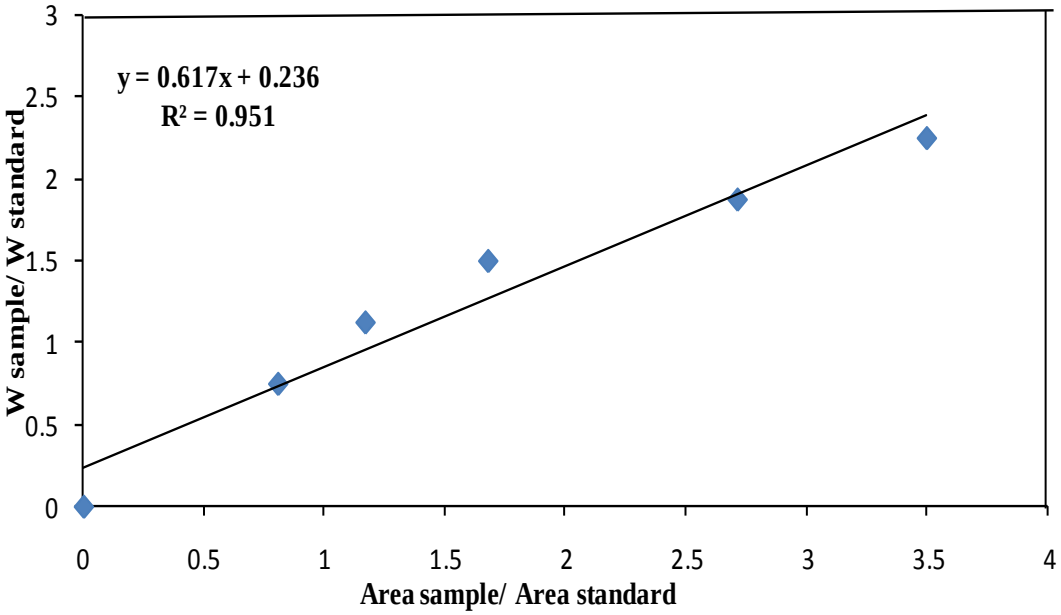


**Figure E-1.** Standard curve of monopalmitin

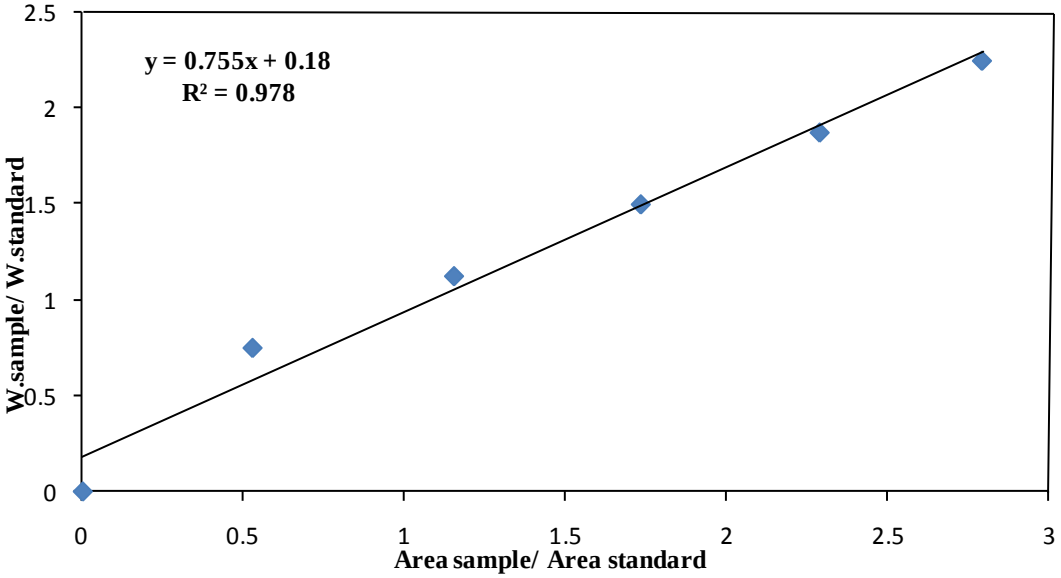


**Figure E-2.** Standard curve of dipalmitin

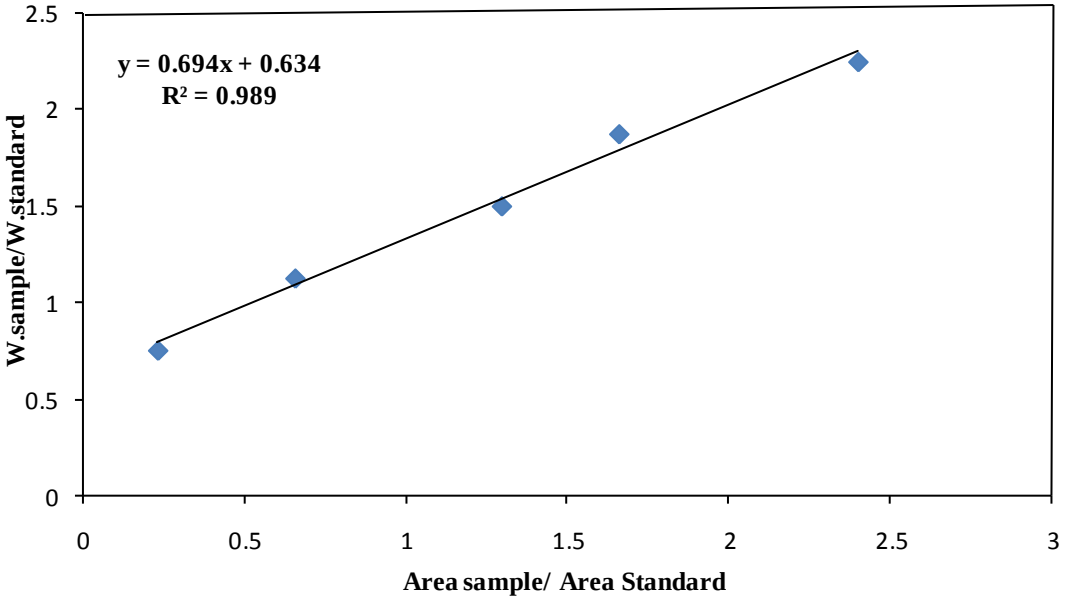


**Figure E-3.** Standard curve of tripalmitin

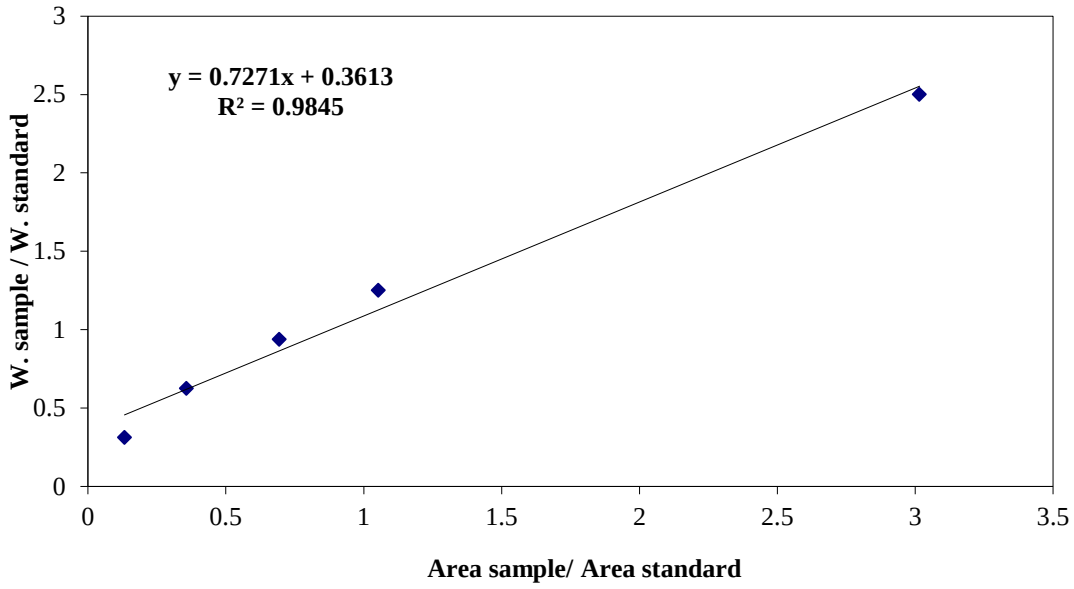


**Figure E-4.** Standard curve of monoolein

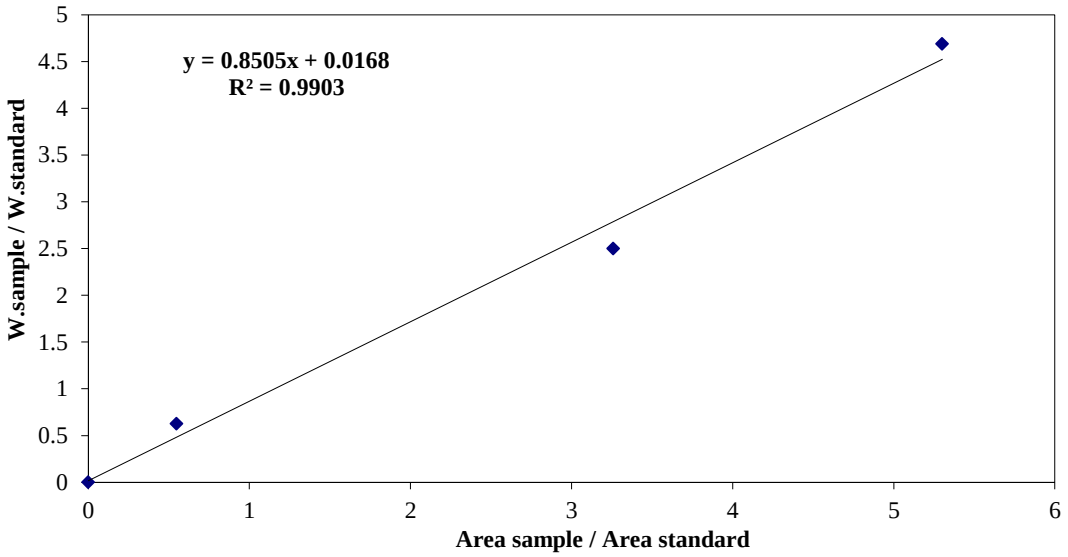


**Figure E-5.** Standard curve of diolein

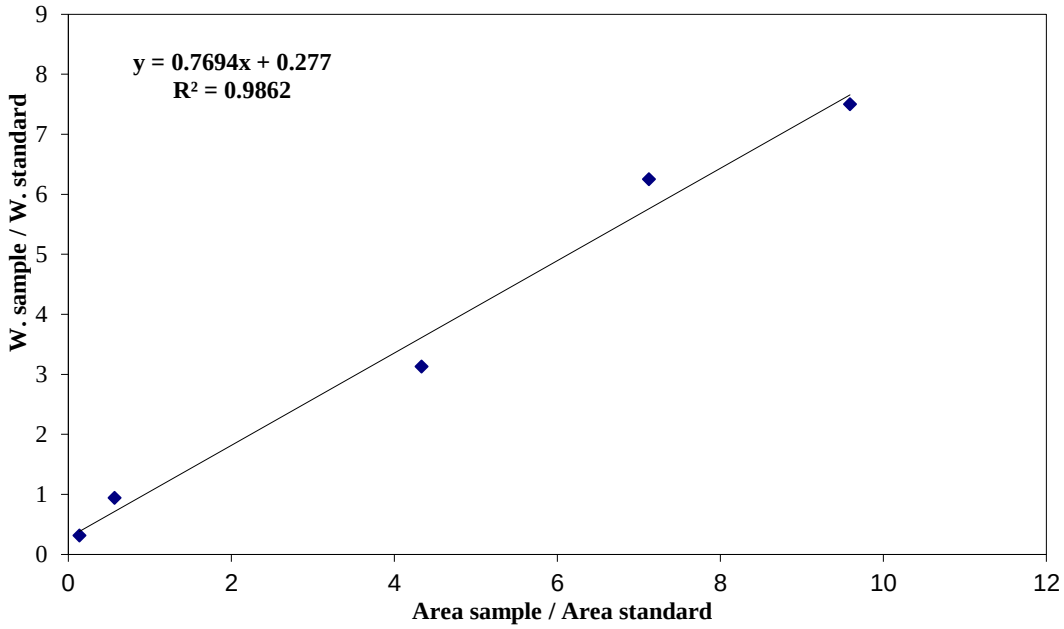


**Figure E-6.** Standard curve of triolein

# VITAE

Miss Thikumbhorn Naree was born on August 10, 1986 in Khon kaen, Thailand. She received a Bachelor‟s degree of Science, majoring in Biochemistry from Khon kaen University in 2008. She has pursued Master‟s degree in Petrochemistry and Polymer Science, Faculty of Science, Chulalongkorn University, Bangkok, Thailand since 2009 and finished her study in 2012.